FUNCTION AND DIAGNOSTIC POTENTIAL OF THE SEZ6 PROTEIN FAMILY - NOVEL SUBSTRATES OF THE ALZHEIMER PROTEASE BACE1

Martina Pigoni

Graduate School of
Systemic Neurosciences

LMU Munich

Dissertation der Graduate School of Systemic Neurosciences
der Ludwig-Maximilians-Universität München

April, 2019

Supervisor
Prof. Dr. Stefan Lichtenthaler
Chair for neuroproteomics at Technical University of Munich
German Center for Neurodegenerative Disease (DZNE), Munich

First Reviewer: Prof. Dr. Stefan Lichtenthaler
Second Reviewer: Prof Dr. Christoph W. Turck
External Reviewer: Dr. Victor Anggono

Date of Submission: 10.04.2019
Date of Defense: 19.11.2019

Table of Contents

List of abbreviations

AD	Alzheimer´s disease
AMPAR	α-amino-3-hydroxy-5-methylisoxazole-4-propionic acid receptor
APP	Amyloid precursor protein
Aβ	Amyloid beta peptide
BACE1	β-secretase or β site amyloid precursor protein cleaving enzyme 1
BACE2	β-site amyloid precursor protein cleaving enzyme 2
CHL1	Neural cell adhesion molecule close homolog of L1
COS	Childhood-onset schizophrenia
CSF0	Cerebrospinal fluid
CTD	C-terminal domain
CTF	C-terminal fragment
CUB	Complement proteases C1r and C1s, embryonic sea urchin protein Uegf, bone morphogenetic protein-1 (BMP-1)
ER	Endoplasmic reticulum
FAD	Familial Alzheimer´s disease
iGluR	Ionotropic glutamate receptor
KAR	Kainate receptor
KO	Knock-out
LBD	Ligand binding domain
NMDAR	N-methyl-D-aspartate receptor
NRG1	Neuregulin 1
NTD	N-terminal domain
PTZ	pentylene-tetrazole
RUSH	Retention using selective hooks system
SCR	Short consensus repeats for complement C3b/C4b-binding site
SEZ6	Seizure protein 6
SEZ6L	Seizure 6-like protein
SEZ6L2	Seizure 6-like protein 2

SNP	Single nucleotide polymorphism
SPECS	Secretome protein enrichment with click sugars
SUSPECS	Surface-spanning protein enrichment with click sugars
TGN	Trans-Golgi network
TKO	Triple knock-out
VGSC β	Voltage-gated sodium channels β subunit
WT	Wild-type

Abstract

BACE1 is the initiating enzyme responsible for the generation of the pathogenic amyloid beta (Aβ) and therefore a major drug target in Alzheimer's disease. On one hand, therapeutic BACE1 inhibition leads to reduced Aβ production but on the other hand it causes unwanted side effects due to loss of cleavage of additional BACE1 substrates besides APP. Different proteomic studies have identified several membrane proteins as potential BACE1 substrate candidates, but most of them have not been validated nor functionally characterized.

Here, seizure protein 6 (SEZ6) was validated as an exclusive BACE1 substrate both in primary neurons and in the brain of BACE1 knock-out (BACE1KO) mice. Additionally, I demonstrate that the soluble ectodomain of SEZ6 (sSEZ6) generated by BACE1 cleavage is strongly reduced in the CSF of BACE1KO mice, suggesting that sSEZ6 is an excellent biomarker for monitoring BACE1 activity. While it is known that BACE1 mediated-cleavage of SEZ6 controls dendritic spine density and LTP, little is known about the molecular functions of SEZ6. To this aim, I applied a novel proteomic technique to determine how loss of SEZ6 affects the surface proteome of primary neurons. Surprisingly, I found that SEZ6 specifically controls surface levels of a subclass of glutamate receptors with key functions in neurotransmission. Mechanistic analyses suggest that SEZ6 is required for glutamate receptor transport and maturation along the secretory pathway and may influence synaptic transmission.

Taken together my results prove that SEZ6 is a major substrate of BACE1, both *in vitro* and *in vivo*. Moreover, I investigated the possibility to use sSEZ6 as a potential companion diagnostic to monitor BACE1 activity in patients treated with BACE inhibitors and I discovered a novel function of SEZ6 as glutamate receptor regulator.

1. Introduction

1.1 Dementia and Alzheimer's disease (AD)

AD is a complex multifactorial neurodegenerative disease, leading to dementia symptoms such as cognitive impairment and neuropsychiatric symptoms [1]. In 2005, Alzheimer Disease International estimated that 24 million people were affected by dementia in the 14 World Health Organization regions considered in this study. Additionally, this study estimated 4.6 million new cases of dementia occur every year (one new case every 7 seconds) and that the number of affected people will be almost double every 20 years to 42.7 million by 2020 and 82 million by 2040 [2]. The same analysis run in 2013, which estimated that 48.1 million and 90.3 million people will be affected by dementia in 2020 and 2040 respectively [3]. Considering that up to 70% of dementias occurring in older adults are attributed in whole or in part to AD, AD is considered the most common cause of dementia nowadays [4,5].
In addition, according to the Alzheimer's Association costs of health care, long-term care and hospice for individuals with AD and other dementias were three times higher than payments for people in the same age group without dementias [6]. It was also estimated that total payments in 2016 in USA for all individuals with AD and other dementias are $236 billion, making AD one of the most expensive chronic diseases to society [6,7]. Yet, current available treatments for AD are only symptomatic and unable to impede the progressive pathogenesis of AD. Therefore, considering the strong impact AD has on patients and society, there is a worldwide effort to better understand its molecular mechanism, delay its onset, and prevent it from developing.

1.1.1 AD: neuropathology and amyloid β

AD leads to specific neuron and synapse loss and is neuropathologically characterized by the presence of neurofibrillary alterations mainly composed by abnormal Tau proteins, and amyloid plaques mainly composed by amyloid beta (Aβ) peptides. Neurofibrillary alterations include strands of abnormal Tau proteins located within nerve cell bodies (neurofibrillary tangles) and within their dendritic processes (neuropil threads), and neuritic plaques as a result of abnormal fibrous material which accumulates in swollen cellular processes and extracellular ‘tombstone’ tangles

localized at the sites at which the host nerve cells are perished [8]. Amyloid plaques are extracellular deposits composed mainly, but not exclusively, of Aβ peptides. Plaques occur in different sizes and shapes and most of them evolve as globular structures with or without a condensed core [8].

Aβ peptides are generally considered the main neurotoxic species in AD pathology. Aβ peptides are arisen from amyloid precursor protein (APP) by a first proteolytic cleavage mediated by BACE1 (β-secretase or β site amyloid precursor protein cleaving enzyme 1 [9]) and a subsequent cleavage by γ-secretase (Fig. 1) [10]. This double cut generates hydrophobic peptides highly prone to aggregate into high order-oligomers and subsequently form insoluble amyloid fibrils [11]. Insoluble amyloid fibrils were believed to be the main source of toxicity that causes synaptic abnormalities and the breakage of neuronal processes [12,13].

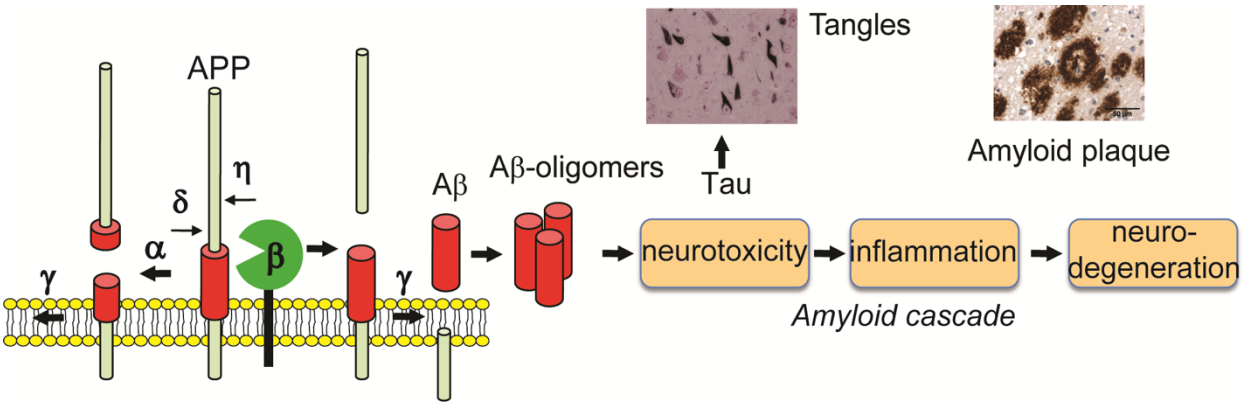

Figure 1: **Amyloid cascade hypothesis and Aβ generation.** Amyloid precursor protein (APP) is first cleaved by β-secretase (also referred to as the aspartyl protease BACE1), followed by γ-secretase cleavage. This double cleavage leads to Aβ generation and secretion. Aβ can form oligomers, which are neurotoxic through mechanisms involving the Tau proteins, leading to inflammation in the brain and neurodegeneration. Aβ aggregates are visible in the brain of AD patients upon autopsy as amyloid plaques, whereas Tau forms hyperphosphorylated-Tau aggregates. APP can also be shed by the α-secretase ADAM10, which cleaves APP in the middle of the Aβ domain, thus preventing APP from being converted to Aβ or being cleaved by other proteases (η- and δ-secretase). Taken from Saftig and Lichtenthaler, 2015 (order number: 4564920472620)

However, it was shown that oligomeric Aβ assemblies cause substantial neuronal dysfunctions even before the appearance of fibrillar amyloid deposits, indicating an important role of oligomeric assemblies in AD pathogenesis [14,15,11]. The mechanism of Aβ toxicity has been studied extensively and many theories have been proposed. Recently, in addition to the well-established role of Aβ in mediating neurotoxicity, emerging evidences show that Aβ can activate a local inflammatory process astrocytes and microglia-mediated [16]. Taken together, pharmacological modulation to slow down Aβ generation may be a potential treatment for AD.

1.1.2 BACE1 in AD

Beta-site amyloid precursor protein cleaving enzyme 1 (BACE1) is the aspartyl protease that mediates the first cleavage of APP; thereby it is the key initiating enzyme to generate the neurotoxic Aβ peptide [9]. Protein levels of BACE1 and its activity have been found to increase in the brain of AD patients as compared to the healthy controls [17-19]. This evidence suggests that increase in BACE1 might initiate or accelerate AD pathogenesis [20]. Additionally, it is known that the APP Swedish mutation (KM670/671NL), which leads to early onset of familial AD, causes enhanced APP cleavage mediated by BACE1, which is sufficient to induce AD pathogenesis [21,22]. On the opposite side, the Icelandic mutation (A673T) in the APP gene, which reduces approximately 40% of Aβ production for the entire lifespan, is protective against AD and cognitive decline [23]. Considering these evidences, BACE1 is a prime target for drug development in AD and the possibility of reducing Aβ production by inhibiting BACE1 have been extensively pursued [24,25].

BACE1 inhibitors have been shown to reduce Aβ levels both in preclinical and clinical phase [26-34]. On the other hand, side effects due to the loss of BACE1 were reported in BACE1KO mice and mice treated with BACE1 inhibitors (see Table 1 and section 1.1.3) [35-38].

For example, Cheret *et al.* showed that BACE1 is required for formation and maturation of muscle spindles and therefore it is essential to maintain motor coordination [38]. Savonenko *et al*. showed a sensori-motor-gating deficiency, behavioral signs of glutamatergic hypo-function, and other typical endophenotypes of schizophrenia-like behavior in BACE1KO mice [39]. Kobayashi *et al.* demonstrated

that BACE1KO mice perform worse than wild-type mice in hippocampal-dependent learning tasks and in a motor coordination test [40]. Additionally, several groups reported impaired synaptic plasticity and impaired spatial and working memory in BACE1KO mice [40-42,36].

Likewise, patients enrolled in different clinical trials reported some side effects upon treatment with BACE inhibitors and this cause the termination of several clinical trials in the last years. For example in 2017 Merck stopped the EPOCH trial (SCH 900931, P07738) of verubecestat in mild to moderate AD for “virtually no chance of finding a positive effect” [43] and just one year later also the Merck’s APECS trial (SCH 900931), aiming to test the same drug in people with prodromal AD, was stopped because “was unlikely that positive benefit/risk could be established if the trial continued” (official Merck communication, pressed February 13, 2018). In the same year Janssen decided to terminate the EARLY phase 2b/3 trial of atabecestat (also known as JNJ-54861911) in preclinical AD because “elevations of liver enzymes, which were serious in nature, have been observed in some study participants who received the Janssen BACE inhibitor, atabecestat” (official Janssen communication, pressed May 18, 2018). Previously, Eli Lilly’s LY2811376 (Phase 1) and LY2886721 (Phase 2) and Roche’s RG7129 were also dismissed because of off-target side effects, including liver toxicity for LY2886721. In addition, some mild memory deficits, psychiatric symptoms and tendency to fall/get injuries were also described upon treatment with BACE inhibitors in subgroups of patients [43]. In addition to the described side effects, no cognitive benefits were reported so far in patients treated with BACE inhibitors.

1.1.3 BACE1 substrates

The phenotypes described in mice lacking BACE1 activity result most likely from the absence of processing of other essential BACE1 substrates besides APP. The loss of neuregulin-1 processing for example, leads to hypomyelination and loss of muscle spindles seen in BACE1KO mice. The neuregulin-1 EGC-like region is no longer released and is therefore not available to stimulate axon myelination [44-46,38]. Likewise, loss of cleavage of the cell adhesion protein CHL1 has been linked to axon guidance defects in BACE1KO mouse brains [47]. Additionally, the hyperexcitability and spontaneous seizures described in the BACE1KO mice may be explained by loss

of cleavage of voltage-gated sodium channels β subunit (VGSC β) [48,49]. Recently, reduced LTP, spine density and spine plasticity were reported in SEZ6KO mice and these features could be reproduced in BACE1 inhibitor treated mice, which indicates that the lack of SEZ6 processing by BACE1 is responsible for these phenotypes [37]. Conclusively, it becomes clear that the substrates and functions of BACE1 need to be carefully examined in order to fully evaluate the therapeutic potential of BACE1 and possible side effects of pharmacological BACE1 inhibition in patients [20].

A part of the most known BACE1 substrates such as APP [50], several novel BACE1 substrates have been identified in different proteomic studies [51-55], among which the seizure protein 6 (SEZ6, also known as seizure related protein 6) and its homolog seizure protein 6 like (SEZ6L) were exclusive substrates of BACE1 [52,55]. A third family member, SEZ6L2, was also among the BACE1 substrates, but was not only cleaved by BACE1 but also by additional proteases, probably including Cathepsin D [52,53,56].

BACE1KO Mouse Phenotype	Reference
Altered neurogenesis and astrogenesis	Hu, X. et al. (2013)
Axonal targeting errors	Rajapaksha, T.W. et al. (2011); Cao, L. et al. (2012) T; Hitt, B. et al. (2012)
Epileptic-like seizures	Hu, X. et al. (2010); Kobayashi, D. et al.; Hitt, B.D. et al. (2010)
Higher lethality	Dominguez, D. et al. (2005); Hu, X. et al. (2010)
Hypomyelination	Willem, M. et al. (2006) Hu, X. et al. (2006); Hu, X. et al. (2008)
Impaired growth cone collapse	Barão, S. et al. (2015)
Impaired spatial and working memory	Laird, F.M. et al. (2005); Kobayashi, D. et al. (2008); Filser, S. et al. (2014)
Impaired synaptic plasticity	Laird, F.M. et al. (2005); Kobayashi, D. et al. (2008); Wang, H. et al. (2008); Filser, S. et al. (2014)
Reduced muscle spindles	Cheret, C. et al. (2013)
Reduced spine density	Savonenko, A.V. et al. (2008)
Retinal pathology	Cai, J. et al. (2012)
Schizophrenia-like phenotypes	Kobayashi, D. et al.; Savonenko, A.V. et al. (2008)
Timid and less exploratory	Harrison, S.M. et al. (2003)

Table 1: **Summary of the phenotypes described in BACE1KO or BACE inhibitor- treated mice.** Modified from Barao *et al*., 2016

1.2 The Seizure protein 6 family

The protein SEZ6 is a particularly interesting BACE1 substrate for several reasons. First, the ectodomain cleavage of the transmembrane protein SEZ6 is almost exclusively dependent on the BACE1 activity. Additionally, SEZ6 was reported to play critical roles in neuronal development and functions [57]. Some phenotypes present in SEZ6KO mice, such as reduced anxiety levels and cognitive deficits were also described in BACE1KO mice, suggesting that BACE1 may regulate the functions of SEZ6 in the nervous system [57].

1.2.1 Expression and domain structure of Seizure protein 6 family

SEZ6 mRNA was found upregulated in cortical neurons treated with the convulsant drug pentylene-tetrazole (PTZ), but, nowadays no prove of SEZ6 involvement in epilepsy- or PTZ-susceptibility was found [58]. Different SEZ6 isoforms are produced by alternative splicing of the *SEZ6* mRNA: two (Sez6 type I and type II) are cell-surface proteins with a single transmembrane domain (transmembrane type 1), and Sez6 type III is a secreted isoform. The third splice form, Sez6 type III, has been described on the mRNA level and is a truncated soluble protein, but has never been detected on the protein level [59,57].

The SEZ6 extracellular region includes protein-protein interaction domains: CUB (complement subcomponent C1r, C1s/sea urchin embryonic growth factor Uegf/bone morphogenetic protein 1) and SCR (short consensus repeat) (Fig. 2). The SEZ6 C-terminal domain was predicted to contain a NPxY binding motif, which is commonly involved in protein endocytosis and it is reported to be important for the internalization of SEZ6L2, another member of the SEZ6 family [60,56].

The other two family members of the SEZ6 family, Seizure-related 6 Like protein (SEZ6L) and Seizure-related 6 Like 2 protein (SEZ6L2) have more than 40% identity and 60% similarity with SEZ6. The similarity is particularly high in the CUB and SCR domains, which are important for protein-protein interaction (alignment done with EMBOSS Stretcher, using SEZ6 Uniprot sequence Q7TSK2, SEZ6L Uniprot sequence Q6P1D5 and SEZ6L2 Uniprot sequence Q4V9Z5-1).

The three family members have a peculiar spatial and temporal expression pattern. SEZ6 is mainly expressed in neurons with highest expression in embryonic and postnatal neocortex [61,59,62,63]. In adult mouse brain, SEZ6 expression is reduced but remains detectable in mid-cortical layers, olfactory tubule, cingulate cortex and hippocampus (mainly in the CA1) [61]. SEZ6L has been mainly studied in brain, but there are mounting evidences indicating that this protein is also expressed in other cell types and organs such as pancreatic cells and lung [55,64].

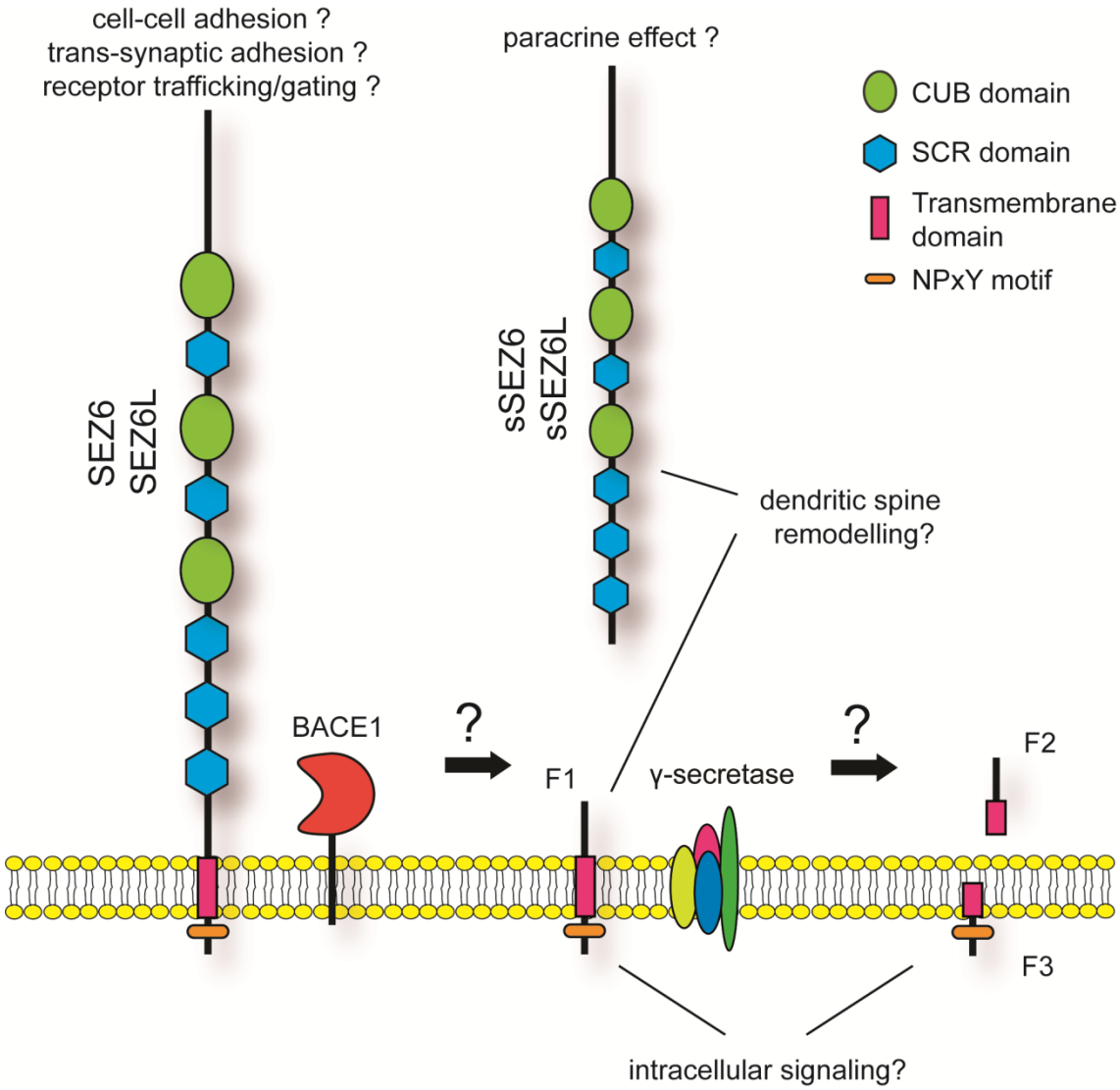

Figure 2: **Schematic representation of SEZ6/SEZ6L structure and hypothesized proteolytic processing.** SEZ6 proteins contain three CUB domains, five SCR domains and a NPxY motif. It was suggested that, similarly to APP, BACE1 cleaves SEZ6/SEZ6L generating a soluble ectodomain (sSEZ6/sSEZ6L) and a C-terminal fragment (F1). F1 would be further cleaved by γ -secretase producing two additional fragments, F2 and F3. The function of these fragments remains unexplored. Figure modified from Pigoni *et al.*, 2017

As compared to SEZ6, SEZ6L levels in the brain are relatively constant during the postnatal stages [59] and it is expressed ubiquitously in all regions with highest expression in the cerebellum and Purkinje cells [59,65]. Similar to SEZ6L, SEZ6L2 was also detected in pancreatic cells and in lung [55,66]. In the brain, SEZ6L2 is widely expressed in the gray matter with high levels in the olfactory bulb, anterior olfactory nuclei, hippocampus and cerebellar cortex and its level remain constant during aging [59].

1.2.2 The SEZ6 family in disease

In general, mutations in SEZ6 have been linked to psychiatric disturbances and neurodevelopmental disorders in several genome-wide association studies, even if no evidence of a mechanism or causative role of SEZ6 was ever shown. Ambalavanan *et al.* described a de novo variant of SEZ6 sequence associated with Childhood-onset schizophrenia (COS) and speculate that SEZ6 might be a good candidate as a COS predisposing gene [67]. Maccarrone *et al.* found significantly increased levels of SEZ6 ectodomain (sSEZ6) in the CSF of bipolar disorder, major depressive disorder and schizophrenia patients in comparison to controls [68]. Additionally, genetic variants of SEZ6 genes have been associated with severe intellectual disability [69] and increased susceptibility for febrile seizures [70,71]. A mutation in the SEZ6L2 gene was associated with bipolar disorder [72] and mutations in both SEZ6L and SEZ6L2 genes with autism [73,74].
SEZ6 was also found to be associated with neurodegenerative diseases, in particular AD. Reduced levels of sSEZ6 have been found in the CSF of AD patients as compared to healthy controls [75] and recently, a rare variant of SEZ6 (R615H) was linked to late-onset AD in a large Italian family carrying no typical FAD-linked mutations [76].

1.2.3 Molecular functions of the SEZ6 family

Even if SEZ6 knock-out (SEZ6KO) mice have been generated more than ten years ago and several phenotypes of SEZ6KO mice have been described [57], the molecular functions of SEZ6 are still largely unknown. However, given that *Sez6* mRNA is highly expressed in the developing forebrain, it is reasonable to assume that

SEZ6 plays a critical role in the development and functions of neocortex, hippocampus and thalamus. At the behavioral level, SEZ6KO mice displayed impaired primary motor ability, long-term memory deficit and decreased anxiety levels [57]. Behavioral phenotypes also correlate with morphological alterations in neurons. As compared to WT control, SEZ6KO neurons increased complexity of dendritic branches but reduced spine numbers [57,37]. Additionally, the number of functional excitatory connections and long term potentiation (LTP) are significantly reduced in SEZ6KO mice [57,37]. A similar reduction of excitatory synaptic transmission was also found in SEZ6L and SEZ6L2 deficient neurons, resulting in reduced frequency and amplitude of intracellular calcium elevations and neuronal network activity [77].

In addition, considering that the structure of SEZ6 is rich in CUB and SCR domains, both are involved in protein-protein interactions [78] and are contained in a number of neurotransmitter receptor-binding proteins such as SOL-1, SOL-2 and LEV-10 [79-86], SEZ6 and related family members might be involved in cell-cell adhesion or in the regulation of ionotropic neurotransmitter receptors. Indeed, supporting this notion, it was recently published that SEZ6L2 binds both glutamate receptor 1 (GluR1) and Adducin, forming a protein complex and acting similarly to a scaffolding protein [87]. Taking all together, I proposed and found a novel function of SEZ6 as a regulator of glutamate ionotropic receptors.

1.3 The Kainate ionotropic receptors GluK2 and GluK3

The ionotropic glutamate receptor (iGluR) family comprises three major subfamilies named after their pharmacological agonists: α-amino-3-hydroxy-5-methylisoxazole-4-propionic acid (AMPA), N-methyl-D-aspartate (NMDA), and kainate (KA) receptors (Table 2) [88]. KARs, similarly to all the other iGluRs, have a tetrameric subunit composition which consists of an extracellular N-terminal domain (NTD), three transmembrane domains, a re-entrant loop penetrating the plasma membrane from the intracellular side, and a cytoplasmic C-terminal domain (CTD) (Fig. 3) [89,90]. The ligand-binding domain (LBD) of KARs consists of two lobes, formed by the S1 and S2 domains of the subunit (Fig. 3). KARs are further classified into two subgroups: low-affinity (GluK1, GluK2 and GluK3) and high-affinity (GluK4 and

	Old nomenclature	HUGO	IUPHAR
NMDA	NR1	*GRIN1*	GluN1
	NR2A	*GRIN2A*	GluN2A
	NR2B	*GRIN2B*	GluN2B
	NR2C	*GRIN2C*	GluN2C
	NR2D	*GRIN2D*	GluN2D
	NR3A	*GRIN3A*	GluN3A
	NR3B	*GRIN3B*	GluN3B
AMPA	**Old nomenclature**	**HUGO**	**IUPHAR**
	GluR1	*GRIA1*	GluA1
	GluR2	*GRIA2*	GluA2
	GluR3	*GRIA3*	GluA3
	GluR4	*GRIA4*	GluA4
Kainate	**Old nomenclature**	**HUGO**	**IUPHAR**
	GluR5	GRIK1	GluK1
	GluR6	GRIK2	GluK2
	GluR7	GRIK3	GluK3
	KA-1	GRIK4	GluK4
	KA-2	GRIK5	GluK5

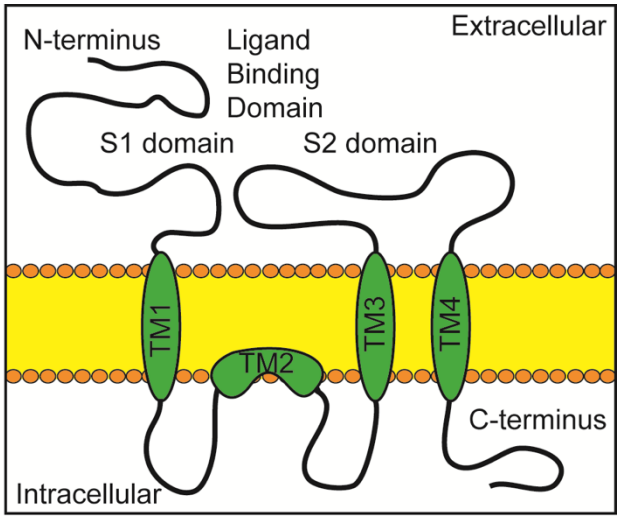

Left side table 2: **Classification and nomenclature of major ionotropic glutamate receptors (iGluRs).** Old nomenclature ("Old nomenclature"), gene name according to the Human Genome Organisation Internationa ("HUGO") and new nomenclature according to the International Union of Basic and Clinical Pharmacology ("IUPHAR") are reported.

Right figure 3: **Schematic representation of iGluRs structure.** TM: transmembrane domain.

GluK5) subunits. Low affinity subunits can assemble as homomeric or heteromeric tetramers, while GluK4 and GluK5 have to co-assemble in a complex with low-affinity subunits to form functional KARs. GluK2 and GluK3 are low affinity subunits, and therefore they can form both homomeric and heteromeric complexes.
Additionally, GluK2 and GluK3 diversity is further increased by alternative splicing that might occur at the CTD and generates GluK2a, GluK2b and GluK2c and GluK3a and GluK3b, respectively.

1.3.1 Regulation and surface localization of GluK2 and GluK3

Multiple mechanisms are known to control trafficking and surface localization of kainate receptors in general and in particular to GluK2 and GluK3. Some of these are dependent from intrinsic properties of the receptors themselves such as alternative splicing, editing of mRNA, differential assembly of different subunits, post-translational modifications. Several other proteins are also known to be important modulators of the trafficking and activity of GluK2 and GluK3 [91].

For example, both splice variants GluK2a and GluK3a contain a cell surface trafficking motif rich in basic residues (873 RRXKXK 878), which makes these subunits be efficiently targeted to the cell surface, while GluK2b and GluK3b are partially retained in the ER [92,93]. Not only GluK2a and GluK3a are efficiently exported when in homomeric structures, but also in heteromeric assembly GluK2a and GluK3a promote the trafficking to the cell surface of otherwise ER-retained subunits [92-94]. This indicates that assembly of different subunits is indeed a critical control step for the membrane trafficking of the receptors. Furthermore, Q/R editing of GluK2 mRNA leads to attenuated oligomerization, decreased ER exit as well as stability, and ultimately leads to a reduced surface expression of GluK2(R)-containing KARs [95]. Moreover, it was shown that disruption in ligand binding domain (LBD) of GluK2 or its co-assembly with mutated GluK5 subunits with reduced agonist-affinity leads to lower surface levels and intracellular retention of the complex [96,97]. These evidences suggest that conformational changes occurring upon agonist binding to the subunits, are a prerequisite for efficient exit from the ER and represent a step of quality control for further trafficking of assembled receptors [97]. Several post-translational modifications influence GluK2 and GluK3 abundance at the cell surface.

Among these, phosphorylation (PKC- and PKA- mediated), palmitoylation and SUMOylation are known to regulate surface levels of KARs and the subsequent kainate-receptor-mediated synaptic transmission in response to different stimuli [98-101].

1.3.2 Proteins interacting and regulating GluK2 and GluK3

GluK2/3 and other KARs are known to interact with several proteins mainly belonging to the SAP family and to other PDZ or CUB domain-containing, or BTB-Kelch protein family members [91]. For example, postsynaptic density protein 95 (also known as PSD-95 or SAP-90), SAP-102 and SAP-97 were proven to directly interact with GluK2 and the interaction with PSD-95 promotes GluK2 clustering and thereby influences the electrophysiological properties GluK2 [102,103]. In addition to the SAP family, other PDZ domain proteins such as PICK1 (protein interacting with PRKCA 1), GRIP (glutamate receptor interacting protein 1), and syntenin bind GluK2 and these interactions not only modulate KARs synaptic transmission, but also seem to be involved in KARs stabilization at the cell surface [99].

More recently, two CUB domain-containing proteins have been identified as accessory subunits essential for the modulation of pharmacological and gating properties of KARs: Neuropilin and Tolloid-like 1 and 2 proteins (NETO 1 and NETO2) [81]. Conflicting data have been reported as to whether these two proteins regulate trafficking and synaptic localization of KARs [104]. Zhang *et al.* showed that NETO2 does not influence the surface abundance of GluK2 in the heterologous *X. laevis* oocyte system [81], whereas Tang *et al.* described a reduction of GluK2-containing KARs in the PSD of cerebella in NETO2 knock-out mice, while the overall GluK2 protein level was not altered [104]. Additionally, Straub *et al.* showed that no obvious change in the surface abundance of GluK2/3 can be observed in acute hippocampal slices of NETO1 knock-out mice [85], but a reduction of GluK2- and GluK5-containing KARs in the PSDs of NETO1 and NETO1/2 knock-out hippocampal neurons has been reported by Tang *et al.* [86]. Additionally, BTB-Kelch protein family plays a critical role in the regulation of KARs. For example, KRIP6 (kainate receptor interacting protein for GluR6) alters functional properties of GluK2 without affecting plasma membrane levels of the receptor [105], whereas actinfilin is implicated in targeting GluK2 for degradation [106].

1.3.3 Kainate ionotropic receptors in disease

Ionotropic kainate receptors play a critical role in the development of synaptic connectivity and in the maturation of neuronal networks both in embryonal and early post-natal stages [107]. Indeed, a two-step model of neuronal synaptogenesis was suggested, in which KARs may be activated by low concentrations of glutamate early in development and this activation may promote neuronal filopodia motility. Once the nascent synapse is established, higher concentrations of glutamate may lead to lower motility and to the stabilization of the new synaptic contact [108].

Considering the important function of KARs in brain development, it is not surprising that KARs have been linked to several brain disorders such as mood disorders and epilepsy. Evidences of altered KARs expression in schizophrenic post-mortem brains have been provided by several groups both at mRNA and protein level [109-113]. For example, Scarr *et al.* showed a reduction of *GluK1* mRNA in the hippocampus, parahippocampus and prefrontal cortex of schizophrenic brains [111] and Garey found a significant reduction of GluK1/2/3-positive neurons in the cortex of schizophrenic patients [112]. On the other hand, no difference of KAR subunits expression was detected in thalamic nuclei of schizophrenic brains by Dracheva *et al.* [114]. Interestingly, Tucholski *et al.* showed that the glycosylation of KARs is also altered in schizophrenia patients, suggesting that the altered glutamate neurotransmission in schizophrenia may involve abnormal trafficking of KARs [115].

In addition, deletions of the *Grik2* gene have been associated to mental retardation [116] and mania [117,118]. SNPs in the Grik3 gene have also been shown in linkage disequilibrium with depressive disorder patients [119,120] and patients with schizophrenia [121,122]. In addition to mood disorders, mounting evidences showed an involvement of KARs in the excitatory to inhibitory imbalances connected to epilepsy. Considering that kainate administration in mice is used as a model of epilepsy and that GluK2 KO mice display reduced sensitivity to develop seizures after KA administration, it was suggested that KARs play an important role in the KA-mediated over-excitability that leads to epilepsy [123]. Indeed, antagonists of GluK1 were shown to be able to abolish epileptic activity and seizures both in in brain slices and *in vivo* in a mouse of epileptiform activity [124]. In addition, mutations of Grik1

gene represent a major genetic risk to the pathogenesis of juvenile absence epilepsy-related phenotypes [125].

On the basis of these important research findings, my aim was to validate SEZ6 as a major BACE1 substrate in neurons and investigate how BACE1 inhibition impacts on SEZ6 proteolytic processing. Furthermore, I extensively studied the molecular functions of SEZ6 in neurons with the aim to identify novel functions for SEZ6 and molecular mechanisms in which SEZ6 in involved. Third, I will investigate how the loss of BACE1-mediated SEZ6 cleavage influences these functions. These aspects will help to better understand how SEZ6 acts physiologically in neurons and to reveal the mechanisms that lead to the previously described phenotypes related to SEZ6 deficiency or BACE1 inhibition.

2.1 Seizure protein 6 and its homolog seizure 6-like protein are physiological substrates of BACE1 in neurons

Martina Pigoni, Johanna Wanngren, Peer-Hendrik Kuhn, Kathryn M. Munro, Jenny M. Gunnersen, Hiroshi Takeshima, Regina Feederle, Iryna Voytyuk, Bart De Strooper, Mikail D. Levasseur, Brian J. Hrupka, Stephan A. Müller and Stefan F. Lichtenthaler

Pigoni et al. Molecular Neurodegeneration (2016) 11:67
DOI 10.1186/s13024-016-0134-z

Molecular Neurodegeneration

RESEARCH ARTICLE Open Access

Seizure protein 6 and its homolog seizure 6-like protein are physiological substrates of BACE1 in neurons

Martina Pigoni[1,2], Johanna Wanngren[1,2], Peer-Hendrik Kuhn[2,3,4], Kathryn M. Munro[5], Jenny M. Gunnersen[5,6], Hiroshi Takeshima[7], Regina Feederle[1,8,13], Iryna Voytyuk[9], Bart De Strooper[9,10,11], Mikail D. Levasseur[12], Brian J. Hrupka[12], Stephan A. Müller[1,2] and Stefan F. Lichtenthaler[1,2,3,13*]

Abstract

Background: The protease BACE1 (beta-site APP cleaving enzyme) is a major drug target in Alzheimer's disease. However, BACE1 therapeutic inhibition may cause unwanted adverse effects due to its additional functions in the nervous system, such as in myelination and neuronal connectivity. Additionally, recent proteomic studies investigating BACE1 inhibition in cell lines and cultured murine neurons identified a wider range of neuronal membrane proteins as potential BACE1 substrates, including seizure protein 6 (SEZ6) and its homolog SEZ6L.

Methods and results: We generated antibodies against SEZ6 and SEZ6L and validated these proteins as BACE1 substrates in vitro and in vivo. Levels of the soluble, BACE1-cleaved ectodomain of both proteins (sSEZ6, sSEZ6L) were strongly reduced upon BACE1 inhibition in primary neurons and also in vivo in brains of BACE1-deficient mice. BACE1 inhibition increased neuronal surface levels of SEZ6 and SEZ6L as shown by cell surface biotinylation, demonstrating that BACE1 controls surface expression of both proteins. Moreover, mass spectrometric analysis revealed that the BACE1 cleavage site in SEZ6 is located in close proximity to the membrane, similar to the corresponding cleavage site in SEZ6L. Finally, an improved method was developed for the proteomic analysis of murine cerebrospinal fluid (CSF) and was applied to CSF from BACE-deficient mice. Hereby, SEZ6 and SEZ6L were validated as BACE1 substrates in vivo by strongly reduced levels in the CSF of BACE1-deficient mice.

Conclusions: This study demonstrates that SEZ6 and SEZ6L are physiological BACE1 substrates in the murine brain and suggests that sSEZ6 and sSEZ6L levels in CSF are suitable markers to monitor BACE1 inhibition in mice.

Keywords: Alzheimer's disease, BACE1, BACE2, Secretase, Neuroproteomics, Biomarker, SEZ6, SEZ6L

Background

The β-secretase BACE1 (β-site APP cleaving enzyme) is a key drug target in Alzheimer's disease (AD) [1]. BACE1 cleaves the amyloid precursor protein (APP) and thus catalyzes the first step in generation of the amyloid β peptide (Aβ) [2–5], which has a critical role in AD pathogenesis [6]. BACE1 is highly expressed in the nervous system and contributes to additional physiological processes besides its role in AD, e.g. through neuregulin-1 cleavage in myelination and CHL1 cleavage in axon targeting [7–12]. Moreover, several phenotypic changes were described in BACE1-/- mice, such as epileptic seizures, schizophrenic symptoms, increased mortality and altered insulin metabolism, but most of the BACE1 substrates contributing to these phenotypes still need to be determined [13]. Their identification and validation would also allow the estimation of potential liabilities of BACE inhibitors in AD clinical trials and the use of BACE1 substrate cleavage products, in addition to Aβ, as possible companion diagnostics to monitor BACE1 inhibition in animals and patients.

More than 40 substrate candidates for BACE1 were identified in recent proteomic studies in murine neurons or cerebrospinal fluid (CSF), but only a few of them have

* Correspondence: stefan.lichtenthaler@dzne.de
[1]German Center for Neurodegenerative Diseases (DZNE), Munich, Germany
[2]Neuroproteomics, Klinikum rechts der Isar, Technische Universität München, Munich, Germany
Full list of author information is available at the end of the article

been validated to date with functional or in vitro assays, including L1, CHL1, ENPP5 and PTPRN2 [12, 14–16].

The three members of the seizure protein 6 (SEZ6) family, namely SEZ6, SEZ6-like (SEZ6L) and SEZ6-like 2 (SEZ6L2) have been identified as candidate BACE1 substrates in different studies [15, 17], but have not yet been validated in detail. The SEZ6 family controls synaptic connectivity and motor coordination in mice [18, 19], but little is known about the functions of these proteins at the molecular level. How BACE1-cleavage influences the function of SEZ6 and SEZ6L has not been investigated so far.

Interestingly, several of the identified BACE1 substrate candidates were also found to be cleaved by other proteases. As a result, substrate cleavage was only partly blocked upon BACE1 inhibition or BACE1-deficiency [14, 15], limiting the use of these substrates or their cleavage products as potential biomarkers to monitor BACE1 inhibition in vivo. In contrast, the two type I membrane proteins SEZ6 and its homolog SEZ6L appeared to be almost exclusively cleaved by BACE1 in neurons [15], making them potential biomarkers for BACE activity in vivo. The third family member, SEZ6L2, appeared to be mostly cleaved by proteases other than BACE1 [15, 17]. After the proteomic identification of SEZ6 as a BACE1 substrate candidate, SEZ6 was also shown to undergo reduced cleavage in BACE1-/- mouse brains [15]. However, the proteomic data for SEZ6L have not been validated by other methods and another proteomic study using pancreatic cells and tissue failed to confirm SEZ6L as a BACE1 substrate. Instead, that study demonstrated that SEZ6L is cleaved by the BACE1-homolog BACE2 in pancreas [17].

To resolve whether SEZ6 and SEZ6L are *bona fide* BACE1 substrates in brain, we generated monoclonal antibodies against both proteins and validated SEZ6 and SEZ6L as BACE1 substrates in murine neurons and brain. Additionally, SEZ6 and SEZ6L levels at the neuronal surface were controlled by BACE1, as demonstrated by cell surface biotinylation. Finally, we used a whole proteome analysis of CSF from BACE-deficient mice and found that the soluble ectodomains of SEZ6 and SEZ6L in CSF were most strongly reduced among all BACE1 substrates identified, suggesting their use as potential biomarkers in CSF to monitor BACE1 activity in mice.

Methods

Materials

The following antibodies were used: pAb SEZ6 [18], newly generated monoclonal SEZ6 and monoclonal SEZ6L (described below), pAb SEZ6L2 (R&D Systems, AF4916), pAb SEZ6L (R&D Systems, AF4804), 3D5 (kindly provided by Robert Vassar), pAb BACE2 (Santa Cruz, sc-10049), calnexin (Enzo, Stressgen, Farmingdale, NY, USA, ADI-SPA-860), β actin (Sigma, A5316), LDLR (R&D system, AF2255), rat mAb HA 3F10 (Roche, 11867423001), Flag M2 (Sigma, F1804), anti-DYKDDDDK (Biolegend, L5), anti-V5 (ThermoFisher, R960-25), HRP coupled anti-mouse and anti-rabbit secondary (DAKO), HRP coupled anti-goat, anti-rat and anti-sheep (Santa Cruz), biotinylated goat anti-rat IgG (Vector Laboratories), SULFO-TAG labelled anti-sheep (MSD, R32AI-1). The following reagents and media were used: neurobasal medium, HBSS and B27 (Invitrogen), C3 (β-secretase inhibitor IV; Calbiochem, 565788, final concentration 2 μM), DAPT (D5942 Sigma, final concentration 1 μM), ON-TARGETplus Bace2 siRNA SMARTpool, ON-TARGETplus Non-targeting Pool (Dharmacon, L-040326-00-0005 and D-001810-10-05, respectively), FlexiTube GeneSolution siRNA for Bace1 and AllStars Negative Control siRNA (Qiagen, GS23821 and SI03650318, respectively).

Mouse strains

The following mice were used in this study: wild type (WT) C57BL/6NCrl (Charles River), BACE1-/- (Jackson Laboratory, strain B6.129- Bace1tm1Pcw/J, BACE1 KO), SEZ6-/- (SEZ6 KO) [18], SEZ6 family triple knockout (TKO) mice lacking SEZ6, SEZ6L and SEZ6L2 [19] and SEZ6L2-/- (SEZ6L2 KO, bred from SEZ6 family TKO [19]). For the CSF experiments the following mice were used: WT, single BACE1-/- (BACE1 KO), single BACE2-/- (BACE2 KO), double BACE1-/- BACE2-/- (BACE DKO) knockout mice [20]. All mice were on a C57BL/6 background and were maintained on a 12/12 h light-dark cycle with food and water *ad libitum*.

Antibody production in rat

Monoclonal antibodies against murine SEZ6 (clone 14E5, IgG1) and murine SEZ6L (clone 21D9, IgG2a) were generated using standard procedures [21]. Briefly, a cDNA (HIS-mmSEZ6-HIS) was generated encoding murine (*mus musculus*) SEZ6 ectodomain (mmSEZ6, aa: 29-869, lacking the endogenous signal peptide) with an N- and C-terminal HIS tag, fused to an N-terminal CD5 signal peptide. The CD5 signal peptide allows for efficient secretion of the recombinant protein and is removed upon expression by signal peptidase, yielding HIS-mmSEZ6-HIS. The other cDNA (mmSEZ6L-1xStrepII) encoded murine SEZ6L ectodomain with its endogenous signal peptide (mmSEZ6L, aa: 1-812) and a C-terminal 1xStrepII tag. cDNA constructs were expressed in HEK293T cells and recombinant proteins were purified from the supernatant and used for immunization of rats.

Immunohistochemistry

DAB immunostaining: Brains from 4 % paraformaldehyde perfusion-fixed SEZ6 TKO ($n = 4$) and WT ($n = 7$) adult mice were cryosectioned and underwent sequential incubation in BLOXALL (Vector Laboratories), 4 % Bovine Serum Albumin (BSA, Sigma Aldrich) and 0.1 %

Triton X-100 (Sigma Aldrich) in phosphate buffered saline (PBS), and avidin/biotin (Avidin/Biotin Blocking Kit, Vector Laboratories). Sections were incubated overnight with monoclonal rat anti-SEZ6 or SEZ6L primary antibodies diluted in 2 % BSA and 0.3 % Triton X-100 in PBS. Sections were washed with PBS, incubated with biotinylated goat anti-rat IgG (Vector Laboratories) and processed using the VECTASTAIN ABC Kit (Vector Laboratories) and ImmPACT DAB peroxidase substrate as chromogen (Vector Laboratories) according to manufacturer's instructions. Some sections were counterstained with haematoxylin. Primary or secondary antibodies were omitted on sections in each experiment to confirm staining specificity. Low power images were acquired on a Mirax slide scanner and high power images were acquired at 63× magnification on a Zeiss Axio microscope.

Molecular biology

pcDNA3.1/HA-SLIC-Flag-mmSEZ6 was generated cloning full-length *Mus musculus* SEZ6, transcript variant 1 (Uniprot Q7TSK2-1) without signal peptide in pcDNA3.1 vector using Gibson assembly protocol as previously described [14]. The signal peptide of SEZ6 was replaced by the CD5 signal peptide, followed by a short tag resulting from sequence and ligase independent cloning (SLIC) [22], and an HA tag (YPYDVPDYA). A FLAG tag (DYKDDDDK) was cloned to the C terminus of the protein. pcDNA3.1/HA-SLIC-Flag-empty was used as control. pcDNA3.1/Flag-V5-hSEZ6-HA was generated cloning full-length *Homo sapiens* SEZ6, transcript variant 1 (Uniprot Q53EL9-1) into pcDNA3.1 vector. Following the endogenous signaling peptide, a Flag and V5 (PIPNPLLGLDST) tag were inserted, separated by a 10 amino acid glycine/serine linker sequence. An HA tag was cloned to the C terminus of the protein.

Transfection and stable line generation

HEK293T stably expressing pcDNA3.1/HA-SLIC-Flag-mmSEZ6 or pcDNA3.1/HA- SLIC-Flag-empty as control were generated and cultured as previously described [14]. Cells were seeded in plates coated with Poly-D-lysine (Sigma, P6407). After 24 h medium was replaced with fresh medium supplemented with either C3, DAPT or DMSO as control. Collection of supernatants and cell lysates (described below) was done after 24 h. MIN6 were cultured in the same conditions, supplementing the medium with 2 mM L-glutamine and 50 μM β-mercaptoethanol (all from Invitrogen). Cells were transfected with 10 nM of BACE1, BACE2 and respective control siRNA using Lipofectamine RNAiMAX (Invitrogen, 13778-150), according to manufacturer's instructions. Forty-eight hours post transfection, medium was replaced and cells were incubated for 24 h before collection of supernatants and cell lysis.

For drug inhibition studies, MIN6 cells were transfected with pcDNA3.1/Flag-V5-hSEZ6-HA as described above. Stable cell lines were generated using Geneticin (Gibco) selection pressure (800 μg/ml). MIN6 cells stably expressing Flag-V5-SEZ6 were seeded at a concentration of 300,000 cells/well in Falcon 24-well tissue culture plates (Corning, 353047). After 72 h, the medium was removed and replaced with fresh medium containing BACE inhibitors. Cells were treated with a nonselective BACE inhibitor (Compound A: (4aR,6R,8aS)-8a-(2,4-difluorophenyl)-6-(3-methylisoxazol-5-yl)-4a,5,6,8-tetrahydro-4H-pyrano[3,4-d] [1, 3] thiazin-2-amine [23], and 2 BACE1-selective inhibitors (Compound B: (5S)-2-amino-5-(2,6-diethyl-4-pyridyl)-3-methyl-5-(3-pyrimidin-5-ylphenyl)imidazol-4-one (AZD3839) [24] or Compound C: (5S)-2-amino-5-(2,6-diethyl-4-pyridyl)-3-methyl-5-(3-pyrimidin-5-ylphenyl)imidazol-4-one [25]. After 24 h of drug incubation, medium was removed, centrifuged to remove floating cells/cell debris (4000xg, 10 min), and analyzed for soluble shed Flag-V5-hSEZ6 as described below. For evaluation of endogenous SEZ6L shedding, wild-type MIN6 cells were seeded as above, and medium was replaced with drug-containing Opti-MEM (Gibco). After 24 h of drug exposure, Opti-MEM was removed and centrifuged to remove cell debris.

Cellular Aβ assay

Cellular activity was assessed using the human SK-N-BE(2) neuroblastoma cell line expressing the wild-type amyloid precursor protein (hAPP695). BACE inhibitors described above were diluted and added to the cells, incubated for 18 h, and then measurements of Aβ42 were taken. Aβ42 was measured by a sandwich αlisa assay using biotinylated antibody (AbN/25) attached to streptavidin-coated beads and antibody (cAb42/26) conjugated acceptor beads. In the presence of Aβ42, the beads come into close proximity. The excitation of the donor beads provokes the release of singlet oxygen molecules that triggers a cascade of energy transfer in the acceptor beads, resulting in light emission. Aβ42 was quantified on an EnVision Multimode plate reader (Perkin Elmer) with excitation at 650 nm and emission at 615 nm.

Enzymatic BACE1 and BACE2 assay

Primary BACE1 and BACE2 enzymatic activity was assessed by a FRET assay using an amyloid precursor protein (APP) derived 13 amino acids peptide contain the "Swedish" Lys-Met/Asn-Leu mutation of the APP β-secretase cleavage site as a substrate (Bachem, M-2465) and soluble BACE1(1 – 454) (Aurigene, Custom made) or soluble BACE2 (Enzo, BML-SE550). The APP peptide substrate (Mca-SEVNLDAEFRL(Dnp)RR-NH_2) contains two fluorophores: 1) (7-methoxycoumarin-4-yl) acetic

acid (Mca), a fluorescent donor with excitation wavelength at 320 nm and emission at 405 nm and, 2) 2,4-dinitrophenyl (Dnp), a proprietary quencher acceptor. An increase in fluorescence is linearly related to the rate of proteolysis. BACE1 or BACE2 were incubated with substrate and the inhibitor for 120 min in a 384-well plate. The amount of proteolysis is measured by fluorescence measurement in the Fluoroskan microplate fluorometer (Thermo Scientific). For the low control, no enzyme was added to the reaction mixture.

Mesoscale (MSD) detection of sFlag-V5-SEZ6 and sSEZ6L

Detection of Flag-V5-SEZ6 and SEZ6L was done in Mesoscale Discovery MULTI-ARRAY 96-well plates (L15XA-3 or L15XB-3 respectively). sFlag-V5-SEZ6 was quantified using anti-DYKDDDDK Tag capture antibody (L5, Biolegend, 10 μg/ml), mouse monoclonal anti-V5 Epitope Tag detection antibody (R960-25, ThermoFisher, 1:20000 dilution) and SULFO-TAG labeled Protein A (1:4000 dilution) for anti-mouse quantification. SEZ6L was quantified by coating 30 μl of Opti-MEM medium diluted 1:25 in PBS to MSD High Bind plates overnight at 4 °C, followed by detection with 25 μl of R&D System anti-SEZ6L (AF4804, 2 μg/ml) and SULFO-TAG labeled Anti-Sheep antibody (MSD, R32AI-1, 1 μg/ml). For both assays, blocking and antibody dilutions were done in 0.1 % Blocker™ Casein (ThermoFisher) in PBS. Detection was done using 2× concentration of Read Buffer T (MSD, R92TC-1). Data were transformed to 0–100 % activity based on low controls (2.5 μM nonselective BACE inhibitor with nM potency) and high controls (0.02 % DMSO) within the same plate. IC50s were calculated in Graphpad Prism using the four parameter variable slope nonlinear fit model. All curves are based on biological replicates with at least two technical replicates.

Isolation of primary neurons

Neurons from WT mice were isolated at E15/E16 and cultured as described previously [26]. After 5 days in vitro (DIV), neurons were washed with PBS and medium was replaced with fresh neurobasal supplemented with C3 or DMSO as control. After 48 h (7 DIV), supernatants from neurons were collected and cells were lysed.

Cell lysate preparation

Supernatants from neurons, HEK293T and MIN6 cells were collected and cells were lysed as described previously [14]. Protein concentrations were quantified with an BCA assay (Uptima Interchim, UP95425) and 15–20 μg of total neuronal lysate, 8–10 μg of HEK293T lysate and 15–20 μg of MIN6 lysate were used for Western Blot analysis.

Brain fractionation

Brains were isolated from P7 BACE1 KO mice and WT littermates. SEZ6 KO, SEZ6L2 KO and SEZ6 TKO and WT brains were collected from 4 to 5 month old male mice. All brains were processed as previously described [15]. Protein concentrations were quantified with an BCA assay (Uptima Interchim, UP95425) and 15–20 μg of total protein were used for Western Blot analysis.

Murine CSF sampling

CSF was extracted from single BACE1 KO, BACE2 KO, BACE DKO mice and WT controls according to a previously described protocol [27]. CSF was put into a 0.5 ml LoBind tube (Eppendorf), centrifuged for 5 min at 800 × g, and transferred to a fresh tube and frozen at −80 °C. For mass spectrometric analysis 7 WT and 7 BACE DKO were sampled and 5 μl of each CSF sample was used. Immunoblots for the analysis of murine CSF were performed using 5 or 4 μl of CSF.

Western blot analysis

Samples were boiled for 5 min at 95 °C in Laemmli buffer. For the detection of SEZ6L, Laemmli buffer without disulfide bridge reducing agents such as β-mercaptoethanol was used. Samples were separated on 8 % SDS-polyacrylamide gels. Schägger gels were used for the detection of C-terminal fragments (16.5 % separation gel, 10 % spacer gel [28]). PVDF membranes (Millipore) were incubated with primary antibody for 1–2 h at room temperature or at 4 °C overnight. After incubation with secondary antibody at room temperature for 1 h, membranes were developed with ECL prime (GE Healthcare, RPN2232V1).

Deglycosylation assay

40 μg of neuronal lysate were treated with endoglycosidase H (Endo H, New England Biolabs, P0702), or Peptide-*N*-Glycosidase (PNGase F, New England Biolabs, P0704) according to the manufacturer's protocol. For SEZ6L, non-reducing conditions were used (denaturation buffer was with 5 % SDS but no DTT). Afterwards, the samples were separated on 8 % SDS-polyacrylamide gel.

Surface biotinylation

At 7 DIV, neurons were biotinylated with EZ-Link™ Sulfo-NHS-Biotin (ThermoFisher, 21217) according to manufacturer's protocol. Quenching was done with ammonium chloride (50 mM) and BSA (1 %) in PBS and lysis with SDS lysis buffer (50 mM Tris-HCl pH 8, 150 mM NaCl, 2 mM EDTA, 1 % SDS). RIPA buffer (10 mM Tris-HCl pH 8, 150 mM NaCl, 2 mM EDTA, 1 % Triton, 0.1 % sodium deoxycholate, 0.1 % SDS) was used to dilute the samples. After sonication, protein concentrations were quantified and 80 μg of total lysate were incubated with 25 μl of High Capacity Streptavidin Agarose Resin

(ThermoFisher, 20361), mixed overnight at 4 °C. Beads were washed in RIPA buffer and bound proteins were eluted by boiling at 95 °C in Laemmli buffer supplemented with 3 mM biotin. Eluted proteins were separated on 8 % SDS-polyacrylamide gel and Western blotting was performed.

BACE1 in vitro digestion and mass spectrometric cleavage site determination

The murine SEZ6 peptide AASLDGFYNGRSLDVAKAPAASSAL (PSL Peptide Specialty Laboratories GmbH, Germany) was resuspended in LC-MS grade water (Chromasolv, Sigma Aldrich, Germany) and 40 μg of peptide were used to determine the cleavage site. Peptides were incubated with recombinant BACE1 with or without C3 inhibitor in 50 mM sodium acetate buffer pH 4.4 from 4 to 16 h as previously described [29].

Samples from the peptide cleavage assay were analyzed by LC-MS/MS. An amount of 500 fmol with respect to the starting material of the synthetic peptide was injected. Samples were separated on a nanoLC system (EASY-nLC 1000, Proxeon – part of Thermo Scientific, US; PRSO-V1 column oven: Sonation, Germany) using an in-house packed C18 column (30 cm × 75 μm ID, ReproSil-Pur 120 C18-AQ, 1.9 μm, Dr. Maisch GmbH, Germany) with a binary gradient of water (A) and acetonitrile (B) containing 0.1 % formic acid at 50 °C column temperature and a flow of 250 nl/min (0 min, 8 % B; 25:00 min, 35 % B; 30:00 min, 95 % B; 40:00 min, 95 % B). The nanoLC was coupled online via a nanospray flex ion source (Proxeon – part of Thermo Scientific, US) to a Q-Exactive mass spectrometer (Thermo Scientific, US). The five most intense ions exceeding an intensity of 1.0×10^4 were chosen for collision induced dissociation. The dynamic exclusion was reduced to 1 s and the m/z values of the proposed cleavage products were put on an inclusion list to get high quality MS/MS spectra.

MS raw data of the peptide cleavage assay were used to check for m/z values of possible cleavage products. Quantification was done by calculating the area under the curve of cleavage products using extracted ion chromatograms. Peak areas of the synthetic peptide incubated with BACE1 were compared with the control incubations of BACE1 and C3 as well as without BACE1. The identity of cleavage products was verified by a database search against the sequence of the synthetic peptide with Maxquant [30]. Non-specific cleavage was applied to identify cleavage products by tandem MS spectra.

Mass spectrometric analysis of CSF samples

Seven WT and seven BACE DKO CSF samples were used for mass spectrometric analysis. A volume of 5 μL of CSF per sample was subjected to proteolytic digestion in 50 mM ammonium bicarbonate with 0.1 % sodium deoxycholate (Sigma Aldrich, Germany). Disulfide bonds were reduced by addition of 2 μL 10 mM dithiothreitol (Biomol, Germany). Cysteine residues were alkylated by addition of 2 μL 55 mM iodoacetamide (Sigma Aldrich, Germany). Proteolytic digestion was performed by consecutive digestion with LysC (0.1 μg; 4 h) and trypsin (0.1 μg; 16 h) at room temperature (Promega, Germany).

Samples were acidified by adding 4 μL of 8 % formic acid (Sigma Aldrich, Germany) and 150 μL of 0.1 % formic acid (Sigma Aldrich Germany). Precipitated deoxycholate was removed by centrifugation at 16,000 g for 10 min at 20 °C. Proteolytic peptides were desalted by stop and go extraction (STAGE) with C18 tips [31], dried by vacuum and dissolved in 20 μL 0.1 % formic acid.

Samples were analyzed with the same LC-MS/MS method as described for the BACE1 in vitro digestion assay with a longer gradient (0 min, 2 % B; 3:30 min, 5 % B; 137:30 min, 25 % B; 168:30 min, 35 % B; 182:30 min, 60 % B; 185 min, 95 % B; 200 min, 95 % B).

Full MS spectra were acquired at a resolution of 70,000. The top ten peptide ions exceeding an intensity of 1.5×10^4 were chosen for collision induced dissociation. Fragment ion spectra were acquired at a resolution of 17,500. A dynamic exclusion of 120 s was used for peptide fragmentation.

MS data analysis of CSF samples

The data were analyzed with Maxquant software (maxquant.org, Max-Planck Institute Munich) version 1.5.3.12 [30]. The MS data were searched against a reviewed canonical fasta database of *Mus musculus* from UniProt (download: January 26th 2016, 16758 entries). Trypsin was defined as protease. Two missed cleavages were allowed for the database search. The option first search was used to recalibrate the peptide masses within a window of 20 ppm. For the main search, peptide and peptide fragment mass tolerances were set to 4.5 and 20 ppm, respectively. Carbamidomethylation of cysteine was defined as static modification. Acetylation of the protein N-term as well as oxidation of methionine were set as variable modifications. False discovery rate for both peptides and proteins was adjusted to less than 1 % using a target and decoy approach (concatenated forward/reverse database). Only unique peptides were used for quantification. Label-free quantification (LFQ) of proteins required at least two ratio counts of unique peptides.

The LFQ intensity values were log2 transformed and a two-sided Welch's t-test was used to evaluate the significance of proteins with changed abundance between KO and WT animals. A p-value less than 5 % was set as significance threshold.

Statistical tests

Statistical differences for Western Blot experiments were determined using two-tailed Mann-Whitney test (GraphPad Prism Software, San Diego, CA, USA). In Fig. 7, one-way ANOVA followed by two-tailed Student's t-Test, was used for Western Blot quantification. Graphs show mean ± SEM.

Results

Validation of new monoclonal antibodies against SEZ6 and SEZ6L

To validate SEZ6 and SEZ6L as BACE1 substrates, rat monoclonal antibodies against both proteins were generated. They were first tested in immunoblots using membrane fractions from mouse brains. As a control, the third family member, SEZ6L2, was also analyzed, using a commercial antibody. To ensure the specificity of the immunoblot signals, brains from wild type (WT) as well as from SEZ6-/- (SEZ6 KO) or SEZ6L2-/- (SEZ6L2 KO) mice were used. As SEZ6L-/- mouse brains were not available, brains from mice lacking all three SEZ6 family members (SEZ6-/-, SEZ6L-/-, SEZ6L2-/-; triple knockout, TKO [16]) were used instead.

In WT brains the SEZ6 antibody detected a major band at 170 kDa and a band of minor intensity at 150 kDa (Fig. 1a). Importantly, both bands were absent in SEZ6 KO and TKO brains, but were clearly visible in SEZ6L2 KO brains, demonstrating the specificity of the SEZ6 antibody. Because SEZ6 has 10 predicted N-glycosylation sites [32], we next determined whether the two SEZ6 bands differ in their extent of glycosylation. In order to detect both the major and the minor band more intensively, a SEZ6 polyclonal antibody was used. Endogenous SEZ6 from neuronal lysates was deglycosylated in vitro using peptide N-glycosidase F (PNGaseF), which removes all N-linked sugars, or endoglycosidase H (EndoH), which only removes high-mannose sugars but not complex glycosylated sugars. PNGaseF induced a band shift and lowered the apparent molecular weight of both SEZ6 bands to 155 and 135 kDa, respectively (Fig. 1b). This demonstrates that SEZ6 is N-glycosylated. However, the fact that still two distinct SEZ6 bands – and not just one - were visible demonstrates that both protein forms must differ by an additional post-translational modification other than N-glycosylation. This is likely to be O-glycosylation as SEZ6 was found to be O-glycosylated in a proteomic study identifying O-glycosylated proteins [33]. Similar to PNGaseF, EndoH induced a band shift of the 150 kDa band, but did not induce a major shift of the 170 kDa band (Fig. 1b). This reveals that the 170 kDa band contains complex sugars (referred to as mature SEZ6), whereas the 150 kDa band (referred to as immature SEZ6), contains only high-mannose sugars.

The SEZ6L antibody detected one major band at 160 kDa and a very weak band at 130 kDa (Fig. 1a). Both bands were not detected in the SEZ6 TKO samples, while they showed unchanged intensity in WT, SEZ6 KO and SEZ6L2 KO brains, thus confirming the specificity of the antibody for SEZ6L. Similar to SEZ6, the major SEZ6L band at 160 kDa was complex N-glycosylated. The glycosylation was removed with PNGaseF, but not with EndoH (Fig. 1b). The 130 kDa band of SEZ6L was not consistently detected in the deglycosylation experiments, but may represent the immature form, similar to SEZ6.

As a control, SEZ6L2 expression was detected in WT and SEZ6 KO brains, but was absent in SEZ6L2 KO and SEZ6 TKO brains (Fig. 1a). Notably, in brains deficient in SEZ6 or SEZ6L2, levels of the other family members were not significantly altered (Fig. 1a), revealing that there are no compensatory changes in protein levels at least for deficiency of SEZ6 and SEZ6L2.

Taken together, these results demonstrate that SEZ6 and SEZ6L are N-glycosylated proteins and that the newly generated antibodies specifically detect endogenous SEZ6 and SEZ6L.

In WT adult mouse brains SEZ6 protein was localized to a number of brain regions including the neocortex and hippocampus (Fig. 1c), with particularly strong immunoreactivity in the striatum and olfactory tubercle (not shown). In the cortex SEZ6 was localized to neuronal cell bodies and processes, predominantly in layers V and VI (Fig. 1c). In the hippocampus, SEZ6 was localized to CA1 pyramidal neuron cell bodies and dendrites, CA2 and a subset of CA3 neurons, and sparsely labeled neurons in the dentate gyrus which resemble interneurons.

SEZ6 immunostaining was completely absent in SEZ6 TKO brain sections (Fig. 1c) and in SEZ6 KO brain sections (data not shown).

Similarly, SEZ6L immunoreactivity (Fig. 1d) appeared strong in the neocortex and hippocampus, and protein localization in these areas was consistent with SEZ6L mRNA expression in the Allen Mouse Brain Atlas [34]. SEZ6L localized to pyramidal neurons throughout the cortex, particularly the apical dendrites (Fig. 1d), and appeared relatively lower in layer IV and VI. All regions of the hippocampus displayed immunoreactivity for SEZ6L (Fig. 1d) although staining was less prominent in neuronal soma than the SEZ6 staining (Fig. 1c). SEZ6L staining was observed in other brain regions including the cerebellum and septal nuclei (data not shown). SEZL6 immunostaining was completely absent in SEZ6 TKO brain sections (Fig. 1d).

Taken together, the newly generated antibodies specifically detect endogenous SEZ6 and SEZ6L by immunohistochemistry as well as Western Blot.

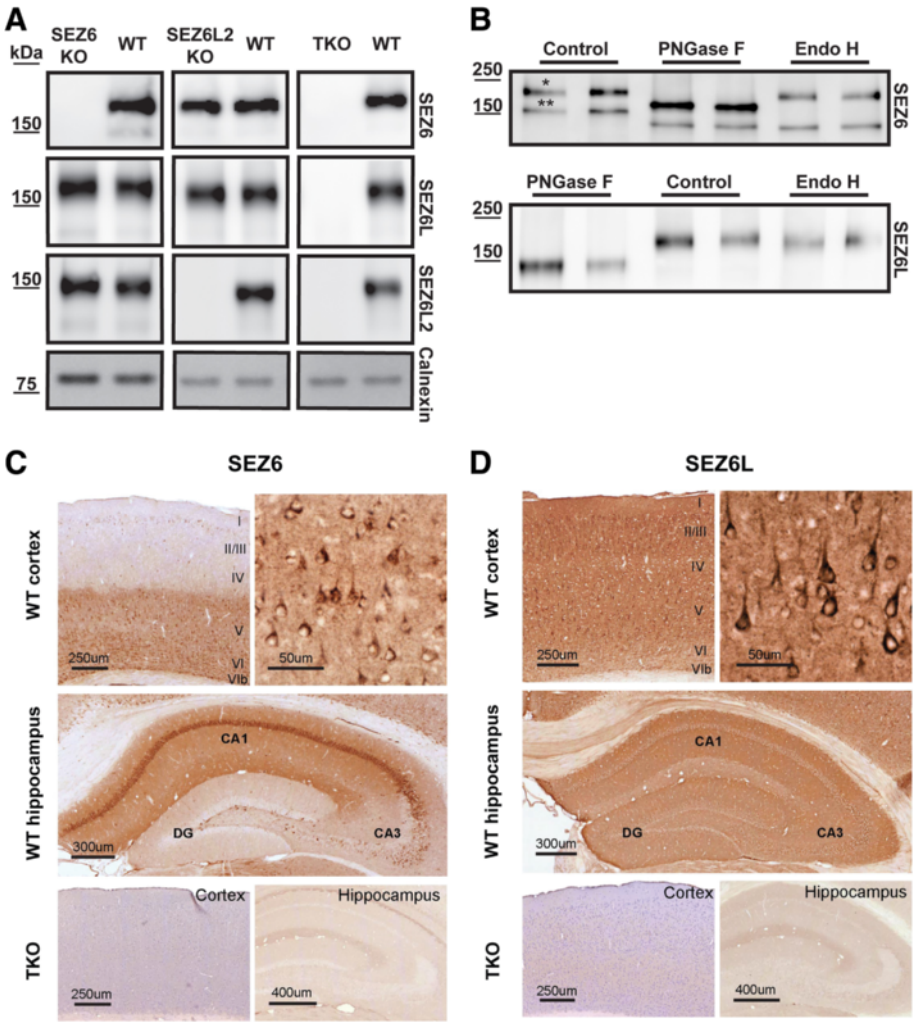

Fig. 1 Specificity of SEZ6 and SEZ6L monoclonal antibodies. **a** Membranes from mouse brains were probed with the indicated antibodies against SEZ6, SEZ6L, SEZ6L2 or calnexin. Brains were collected from wild type (WT), SEZ6-/- (SEZ6 KO), SEZ6L2-/- (SEZ6L2 KO) or triple knock-out (TKO) mice lacking SEZ6, SEZ6L and SEZ6L2. **b** Lysates from primary neurons were treated with peptide N-glycosidase F (PNGaseF) or endoglycosidase H (EndoH) and blotted for SEZ6 and SEZ6L. For SEZ6, a polyclonal antibody was used in the deglycosylation experiment. * indicates mature SEZ6, ** indicates immature SEZ6. **c**, **d** Immunohistochemistry of TKO and WT brains using antibody against SEZ6 (**c**) or SEZ6L (**d**)

BACE1 cleavage of SEZ6 and SEZ6L in primary neurons and mouse brain

As a result of BACE1 cleavage, the soluble ectodomains of SEZ6 and SEZ6L (sSEZ6 and sSEZ6L) should be shed into the conditioned medium of primary neurons and into the extracellular space in mouse brains (Fig. 2a). However, when BACE1 is inhibited or deleted, sSEZ6 and sSEZ6L might be absent or strongly reduced. In fact, treatment of primary neurons with the established BACE1 inhibitor C3 (also known as BACE1 inhibitor IV) [35] strongly reduced sSEZ6L levels compared to the control treatment with a concomitant moderate increase of full-length SEZ6L levels in the cell lysate (Fig. 2b). Likewise, in P7 BACE1 KO mouse brains sSEZ6L was strongly reduced in the diethylamine soluble DEA brain fraction, while full-length SEZ6L was increased in the membrane fraction (Fig. 2c). In agreement with our previous study on SEZ6 [15], similar results were obtained for sSEZ6 and full-length SEZ6 both in C3-treated neurons and in BACE1 KO mouse brains (Fig. 2b and c). Taken together, these results reveal that ectodomain shedding of sSEZ6 and sSEZ6L requires BACE1 activity both in primary neurons and in mouse brains.

BACE1 cleavage of SEZ6 and SEZ6L in pancreatic MIN6 cells

A previous proteomic study showed that SEZ6L was cleaved by BACE2, but not by BACE1 in the pancreatic β-cell line MIN6 [17], which is different from our findings in neurons and brain. SEZ6 was not detected in that study. To investigate whether the same differences can

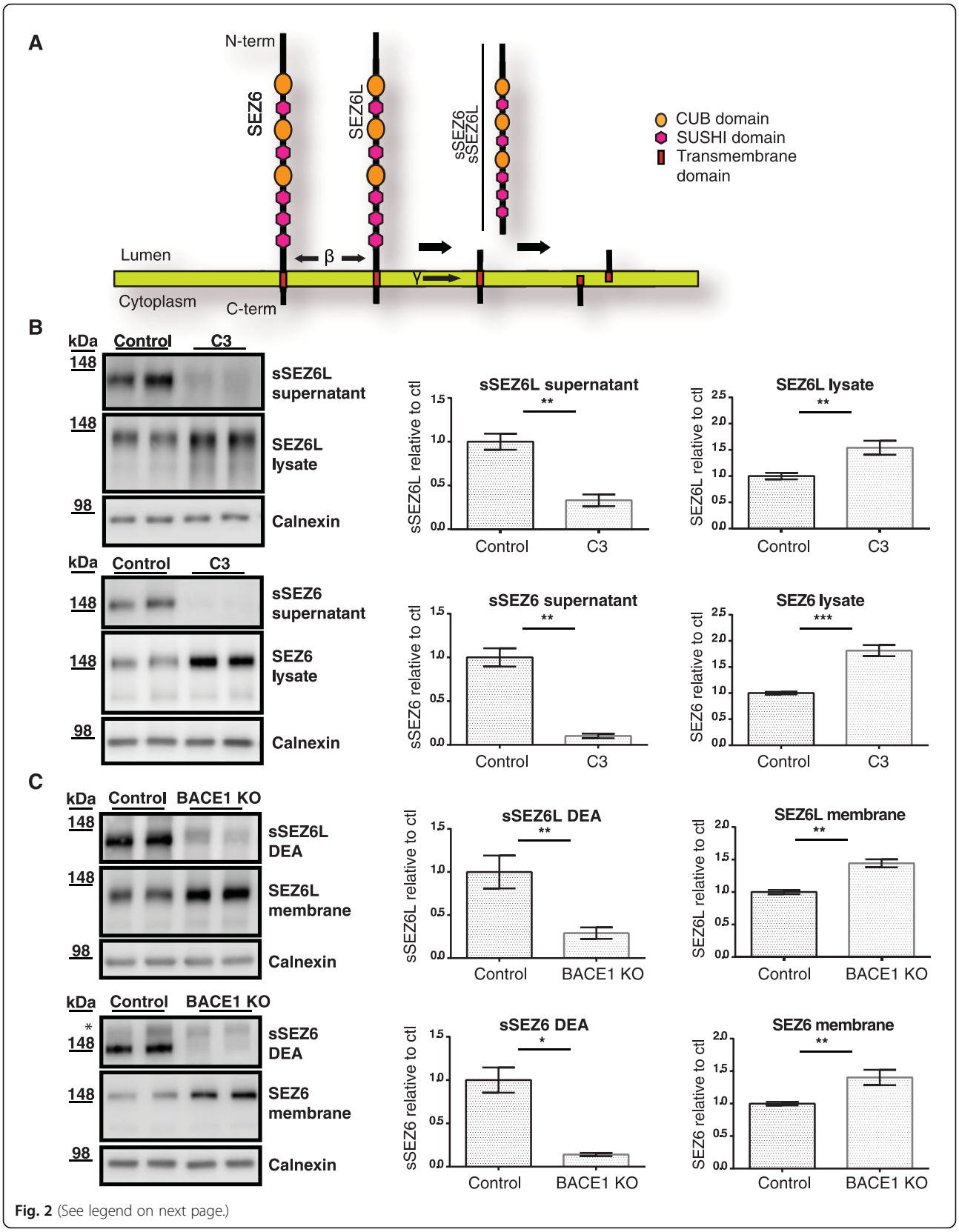

Fig. 2 (See legend on next page.)

(See figure on previous page.)
Fig. 2 BACE1 is required for SEZ6 and SEZ6L shedding in primary neurons and mouse brain. **a** Schematic diagram of SEZ6 and SEZ6L domain structure and proposed proteolytic processing. **b** Detection of soluble SEZ6 and SEZ6L ectodomains (sSEZ6 and sSEZ6L) and full-length SEZ6 and SEZ6L in neuronal supernatant and lysate upon C3 treatment. **c** Detection of sSEZ6 and sSEZ6L and full-length SEZ6 and SEZ6L in BACE1 KO and WT brains. Brains were separated into soluble fraction (DEA) and membranes (membrane). Note that in this figure, a different molecular weight marker has been used compared to Fig. 1. The 148 kDa band corresponds to the band detected at 170 kDa in Fig. 1. The upper band in panel 2C (*) is due to unspecific signal. Densitometric quantitations of the Western blots are shown, (*; $p < 0.05$, **; $p < 0.01$, two-tailed Mann-Whitney test $n = 6$)

be observed for SEZ6, we used the same cell line MIN6 and knocked-down BACE1 or BACE2 with siRNAs (Fig. 3a). As a control, cleavage of SEZ6L was also monitored. In agreement with the previous study [17], sSEZ6L was reduced upon knock-down of BACE2, but not of BACE1. Interestingly, sSEZ6 was also not reduced upon knock-down of BACE1, but mildly reduced upon knock-down of BACE2. This shows that both SEZ6 and SEZ6L are not substrates for BACE1 in the pancreatic cell line. Full-length SEZ6 and SEZ6L levels were increased upon BACE2 knock-down, in line with the reduced cleavage of both proteins (Fig. 3a). Taken together, this demonstrates that both SEZ6 and SEZ6L are cleaved by different proteases in a tissue-specific manner. One possible scenario might be that the tissue-specificity reflects the relative amounts of BACE1 and BACE2 in different tissues. For example, BACE1 – which was the major SEZ6 and SEZ6L protease in neurons – was found to be expressed at higher levels in neurons compared to MIN6 cells (Additional file 1: Figure S1). The opposite was seen for BACE2, which was the primary protease cleaving SEZ6 and SEZ6L in MIN6 cells. This tissue- specificity is reminiscent of two other BACE1 substrates, APP and L1, which are mostly cleaved by BACE1 in neurons, but by ADAM10 in non-neuronal cells [15, 36–39].

The cleavage of SEZ6 and SEZ6L in MIN6 cells by BACE2, but not BACE1, was further evaluated using nonselective (inhibiting both BACE1 and BACE2) and BACE1-selective pharmacological inhibitors by assessing shedding of SEZ6 and SEZ6L in MIN6 cells. Because SEZ6 is expressed at low levels in MIN6 cells (Additional file 1: Figure S1), human SEZ6 tagged with an N-terminal Flag- and V5-tag (Flag-V6-hSEZ6) was mildly overexpressed in MIN6 cells. To validate the efficacy of BACE1 inhibition, Aβ42 (a BACE cleavage product of APP) was measured in the SK-N-BE(2) neuroblastoma cell model, and sFlag-V5-hSEZ6 and endogenous sSEZ6L in MIN6 cells. IC50s for the released substrate cleavage products (sFlag-V5-SEZ6 sSEZ6L) were compared with IC50s determined in enzymatic BACE1 and BACE2 assays. Cleavage of Aβ42 and sFlag-V5-SEZ6 and sSEZ6L were similar after addition of nonselective BACE inhibitor A and was consistent with equipotent inhibition of BACE1 and BACE2 in enzymatic assays. However, cleavage of sFlag-V5-SEZ6 and sSEZ6L was less impacted than Aβ42 upon inhibition with BACE1-selective inhibitors (B and C) and followed the enzymatic inhibition curves of BACE2 rather than BACE1 (Fig. 3b). This confirms the findings in Fig. 3a and demonstrates that in MIN6 cells SEZ6 and SEZ6L are predominantly cleaved by BACE2, but not by BACE1.

BACE1 inhibition increases neuronal cell surface levels of SEZ6 and SEZ6L

The deglycosylation experiment (Fig. 1b) had revealed that mature SEZ6 and SEZ6L carry complex N-linked sugars and are resistant to EndoH treatment. Complex sugars are added as proteins move through the Golgi apparatus. Thus, the mature forms of SEZ6 and SEZ6L are likely to be located in late compartments of the secretory pathway or at the plasma membrane. Indeed, using cell surface biotinylation the mature, but not the immature forms of both proteins were detected at the cell surface of primary neurons (Fig. 4). Treatment with the BACE inhibitor C3 increased full-length, mature SEZ6 and SEZ6L in whole cell lysates (Fig. 2b) and also at the cell surface (Fig. 4). As a control, surface levels of the LDL-receptor (LDLR), which is a substrate of ADAM10, but not of BACE1 [38], were not altered upon BACE inhibition. To demonstrate the specificity of the surface biotinylation, β-actin was detected in whole lysates, but strongly reduced in the pull-down of the biotinylated cell surface proteins (Fig. 4), as expected for a cytoplasmic protein. Taken together, BACE1 activity negatively controls the levels of SEZ6 and SEZ6L at the neuronal cell surface and in whole lysates.

BACE1 cleaves SEZ6 within its juxtamembrane domain

Next, we determined the cleavage site of BACE1 within the juxtamembrane domain of SEZ6 and compared it to the previously identified cleavage site within its homolog SEZ6L [15]. In the previous proteomic study which identified SEZ6 as a BACE1 substrate candidate, several tryptic peptides of the secreted SEZ6 ectodomain were identified. The most C-terminal of these peptides encompassed amino acids 894 to 904 (AASLDGFYNGR) of murine SEZ6 (Fig. 5a). This was a tryptic peptide ending with arginine (R), but BACE1 preferentially cleaves C-terminally to leucine or other hydrophobic amino acids [40]. Thus, the BACE1 cleavage site is likely to be

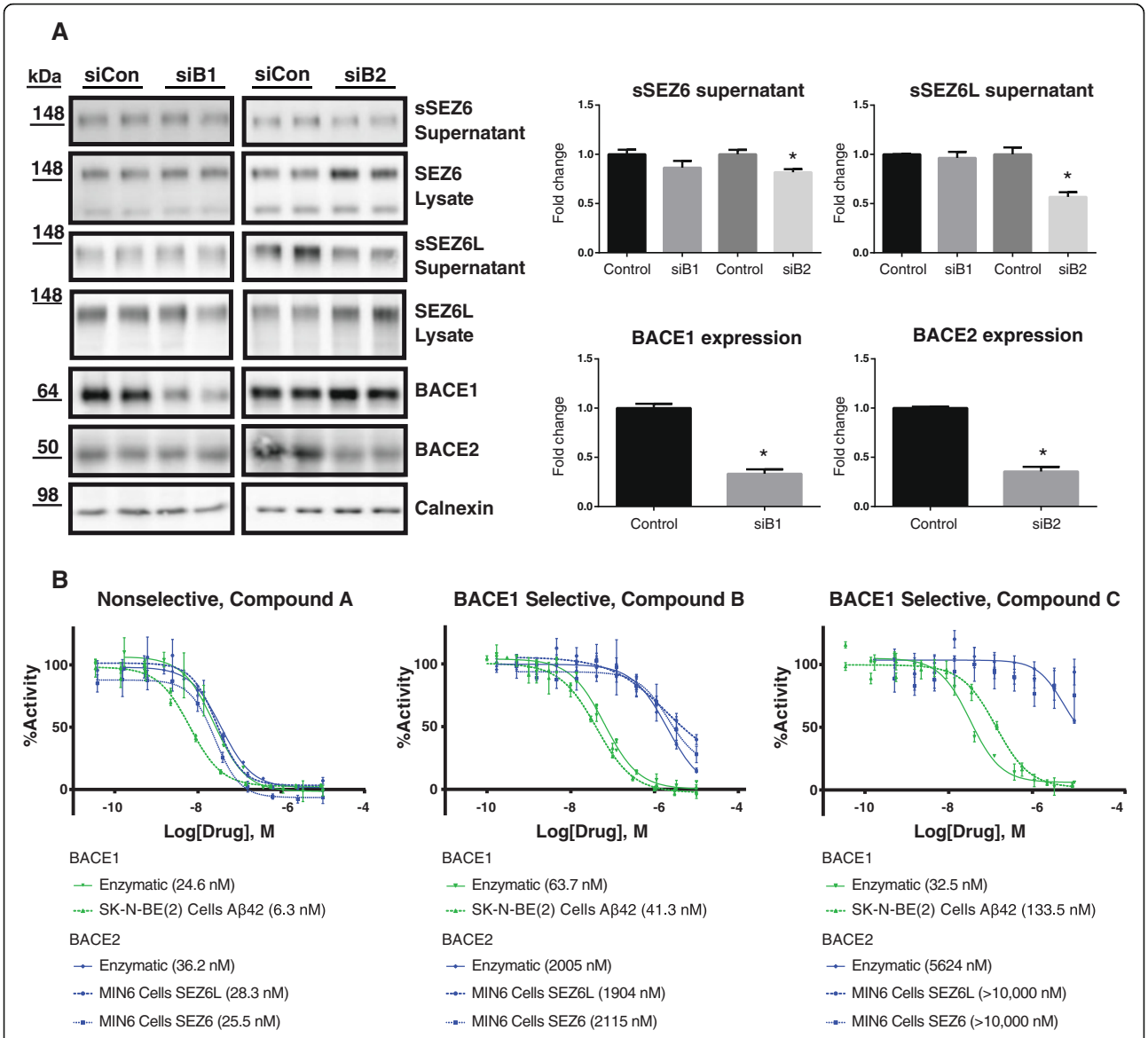

Fig. 3 BACE2 but not BACE1 cleaves SEZ6 and SEZ6L in a pancreatic β-cell line. **a** sSEZ6 and sSEZ6L were detected in the supernatant and full-length SEZ6 and SEZ6L in the lysate of the pancreatic β-cell line MIN6 upon BACE1 and BACE2 knock-down by siRNA (siB1, siB2). As a control, cells were treated with non-silencing control siRNA (siCon). Densitometric quantitations of the Western blots are shown, (*; $p < 0.05$, two-tailed Mann-Whitney test $n = 4$). **b** BACE1 (*green lines*) and BACE2 (*blue lines*) activity were quantified in enzymatic (*solid lines*) and cellular (*dotted lines*) models after pharmacological inhibition with nonselective (inhibiting both BACE1 and BACE2, compounds B and C) and BACE1-selective inhibitors (compound A). Soluble Aβ42 as well as sSEZ6 and sSEZ6L were detected in the supernatant of the neuroblastoma cell line SK-N-BE(2) or in the MIN6 respectively, as indicated. Data were standardized to low and high controls within each assay. Data represent biological duplicates with two or more technical replicates

located between this tryptic peptide and the transmembrane domain (start: leucine 923). To determine this site precisely, an in vitro peptide assay was used. The 25 amino acid peptide AASLDGFYNGRSLDVAKAPAASSAL (Fig. 5a, amino acids 894 to 918), comprising the tryptic peptide and ending shortly before the transmembrane domain, was incubated in the presence or absence of recombinant BACE1 with or without the BACE1 inhibitor C3 (Fig. 5b). Full-length peptide and cleavage fragments were separated by nano liquid chromatography and analyzed by high resolution mass spectrometry (nanoLC/MS). The non-cleaved, full-length peptide eluted from the nLC column at ~ 22 min (Fig. 5b). The correct sequence was verified by MS/MS-based fragmentation (Fig. 5c). Upon addition of BACE1, the full-length peptide levels were decreased in the chromatogram and two additional peptides with elution times of ~16 and ~21 min were detected (Fig. 5b). Addition

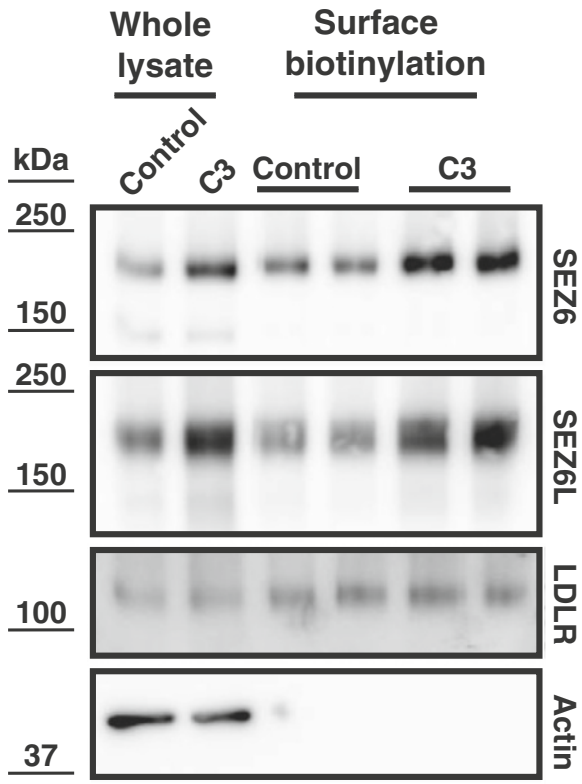

Fig. 4 BACE1 controls neuronal cell surface levels of SEZ6 and SEZ6L. Primary, murine neurons were treated with the BACE inhibitor C3 or DMSO as a control. Proteins at the surface were labeled with biotin and enriched using streptavidin pull-down. Biotinylated SEZ6 and SEZ6L were detected by immunoblot. As a control, both proteins were also detected in whole cell lysates. Note, that only the mature 170 kDa form of SEZ6 was biotinylated at the cell surface. As a control, the ADAM10 substrate LDL receptor (LDLR) did not show a change in surface levels upon C3-treatment. As a further control, the cytosolic protein actin was only detected in whole lysates, but not among the surface biotinylated proteins

of C3 inhibited the production of both peptides, demonstrating that they are BACE1 cleavage products of the full-length peptide. The two peptides were identified as AASLDGFYNGRSL (N-terminal cleavage product, Fig. 5d) and DVAKAPAASSAL (C-terminal cleavage product 2, Fig. 5e) by fragment spectra. Thus, we conclude that the BACE1 cleavage site in SEZ6 is the peptide bond between leucine906 and aspartate907 (Fig. 5a). Interestingly, this site comprises the same amino acids in the P1 and P1' position (L-D) as Swedish mutant APP (Fig. 5a), which is very efficiently cleaved by BACE1 [4]. The previously identified cleavage site in SEZ6L [15] is not identical, but similar to SEZ6, as it also has a hydrophobic amino acid in the P1 and a negatively charged amino acid in the P1' position (Fig. 5a). Moreover, SEZ6 and SEZ6L are both cleaved at a similar distance from the transmembrane domain, i.e. 16 and 14 amino acids for SEZ6 and SEZ6L, respectively (Fig. 5a).

SEZ6 is a substrate for γ-secretase

After initial BACE1 cleavage, the resulting C-terminal, membrane-bound protein fragments of several membrane proteins, including APP and SEZ6L [17], are further processed within their transmembrane domains by γ-secretase, in a process referred to as regulated intramembrane proteolysis [41] (for schematic overview see Fig. 2a). The accumulation of C-terminal fragments upon pharmacological inhibition of γ-secretase with DAPT can be used to identify γ-secretase substrates [42]. To examine if SEZ6 is also cleaved by γ-secretase, we generated a human embryonic kidney 293 (HEK293T) cell line stably expressing murine SEZ6. Due to the lack of an antibody against the SEZ6 C-terminus, the full-length SEZ6 construct was tagged with an N-terminal HA and a C-terminal FLAG epitope tag. The full-length SEZ6 in the cell lysate and the shed ectodomain (sSEZ6) in the supernatant were detected by immunoblots in the transfected cells, but not in control transfected cells (Fig. 6a). Addition of the BACE inhibitor C3 decreased the sSEZ6 (Fig. 6a), in agreement with the results in neurons (Fig. 2b). The expected C-terminal fragment arising through BACE1 cleavage was not detected in control cells without the γ-secretase inhibitor DAPT, presumably because of its fast turnover. However, γ-secretase inhibition led to a strong accumulation of the SEZ6 C-terminal fragment at a molecular weight of around 13 kDa (Fig. 6b), which is consistent with the theoretical molecular weight of about 10 kDa for the C-terminal fragment starting at the BACE1 cleavage site and ending with the C-terminal FLAG-tag. These results indicate that SEZ6 is a γ-secretase substrate.

sSEZ6 and sSEZ6L are detected in murine CSF in BACE1-dependent manner

Finally, we tested in vivo whether levels of sSEZ6 and sSEZ6L in murine CSF may be useful biomarkers for BACE1 activity in vivo. A previous proteomic study demonstrated that the soluble ectodomains of other BACE1 substrates, such as APLP1, PLXDC2 and CHL1, were reduced in the CSF of BACE1-deficient mice [14]. However, sSEZ6 and sSEZ6L were not consistently detected and could not be quantified in murine CSF, potentially because their levels were below the detection limit. Thus, we first improved the method for proteomic analysis of murine CSF in order to identify and quantify a larger number of proteins compared to the previous study. Most BACE1 inhibitors currently tested in clinical trials for AD are not specific for BACE1, but also inhibit BACE2. To mimic this situation we applied the improved proteomic method to the analysis of CSF from seven 4-month old BACE1/BACE2 double knock-out (BACE DKO) and seven age-matched WT mice.

In our previous protocol for mouse CSF proteomics, proteins were digested in the presence of urea and

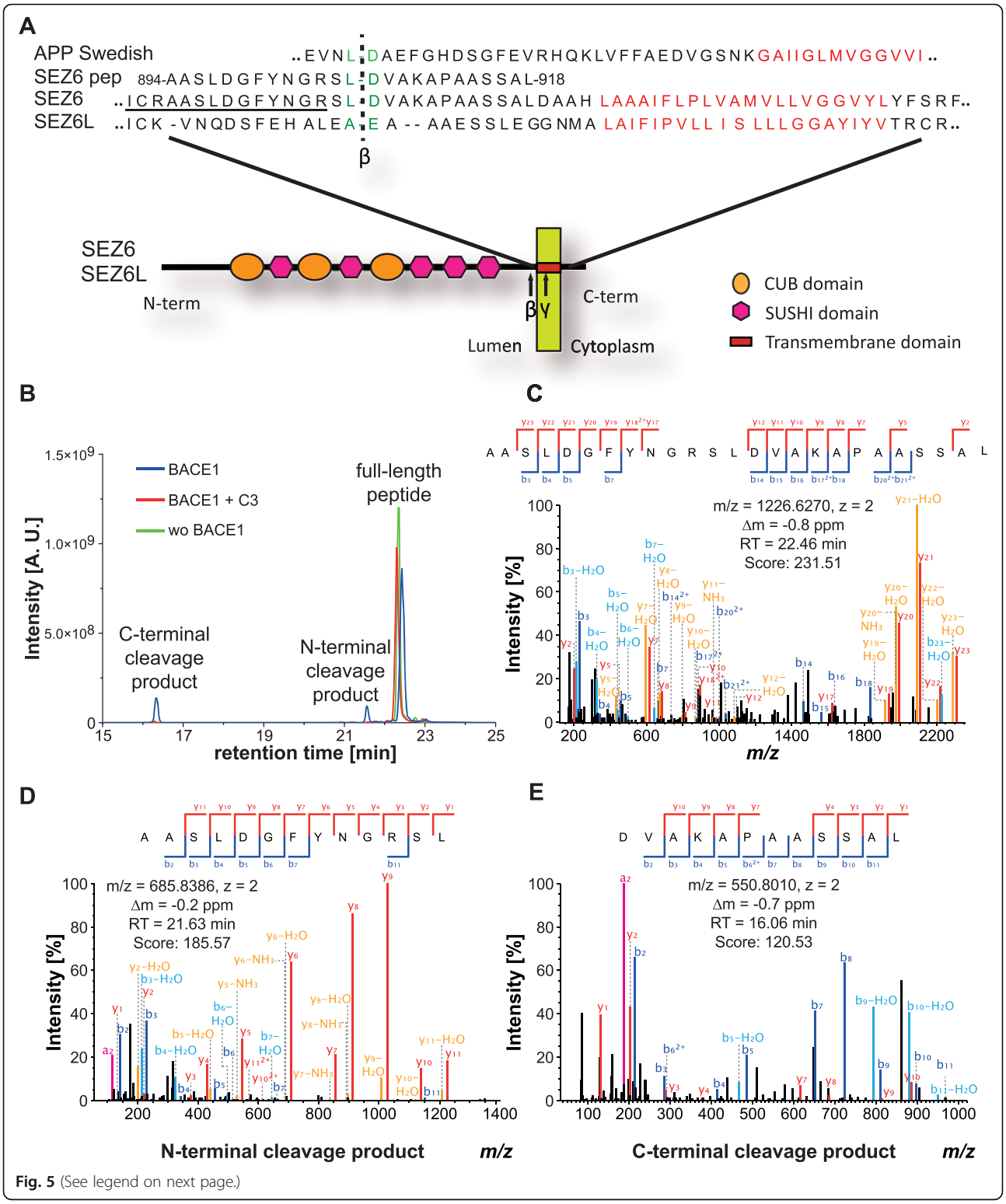

Fig. 5 (See legend on next page.)

(See figure on previous page.)
Fig. 5 Cleavage site determination of SEZ6. **a** Comparison of BACE1 cleavage sites in the known APP Swedish mutant, in SEZ6 and SEZ6L. Additionally, the peptide (SEZ6 pep) used for the in vitro assay is aligned. Numbers next to the N- and C-terminal amino acids of the peptide indicate the amino acid number within the sequence of the full-length protein. Amino acids at the cleavage site are shown in *green*. Amino acids of the transmembrane domains are in *red*. Domains of SEZ6 and SEZ6L are shown with indicated symbols. The most C-terminal tryptic peptide of the secreted SEZ6 ectodomain detected in our previous study is underlined in *black*. **b** Extracted ion chromatogram of full-length peptide incubated with BACE1, BACE1 plus C3 or without BACE1 showing the peaks of the two cleavage products as well as the full-length peptide. Identification of the full-length peptide (**c**), the N-terminal (**d**) and the C-terminal cleavage product (**e**) by fragment ion spectra. The mapped y and b fragment ions are indicated in the sequences as well as in fragment ion spectra. Neutral loss fragment ions are indicated in *light blue* for b and *orange* for y ions

thiourea [14]. We replaced these nonionic chaotropes with the mild ionic detergent sodium deoxycholate (SDC), which has been shown to improve trypsin digestion of membrane proteins [43, 44]. A concentration of 0.1 % SDC was sufficient to improve the digestion efficiency. Triplicates of a pooled mouse CSF sample were digested with either the urea or the SDC-supported digestion protocol. The number of identified unique peptides was 6.6 % lower for the SDC supported protocol (Table 1). However, digestion efficiency was strongly increased which was detected by the 58.1 % lower number of average missed cleavages per peptide (Table 1). Additionally, the average number of identified and quantified proteins was 10.3 and 7.5 % higher for the SDC supported digestion protocol, respectively. Subcellular locations of proteins quantified in all replicates of SDC or urea supported digestions were similar (Additional file 1: Figures S2 and S3). However, the number of quantified membrane proteins was 8.9 % higher for the samples digested in the presence of SDC (135 vs. 124).

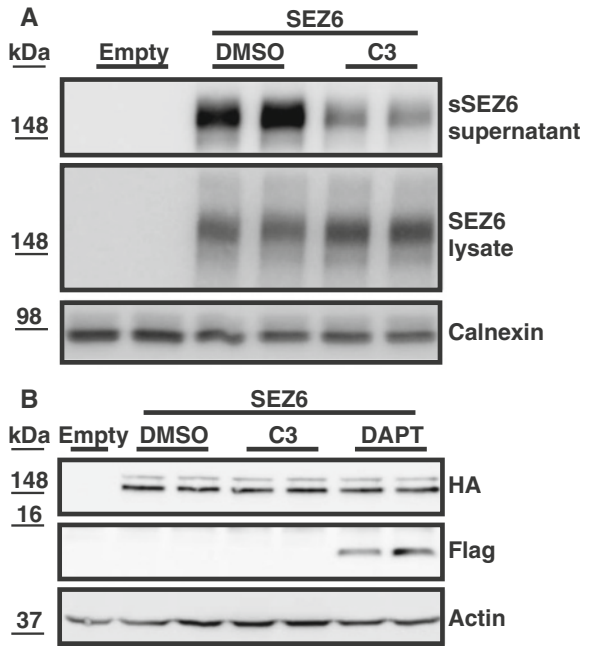

Fig. 6 SEZ6 is a substrate for γ-secretase. **a** HEK293T cells were stably transfected with empty vector (Empty) or SEZ6 expression construct with an N-terminal HA-tag and a C-terminal FLAG epitope tag. Cells were treated with C3 or DMSO as a control. sSEZ6 was detected in the cell supernatant and full-length SEZ6 in the lysate. Calnexin was used as a loading control. **b** Cells were treated with DMSO, C3 or the γ-secretase inhibitor DAPT. The C-terminal SEZ6 fragment was detected by immunoblot using an anti-FLAG-tag antibody

Next, BACE DKO CSF was compared to WT CSF. In contrast to our previous proteomic study of CSF from BACE1 deficient mice [14], we were able to quantify SEZ6 and SEZ6L with the optimized protocol (Additional file 2: Supplementary Data: proteins BACE DKO vs WT CSF). The levels of several known or proposed BACE1 substrates such as SEZ6, SEZ6L, SCN4B, LRRN1, APLP1, APLP2, CACHD1 and NLGN4L were significantly reduced in BACE DKO CSF (Fig. 7a). Among these proteins, SEZ6 (DKO/WT = 13 %, p = 5.99E-06) and SEZ6L (DKO/WT = 20 %, p = 5.10E-05) showed the strongest reduction as well as the highest statistical significance (Fig. 7a). Changes in sSEZ6 and sSEZ6L also remained significant, when applying the Benjamini-Hochberg false discovery rate adjustment (α = 5 %) to correct for multiple hypothesis testing. In contrary, the third SEZ6 family member, SEZ6L2, did not show a significantly lower abundance in BACE DKO CSF, indicating that it is mostly cleaved by protease other than BACE1 or BACE2 (Fig. 7a).

Interestingly, the interleukin-6 receptor subunit beta (IL6ST) was quantified in all WT CSF samples by four unique peptides but in none of the BACE DKO CSF samples. This indicates that IL6ST may be an additional BACE1 and/or BACE2 substrate. Another BACE substrate candidate could be the type-1 transmembrane protein hephaestin (HEPH), which was significantly reduced by 53 % in BACE DKO CSF. Hephaestin is known to be expressed in the brain [45]. Additionally, peptide sequences of transmembrane and GPI-anchored proteins

Table 1 Comparison of urea and SDC supported digestion of mouse CSF

	SDC	Urea	Difference
Unique peptides	5955.3	6376.7	−6.6 %
Average missed cleavages per peptide	0.26	0.62	−58.1 %
Protein identifications (≥2 unique peptides)	814.0	738.0	+10.3 %
Protein quantifications	847.7	788.3	+7.5 %

Values are averaged over three replicates

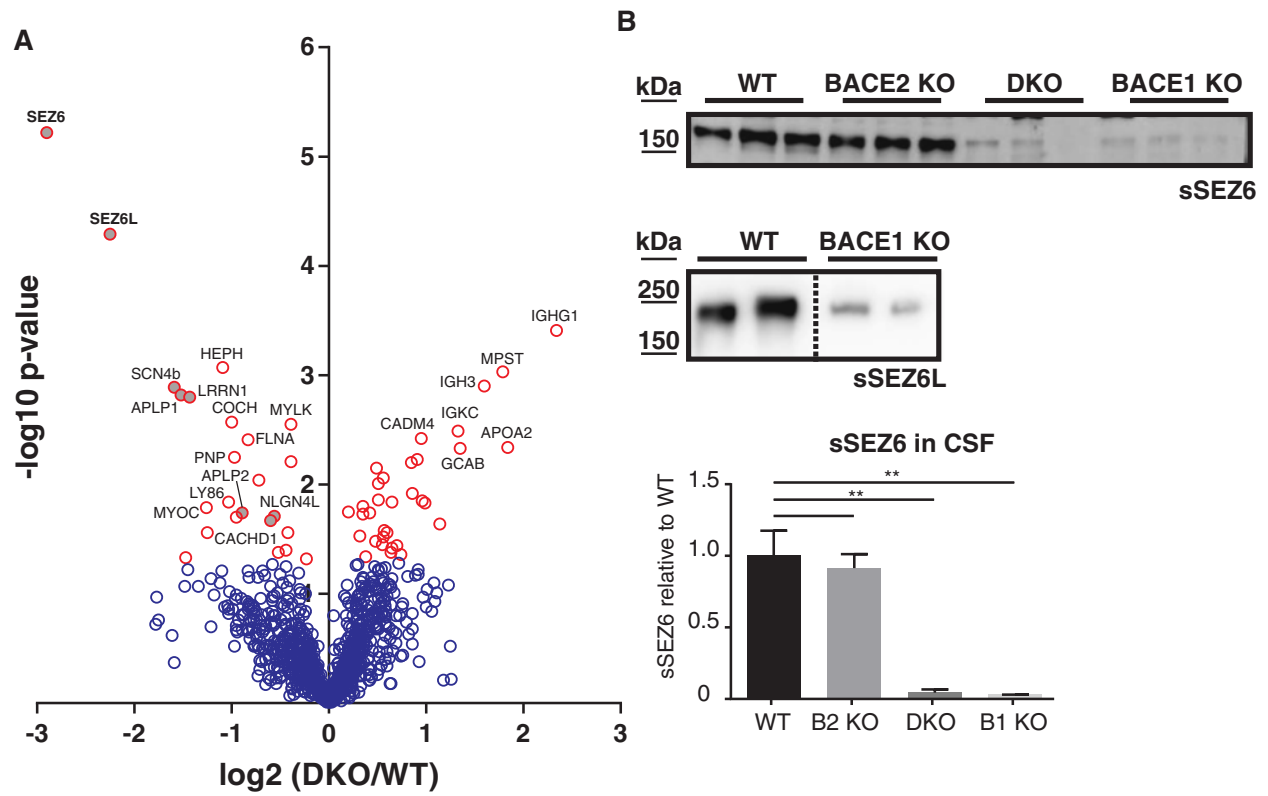

Fig. 7 Proteomic analysis of CSF from BACE DKO and WT mice. **a** Volcano plot of proteomic analysis of BACE1 and BACE2 double knockout (BACE DKO) and WT mouse CSF. The minus log10 transformed t-test *p*-values are plotted against the log2 transformed label-free quantification intensity ratios of BACE DKO and WT CSF for every relatively quantified protein. Proteins with a t-test *p*-value < 0.05 are shown as *red circles*. Already known BACE substrate candidates with a *p*-value < 0.05 are marked with *gray* filling. Proteins that remain significant after Benjamini-Hochberg false discovery rate correction (FDR < 0.05) have bold letters (SEZ6 and SEZ6L). **b** Detection of sSEZ6 and sSEZ6L in mouse CSF. Densitometric quantitation of the Western blot is shown, (**; $p < 0.01$, one-way ANOVA followed by two-tailed Student's t-Test, $n = 3$). The dotted line indicates that the samples were loaded onto the same blot, but not next to each other

were loaded into the bioinformatics software tool QARIP [46] to check for their position within the protein sequences. Peptides were almost exclusively mapped to extracellular domains of transmembrane proteins (Additional file 3: Tables S1-S6). This indicates that most transmembrane proteins in the CSF are derived from proteolytic shedding and not from contaminating cells. For SEZ6, SEZ6L and SEZ6L2 only peptides from the ectodomain were identified (Additional file 3: Table S1).

To validate the proteomic results, reduced abundance of sSEZ6 and sSEZ6L were confirmed using immunoblots of independent CSF samples (Fig. 7b). In agreement with the proteomic analysis, sSEZ6 was nearly completely absent in BACE DKO CSF. The same reduction was observed in CSF from BACE1 KO, but not for BACE2 KO mice. This demonstrates that sSEZ6 is generated specifically by BACE1, but not by BACE2 in murine CSF. Likewise, sSEZ6L was strongly reduced in BACE1 KO CSF. Taken together, these results show that sSEZ6 and sSEZ6L levels can be used to monitor BACE1 activity in murine CSF.

Discussion

BACE1 is a major drug target in AD, but has additional substrates and thus contributes to various biological processes [1, 13], which may limit its therapeutic potential. Recent proteomic studies have identified more than 40 membrane proteins as potential BACE1 substrates [14–16]. However, only few of them have been validated in vitro and in vivo. Using different techniques, our study validates SEZ6 and SEZ6L as BACE1 substrates in vitro and in vivo and demonstrates that, in contrast to other BACE1 substrates, SEZ6 and SEZ6L are nearly exclusively cleaved by BACE1 and not by other proteases in the brain. Levels of the soluble ectodomains (sSEZ6, sSEZ6L) were reduced to less than 10 % of the control levels upon pharmacological inhibition of BACE1 in primary neurons. Additionally, SEZ6 and SEZ6L were validated in vivo as BACE1 substrates using brains and CSF from BACE1 KO, BACE2 KO and/or BACE DKO mice. Thus, we propose that in addition to Aβ and sAPPβ, which are two BACE1 cleavage products of APP, sSEZ6 and sSEZ6L may be suitable as biomarkers to monitor BACE1 activity in vivo in CSF.

Several other previously identified BACE1 substrates, such as CHL1, L1, contactin-2, APP and its homolog APLP2, are not exclusively cleaved by BACE1, but also by other proteases, including ADAM10 [15, 38]. For example, the APP homolog APLP2 is cleaved to about 60 % by BACE1 and to 40 % by ADAM10 in neurons, but the percentages may strongly vary for each substrate [38]. Additionally, the different proteases may compensate for each other, if one of them is blocked. One example is APP. BACE1 inhibition increases the ADAM10 cleavage of APP, such that total APP cleavage is only mildly reduced [36, 47]. Potentially, this is also true for the third SEZ6 family member, SEZ6L2, which shows only moderately reduced shedding upon BACE1 inhibition [15]. A similar compensation does not occur for SEZ6 and SEZ6L in brain, where total cleavage was nearly completely abolished upon BACE1 inhibition. However, in other cell types and tissues both proteins may be cleaved by proteases different than BACE1. A previous study reported that in pancreatic cells SEZ6L is predominantly cleaved by BACE2, but not by BACE1 [17]. We confirm this finding and also extend it to SEZ6. Importantly, we show that neither SEZ6 nor SEZ6L are substrates for BACE1 in the pancreatic cell line, which is in contrast to brain, demonstrating that SEZ6 and SEZ6L are cleaved by different proteases in a tissue-specific manner. Precedents for such a tissue-specific proteolytic cleavage are the BACE1 substrates CHL1 and L1, which are mostly cleaved by BACE1 in the nervous system, but by ADAM proteases in non-neuronal cells [15, 37]. We found opposite expression patterns of BACE1 and BACE2 in MIN6 cells and in neurons, which correlated with the tissue-specific cleavage of SEZ6 and SEZ6L. Whether the distinct protease cleavage events also lead to a different functional outcome for the substrates remains to be investigated. This is particularly relevant as different proteases may cleave at distinct peptide bonds and thus generate ectodomains of different lengths and potentially different functions. For example, in APP the ADAM10 and BACE1 cleavage sites are 16 amino acids apart from each other and yield APP ectodomains with diverging functions [48, 49].

The molecular functions of SEZ6 and SEZ6L are not yet well understood. The name SEZ6 comes from the initial finding that SEZ6 expression was upregulated in cortical murine cells treated with the seizure-inducing drug pentylene tetrazole [32]. SEZ6 has been genetically linked to febrile seizures and epilepsy [50, 51], whereas SEZ6L was associated with bipolar disorder [52]. The extracellular regions of SEZ6/SEZ6L contain three CUB (complement subcomponent C1r, C1s /sea urchin embryonic growth factor Uegf / bone morphogenetic protein 1) and five short consensus repeat domains, which are protein-binding domains that are also found in a variety of cell surface receptors. This suggests that SEZ6/SEZ6L may act as receptors at the cell surface. Importantly, our study demonstrates that BACE1 cleavage negatively regulates SEZ6 and SEZ6L surface levels in neurons, suggesting that BACE1 may directly control SEZ6/SEZ6L surface functions. This could be a more general function of BACE1, because BACE1 also negatively regulates surface levels and/or function of two other substrates, contactin-2 and CHL1 [12, 15, 53]. However, the function of SEZ6 and SEZ6L may not only be exerted by the full-length proteins, but also by sSEZ6 and sSEZ6L or even by the C-terminal fragments resulting from BACE1 cleavage, as recently found for the BACE1 substrate CHL1 [12].

Future studies need to address how exactly BACE1 alters SEZ6 and SEZ6L function and whether such alterations contribute to the multiple phenotypes observed in BACE1-deficient mice. Notably, both BACE1- and SEZ6-deficient mice have deficits in hippocampal learning paradigms [18, 54–56] and in motor coordination [18, 57]. Moreover, both mouse lines appear to have reduced levels of anxiety and/or cognitive deficits [18, 56], reduced glutamatergic synapse function and reduced dendritic spine densities [18, 58]. Given the substantial overlap, at least some of these phenotypes may result from the reduced cleavage products of SEZ6/SEZ6L.

Another major outcome of our study is an improved protocol for efficient proteomic analysis of murine CSF. While human CSF is available in milliliter quantities, only approximately 10 μl of murine CSF are obtainable. Here, we improved the digestion efficiency of murine CSF in comparison to our previous protocol by using 0.1 % SDC in 50 mM ammonium bicarbonate as digestion buffer. This was demonstrated by the strong reduction of the average missed cleavages per peptide as well as the increased number of identified and quantified proteins (Table 1). The improved method may be of wide relevance for studying murine CSF in the context of different neurological and neurodegenerative diseases. Importantly, the new workflow allowed the quantification of SEZ6 and SEZ6L, which were not quantified in the previous study [14]. The nearly complete absence of sSEZ6 and sSEZ6L in murine CSF makes both cleavage products suitable markers to monitor BACE1 inhibition in mice. This may be particularly useful for determining the target engagement and potential side effects of BACE inhibitors in animal models. If confirmed in human CSF, sSEZ6 and sSEZ6L may even be useful as companion diagnostics to guide BACE inhibitor dosing in individual patients and monitor BACE1 inhibitor selectivity.

Conclusions

We demonstrate that SEZ6 and SEZ6L are physiological BACE1 substrates in the murine brain and that, in

contrast to most other BACE1 substrates, these two proteins are nearly exclusively cleaved by BACE1. Levels of sSEZ6 and sSEZ6L were strongly reduced upon pharmacological inhibition or genetic deficiency of BACE1 in primary neurons and mouse brain. Additionally, we developed an improved method for whole proteome analysis of murine CSF and found that in the CSF of BACE DKO mice the soluble ectodomains of SEZ6 and SEZ6L were most strongly reduced among all BACE1 substrates identified, suggesting their use as potential biomarkers in CSF to monitor BACE1 activity in vivo in mice.

Additional files

Additional file 1: Figure S1. Comparison of BACE1 and BACE2 expression in MIN6 and WT primary neurons; **Figure S2**. UniProt subcellular location of proteins quantified in 3 out of 3 replicates of urea and SDC supported digestion; **Figure S3**. Sub-classification of membrane proteins quantified in three out of three replicates of urea and SDC supported digestion. (PDF 243 kb)

Additional file 2: Supplementary Data. Proteins and peptides identified and quantified in BACE DKO and WT CSF. This file contains four sheets, the first one of which contains the list and quantification of all proteins identified in the CSF. (XLSX 17716 kb)

Additional file 3: Tables S1-S6. They contain the proteins and peptides identified in BACE DKO and WT CSF. (PDF 918 kb)

Abbreviations

AD: Alzheimer's disease; APP: Amyloid precursor protein; Aβ: Amyloid β peptide; BACE1: β-site APP cleaving enzyme; BSA: Bovine Serum Albumin; CSF: Cerebrospinal fluid; DIV: Days in vitro; Endo H: Endoglycosidase H; HEK293T: Human embryonic kidney 293; HEPH: Hephaestin; IL6ST: Interleukin-6 receptor subunit beta; KO: Knock out; LDLR: LDL-receptor; LFQ: Label-free quantification; MSD: Mesoscale discovery; PBS: Phosphate buffered saline; PNGase F: Peptide-N-Glycosidase; SDC: Sodium deoxycholate; SEZ6: Seizure protein 6; SEZ6L: SEZ6-like; SEZ6L2: SEZ6-like 2; SLIC: Ligase independent cloning; sSEZ6, sSEZ6L: Soluble SEZ6 and SEZ6L; WT: Wild type

Acknowledgement

The authors thank M. Haseldonck and H. Borghys for providing CSF material.

Funding

We are grateful for financial support by the BMBF (JPND-RiModFTD), the Agency for Innovation by Science and Technology (IWT), the DFG (FOR2290), the Center of Excellence in Neurodegeneration CoEN), the Alzheimer Research Price of the Breuer Foundation, the Swedish Society of Medicine and the Swedish Society for Medical Research, the National Health and Medical Research Council (NHMRC) and the German Academic Exchange Service (DAAD).

Availability of data and materials

Data supporting the conclusions are included within the article and its additional files.

Authors' contributions

MP, JW, PHK, KMM, IV, MDL, SAM collected the samples, performed the experiments and analyzed the data. JMG, BDS, BJH supervised the analysis and participated in the drafting of the manuscript. HT and RF provided reagents. SFL designed the study and wrote the manuscript. All authors read and approved the final manuscript.

Competing interests

MDL and BJH are employees of Janssen Pharmaceuticals. The authors declare that they have no competing interests.

Consent for publication

Not applicable.

Ethics approval and consent to participate

All animal procedures were carried out in accordance with either the European Communities Council Directive (86/609/EEC) or Australian Code of Practice for the Care and Use of Animals for Scientific Purposes. Animal protocols were approved by the Ludwigs-Maximilians-University Munich and the government of Upper Bavaria, or ethics committee of the University of Leuven, or alternatively the Anatomy & Neuroscience, Pathology, Pharmacology, and Physiology Animal Ethics Committee of the University of Melbourne, Australia.

Author details

[1]German Center for Neurodegenerative Diseases (DZNE), Munich, Germany. [2]Neuroproteomics, Klinikum rechts der Isar, Technische Universität München, Munich, Germany. [3]Institute for Advanced Study, Technische Universität München, Munich, Germany. [4]Institute for Pathology und Pathological Anatomy, Technische Universität München, Munich, Germany. [5]Department of Anatomy and Neuroscience, University of Melbourne, Victoria, Australia. [6]The Florey Institute of Neuroscience and Mental Health, University of Melbourne, Victoria, Australia. [7]Division of Pharmaceutical Sciences, Graduate School and Faculty of Pharmaceutical Sciences, Kyoto University, Kyoto, Japan. [8]Institute for Diabetes and Obesity, Monoclonal Antibody Research Group, Helmholtz Zentrum München, German Research Center for Environmental Health (GmbH), Munich, Germany. [9]VIB Center for the Biology of Disease, Leuven, Belgium. [10]Center for Human Genetics, and Leuven Institute for Neurodegenerative Diseases (LIND), University of Leuven (KU Leuven), Leuven, Belgium. [11]Institute of Neurology, University College London, London, UK. [12]Department of Neuroscience, Janssen Pharmaceutica NV, Beerse, Belgium. [13]Munich Cluster for Systems Neurology (SyNergy), Munich, Germany.

Received: 2 July 2016 Accepted: 28 September 2016
Published online: 05 October 2016

References

1. Vassar R, Kuhn PH, Haass C, Kennedy ME, Rajendran L, Wong PC, Lichtenthaler SF. Function, therapeutic potential and cell biology of BACE proteases: current status and future prospects. J Neurochem. 2014;130:4–28.
2. Hussain I, Powell D, Howlett DR, Tew DG, Meek TD, Chapman C, Gloger IS, Murphy KE, Southan CD, Ryan DM, et al. Identification of a novel aspartic protease (Asp 2) as beta-secretase. Mol Cell Neurosci. 1999;14:419–27.
3. Sinha S, Anderson JP, Barbour R, Basi GS, Caccavello R, Davis D, Doan M, Dovey HF, Frigon N, Hong J, et al. Purification and cloning of amyloid precursor protein beta-secretase from human brain. Nature. 1999;402:537–40.
4. Vassar R, Bennett BD, Babu-Khan S, Kahn S, Mendiaz EA, Denis P, Teplow DB, Ross S, Amarante P, Loeloff R, et al. Beta-secretase cleavage of Alzheimer's amyloid precursor protein by the transmembrane aspartic protease BACE. Science. 1999;286:735–41.
5. Yan R, Bienkowski MJ, Shuck ME, Miao H, Tory MC, Pauley AM, Brashier JR, Stratman NC, Mathews WR, Buhl AE, et al. Membrane-anchored aspartyl protease with Alzheimer's disease beta-secretase activity. Nature. 1999;402:533–7.
6. Selkoe DJ, Hardy J. The amyloid hypothesis of Alzheimer's disease at 25 years. EMBO Mol Med. 2016;8:595–608.
7. Willem M, Garratt AN, Novak B, Citron M, Kaufmann S, Rittger A, DeStrooper B, Saftig P, Birchmeier C, Haass C. Control of peripheral nerve myelination by the beta-secretase BACE1. Science. 2006;314:664–6.
8. Hu X, Hicks CW, He W, Wong P, Macklin WB, Trapp BD, Yan R. Bace1 modulates myelination in the central and peripheral nervous system. Nat Neurosci. 2006;9:1520–5.
9. Fleck D, van Bebber F, Colombo A, Galante C, Schwenk BM, Rabe L, Hampel H, Novak B, Kremmer E, Tahirovic S, et al. Dual cleavage of neuregulin 1 type III by BACE1 and ADAM17 liberates its EGF-like domain and allows paracrine signaling. J Neurosci. 2013;33:7856–69.
10. Cheret C, Willem M, Fricker FR, Wende H, Wulf-Goldenberg A, Tahirovic S, Nave KA, Saftig P, Haass C, Garratt AN, et al. Bace1 and Neuregulin-1 cooperate to control formation and maintenance of muscle spindles. Embo J. 2013;32:2015–28.

11. Hitt B, Riordan SM, Kukreja L, Eimer WA, Rajapaksha TW, Vassar R. beta-Site amyloid precursor protein (APP)-cleaving enzyme 1 (BACE1)-deficient mice exhibit a close homolog of L1 (CHL1) loss-of-function phenotype involving axon guidance defects. J Biol Chem. 2012;287:38408–25.
12. Barao S, Gartner A, Leyva-Diaz E, Demyanenko G, Munck S, Vanhoutvin T, Zhou L, Schachner M, Lopez-Bendito G, Maness PF, De Strooper B. Antagonistic effects of BACE1 and APH1B-gamma-secretase control axonal guidance by regulating growth cone collapse. Cell Rep. 2015;12:1367–76.
13. Barao S, Moechars D, Lichtenthaler SF, De Strooper B. BACE1 physiological functions may limit its use as therapeutic target for alzheimer's disease. Trends Neurosci. 2016;39:158–69.
14. Dislich B, Wohlrab F, Bachhuber T, Müller SA, Kuhn P-H, Hogl S, Meyer-Luehmann M, Lichtenthaler SF. Label-free quantitative proteomics of mouse cerebrospinal fluid detects β-Site APP Cleaving Enzyme (BACE1) protease substrates in vivo. Mol Cell Proteomics. 2015;14:2550–63.
15. Kuhn PH, Koroniak K, Hogl S, Colombo A, Zeitschel U, Willem M, Volbracht C, Schepers U, Imhof A, Hoffmeister A, et al. Secretome protein enrichment identifies physiological BACE1 protease substrates in neurons. Embo J. 2012;31:3157–68.
16. Zhou L, Barao S, Laga M, Bockstael K, Borgers M, Gijsen H, Annaert W, Moechars D, Mercken M, Gevaert K, De Strooper B. The neural cell adhesion molecules L1 and CHL1 are cleaved by BACE1 protease in vivo. J Biol Chem. 2012;287:25927–40.
17. Stutzer I, Selevsek N, Esterhazy D, Schmidt A, Aebersold R, Stoffel M. Systematic proteomic analysis identifies beta-site amyloid precursor protein cleaving enzyme 2 and 1 (BACE2 and BACE1) substrates in pancreatic beta-cells. J Biol Chem. 2013;288:10536–47.
18. Gunnersen JM, Kim MH, Fuller SJ, De Silva M, Britto JM, Hammond VE, Davies PJ, Petrou S, Faber ES, Sah P, Tan SS. Sez-6 proteins affect dendritic arborization patterns and excitability of cortical pyramidal neurons. Neuron. 2007;56:621–39.
19. Miyazaki T, Hashimoto K, Uda A, Sakagami H, Nakamura Y, Saito SY, Nishi M, Kume H, Tohgo A, Kaneko I, et al. Disturbance of cerebellar synaptic maturation in mutant mice lacking BSRPs, a novel brain-specific receptor-like protein family. FEBS Lett. 2006;580:4057–64.
20. Dominguez D, Tournoy J, Hartmann D, Huth T, Cryns K, Deforce S, Serneels L, Camacho IE, Marjaux E, Craessaerts K, et al. Phenotypic and biochemical analyses of BACE1- and BACE2-deficient mice. J Biol Chem. 2005;280:30797–806.
21. Kohler G, Milstein C. Continuous cultures of fused cells secreting antibody of predefined specificity. Nature. 1975;256:495–7.
22. Li MZ, Elledge SJ. Harnessing homologous recombination in vitro to generate recombinant DNA via SLIC. Nat Methods. 2007;4:251–6.
23. Brodney MA, Beck EM, Butler CR, Barreiro G, Johnson EF, Riddell D, Parris K, Nolan CE, Fan Y, Atchison K, et al. Utilizing structures of CYP2D6 and BACE1 complexes to reduce risk of drug-drug interactions with a novel series of centrally efficacious BACE1 inhibitors. J Med Chem. 2015;58:3223–52.
24. Jeppsson F, Eketjall S, Janson J, Karlstrom S, Gustavsson S, Olsson LL, Radesater AC, Ploeger B, Cebers G, Kolmodin K, et al. Discovery of AZD3839, a potent and selective BACE1 inhibitor clinical candidate for the treatment of Alzheimer disease. J Biol Chem. 2012;287:41245–57.
25. Malamas MS, Barnes K, Johnson M, Hui Y, Zhou P, Turner J, Hu Y, Wagner E, Fan K, Chopra R, et al. Di-substituted pyridinyl aminohydantoins as potent and highly selective human beta-secretase (BACE1) inhibitors. Bioorg Med Chem. 2010;18:630–9.
26. Mitterreiter S, Page RM, Kamp F, Hopson J, Winkler E, Ha HR, Hamid R, Herms J, Mayer TU, Nelson DJ, et al. Bepridil and amiodarone simultaneously target the Alzheimer's disease beta- and gamma-secretase via distinct mechanisms. J Neurosci. 2010;30:8974–83.
27. Liu L, Duff K. A technique for serial collection of cerebrospinal fluid from the cisterna magna in mouse. J Vis Exp. 2008. doi:10.3791/960.
28. Schagger H. Tricine-SDS-PAGE. Nat Protoc. 2006;1:16–22.
29. Lichtenthaler SF, Dominguez DI, Westmeyer GG, Reiss K, Haass C, Saftig P, De Strooper B, Seed B. The cell adhesion protein P-selectin glycoprotein ligand-1 is a substrate for the aspartyl protease BACE1. J Biol Chem. 2003;278:48713–9.
30. Cox J, Hein MY, Luber CA, Paron I, Nagaraj N, Mann M. Accurate proteome-wide label-free quantification by delayed normalization and maximal peptide ratio extraction, termed MaxLFQ. Mol Cell Proteomics. 2014;13:2513–26.
31. Rappsilber J, Ishihama Y, Mann M. Stop and go extraction tips for matrix-assisted laser desorption/ionization, nanoelectrospray, and LC/MS sample pretreatment in proteomics. Anal Chem. 2003;75:663–70.
32. Shimizu-Nishikawa K, Kajiwara K, Kimura M, Katsuki M, Sugaya E. Cloning and expression of SEZ-6, a brain-specific and seizure-related cDNA. Brain Res Mol Brain Res. 1995;28:201–10.
33. Halim A, Ruetschi U, Larson G, Nilsson J. LC-MS/MS characterization of O-glycosylation sites and glycan structures of human cerebrospinal fluid glycoproteins. J Proteome Res. 2013;12:573–84.
34. Allen Mouse Brain Atlas [http://mouse.brain-map.org/]
35. Stachel SJ, Coburn CA, Steele TG, Jones KG, Loutzenhiser EF, Gregro AR, Rajapakse HA, Lai MT, Crouthamel MC, Xu M, et al. Structure-based design of potent and selective cell-permeable inhibitors of human beta-secretase (BACE-1). J Med Chem. 2004;47:6447–50.
36. Colombo A, Wang H, Kuhn PH, Page R, Kremmer E, Dempsey PJ, Crawford HC, Lichtenthaler SF. Constitutive alpha- and beta-secretase cleavages of the amyloid precursor protein are partially coupled in neurons, but not in frequently used cell lines. Neurobiol Dis. 2013;49:137–47.
37. Reiss K, Cornelsen I, Husmann M, Gimpl G, Bhakdi S. Unsaturated fatty acids drive disintegrin and metalloproteinase (ADAM)-dependent cell adhesion, proliferation, and migration by modulating membrane fluidity. J Biol Chem. 2011;286:26931–42.
38. Kuhn PH, Colombo AV, Schusser B, Dreymueller D, Wetzel S, Schepers U, Herber J, Ludwig A, Kremmer E, Montag D, et al. Systematic substrate identification indicates a central role for the metalloprotease ADAM10 in axon targeting and synapse function. Elife. 2016; 5, doi: 10.7554/eLife.12748.
39. Jorissen E, Prox J, Bernreuther C, Weber S, Schwanbeck R, Serneels L, Snellinx A, Craessaerts K, Thathiah A, Tesseur I, et al. The disintegrin/metalloproteinase ADAM10 is essential for the establishment of the brain cortex. J Neurosci. 2010;30:4833–44.
40. Gruninger-Leitch F, Schlatter D, Kung E, Nelbock P, Dobeli H. Substrate and inhibitor profile of BACE (beta-secretase) and comparison with other mammalian aspartic proteases. J Biol Chem. 2002;277:4687–93.
41. Lichtenthaler SF, Haass C, Steiner H. Regulated intramembrane proteolysis–lessons from amyloid precursor protein processing. J Neurochem. 2011;117:779–96.
42. Hemming ML, Elias JE, Gygi SP, Selkoe DJ. Proteomic profiling of gamma-secretase substrates and mapping of substrate requirements. PLoS Biol. 2008;6:e257.
43. Lin Y, Lin H, Liu Z, Wang K, Yan Y. Improvement of a sample preparation method assisted by sodium deoxycholate for mass-spectrometry-based shotgun membrane proteomics†. J Sep Sci. 2014;37:3321–9.
44. Lin Y, Wang K, Liu Z, Lin H, Yu L. Enhanced SDC-assisted digestion coupled with lipid chromatography-tandem mass spectrometry for shotgun analysis of membrane proteome. J Chromatogr B. 2015;1002:144–51.
45. Sharma K, Schmitt S, Bergner CG, Tyanova S, Kannaiyan N, Manrique-Hoyos N, Kongi K, Cantuti L, Hanisch U-K, Philips M-A, et al. Cell type- and brain region-resolved mouse brain proteome. Nat Neurosci. 2015;18:1819–31.
46. Ivankov DN, Bogatyreva NS, Hönigschmid P, Dislich B, Hogl S, Kuhn P-H, Frishman D, Lichtenthaler SF. QARIP: a web server for quantitative proteomic analysis of regulated intramembrane proteolysis. Nucleic Acids Res. 2013;41:W459–64.
47. May PC, Dean RA, Lowe SL, Martenyi F, Sheehan SM, Boggs LN, Monk SA, Mathes BM, Mergott DJ, Watson BM, et al. Robust central reduction of amyloid-beta in humans with an orally available, non-peptidic beta-secretase inhibitor. J Neurosci. 2011;31:16507–16.
48. Ring S, Weyer SW, Kilian SB, Waldron E, Pietrzik CU, Filippov MA, Herms J, Buchholz C, Eckman CB, Korte M, et al. The secreted beta-amyloid precursor protein ectodomain APPs alpha is sufficient to rescue the anatomical, behavioral, and electrophysiological abnormalities of APP-deficient mice. J Neurosci. 2007;27:7817–26.
49. Li H, Wang B, Wang Z, Guo Q, Tabuchi K, Hammer RE, Sudhof TC, Zheng H. Soluble amyloid precursor protein (APP) regulates transthyretin and Klotho gene expression without rescuing the essential function of APP. Proc Natl Acad Sci U S A. 2010;107:17362–7.
50. Mulley JC, Iona X, Hodgson B, Heron SE, Berkovic SF, Scheffer IE, Dibbens LM. The role of seizure-related SEZ6 as a susceptibility gene in febrile seizures. Neurol Res Int. 2011;2011:917565.
51. Yu ZL, Jiang JM, Wu DH, Xie HJ, Jiang JJ, Zhou L, Peng L, Bao GS. Febrile seizures are associated with mutation of seizure-related (SEZ) 6, a brain-specific gene. J Neurosci Res. 2007;85:166–72.
52. Xu C, Mullersman JE, Wang L, Bin Su B, Mao C, Posada Y, Camarillo C, Mao Y, Escamilla MA, Wang KS. Polymorphisms in seizure 6-like gene are associated with bipolar disorder I: evidence of gene x gender interaction. J Affect Disord. 2013;145:95–9.

53. Gautam V, D'Avanzo C, Hebisch M, Kovacs DM, Kim DY. BACE1 activity regulates cell surface contactin-2 levels. Mol Neurodegener. 2014;9:4.
54. Ohno M, Sametsky EA, Younkin LH, Oakley H, Younkin SG, Citron M, Vassar R, Disterhoft JF. BACE1 deficiency rescues memory deficits and cholinergic dysfunction in a mouse model of Alzheimer's disease. Neuron. 2004;41:27–33.
55. Ohno M, Chang L, Tseng W, Oakley H, Citron M, Klein WL, Vassar R, Disterhoft JF. Temporal memory deficits in Alzheimer's mouse models: rescue by genetic deletion of BACE1. Eur J Neurosci. 2006;23:251–60.
56. Laird FM, Cai H, Savonenko AV, Farah MH, He K, Melnikova T, Wen H, Chiang HC, Xu G, Koliatsos VE, et al. BACE1, a major determinant of selective vulnerability of the brain to amyloid-beta amyloidogenesis, is essential for cognitive, emotional, and synaptic functions. J Neurosci. 2005;25:11693–709.
57. Kobayashi D, Zeller M, Cole T, Buttini M, McConlogue L, Sinha S, Freedman S, Morris RG, Chen KS. BACE1 gene deletion: impact on behavioral function in a model of Alzheimer's disease. Neurobiol Aging. 2008;29:861–73.
58. Savonenko AV, Melnikova T, Laird FM, Stewart KA, Price DL, Wong PC. Alteration of BACE1-dependent NRG1/ErbB4 signaling and schizophrenia-like phenotypes in BACE1-null mice. Proc Natl Acad Sci U S A. 2008;105:5585–90.

2.2 Seizure protein 6 (SEZ6) controls glycosylation, trafficking and function of kainate receptors GluK2 and GluK3

Martina Pigoni, Rohit Kumar, Merav D Shmueli, Stephan A Muller, Peer H Kuhn, Jasenka Njavro, Pan Gao, Birgit Blank, Mai Ly Tran, Agnes L. Hipgrave Ederveen, Julia Von Blume, Christophe Mulle, Jenny M Gunnersen, Manfred Wuhrer, Gerhard Rammes, Thomas Koeglsperger and Stefan F Lichtenthaler

Seizure protein 6 controls glycosylation, trafficking and function of kainate receptor subunits GluK2 and GluK3

Martina Pigoni [1,2], Jana Hartmann[3], Jasenka Njavro [1,2], Merav D Shmueli [1,2,4], Stephan A Müller [1,2], Peer-Hendrik Kuhn [1,2,5], Pan Gao [6,7], Mai Ly Tran [8,9], Birgit Blank [9], Agnes L. Hipgrave Ederveen [10], Julia Von Blume [8,9], Christophe Mulle[11], Jenny M Gunnersen [12,13], Manfred Wuhrer [10], Gerhard Rammes [14], Marc Aurel Busche[3], Thomas Koeglsperger [6,7] and Stefan F Lichtenthaler *[1,2,15,16]

Keywords

BACE1/ GluK2/3 / HNK-1/ Protein trafficking / SEZ6

Affiliations

1: Deutsches Zentrum für Neurodegenerative Erkrankungen (DZNE), 81377, Munich, Germany

2: Neuroproteomics, Klinikum rechts der Isar, Technische Universität München, 81675, Munich, Germany

3: UK Dementia Research Institute at UCL, University College London, WC1E 6BT London, Great Britain

4: Department of Immunology, the Weizmann Institute of Science, 76100, Rehovot, Israel

5: Institut für Allgemeine Pathologie und pathologische Anatomie, Technische Universität München, 81675, Munich, Germany

6: Department of Neurology, Ludwig Maximilians University, 81377, Munich, Germany

7: Department of Translational Neurodegeneration, German Center for Neurodegenerative Diseases (DZNE), 81377, Munich, Germany

8: Max Planck Institute of Biochemistry, Am Klopferspitz 18, 82152 Martinsried, Germany

9: Department of Cell Biology, Yale University School of Medicine, 06520-8002, New Haven, CT USA

10: Center for Proteomics and Metabolomics, Leiden University Medical Center, 2333ZA Leiden, The Netherlands

11: University of Bordeaux, Interdisciplinary Institute for Neuroscience, CNRS UMR 5297, F-33000 Bordeaux, France

12: Department of Anatomy and Neuroscience, University of Melbourne, VIC 3010, Melbourne, Victoria, Australia

13: The Florey Institute of Neuroscience and Mental Health, University of Melbourne, VIC 3010, Melbourne, Victoria, Australia

14: Department of Anesthesiology, Klinikum rechts der Isar, Technische Universität München, 81675, Munich, Germany.

15: Institute for Advanced Study, Technische Universität München, 85748 Garching, Germany

16: Munich Cluster for Systems Neurology (SyNergy), 81377, Munich, Germany

*Correspondence: stefan.lichtenthaler@dzne.de +49 89 4400-46426

Abstract

Seizure protein 6 (SEZ6) is required for development and maintenance of the nervous system, is a major substrate of the protease BACE1 and is linked to Alzheimer's disease (AD) and psychiatric disorders, but its molecular functions are not well understood. Here we demonstrate that SEZ6 controls glycosylation, cell surface localization and function of kainate receptors composed of GluK2/3 subunits. Loss of SEZ6 reduced surface levels of GluK2/3 in primary neurons and reduced kainate-evoked currents in CA1 pyramidal neurons in acute hippocampal slices. Mechanistically, loss of SEZ6 in vitro and in vivo prevented modification of GluK2/3 with the human natural killer-1 (HNK-1) glycan, a modulator of GluK2/3 function. In heterologous cells, SEZ6 interacted with GluK2 through its ectodomain and promoted post-endoplasmic reticulum transport of GluK2 in the secretory pathway. Taken together, SEZ6 acts as a new trafficking factor for GluK2/3, thereby fine-tuning neurotransmission which is essential for a healthy nervous system.

Introduction

Precise development and maintenance of the nervous system is essential for the functioning of the brain. Defects in these processes cause various psychiatric and neurological diseases, including neurodevelopmental disorders and Alzheimer's disease (AD), the most common neurodegenerative disorder (Brookmeyer, Evans et al., 2011, Goodman, Lochner et al., 2017). One protein with links to different brain diseases is seizure protein 6 (SEZ6). SEZ6 is an N-glycosylated type I transmembrane protein with predominant expression in neurons, where it localizes to the somatodendritic compartment, including the cell surface (Gunnersen, Kim et al., 2007, Herbst & Nicklin, 1997, Pigoni, Wanngren et al., 2016). SEZ6-deficient mice revealed basic functions for SEZ6 in nervous system development and maintenance, such as in dendritic branching, dendritic spine dynamics, correct synapse formation and proper synaptic transmission, in particular excitatory postsynaptic responses, as well as long-term potentiation (Gunnersen et al., 2007, Zhu, Xiang et al., 2018). Several of these functions seem to be mediated by full-length SEZ6, but SEZ6 can also undergo ectodomain shedding (Lichtenthaler, Lemberg et al., 2018), similar to the AD-linked amyloid precursor protein (APP). This proteolytic removal of the large extracellular domain of SEZ6 is mediated by the AD-linked protease β-site APP cleaving enzyme 1 (BACE1) and contributes to SEZ6 function in controlling dendritic spine dynamics and long-term potentiation in mice (Pigoni et al., 2016, Zhu et al., 2018). The cleaved, soluble form of SEZ6 (sSEZ6) is released from neurons and is found in CSF, where it is increased in depressed, bipolar and schizophrenic patients as well as in inflammatory pain and may be a biomarker for monitoring BACE1 activity in clinical trials for AD (Maccarrone, Ditzen et al., 2013, Pigoni et al., 2016, Roitman, Edgington-Mitchell et al., 2019).

Genetic variants of SEZ6 are linked to psychiatric and neurological disorders. For example, deletions in the SEZ6 ectodomain are found in childhood onset schizophrenia (Ambalavanan, Girard et al., 2015). Other genetic variants have been reported in intellectual disability (Gilissen, Hehir-Kwa et al., 2014) while the rare SEZ6 mutation R615H has been suggested to cause a familial form of AD (Paracchini, Beltrame et al., 2018). Consistent with the disease link, SEZ6-deficient mice, which are viable and fertile, display an anxiety- and depression-related behavior (Gunnersen et al., 2007). Moreover, they show exploratory, motor, and cognitive deficits, which are more severe in mice lacking not only SEZ6, but also its two homologs SEZ6-like (SEZ6L) and SEZ6L2 (Gunnersen et al., 2007, Miyazaki, Hashimoto et al., 2006).

Despite the fundamental functions of SEZ6 in the brain, the molecular mechanisms through which wild-type and mutated SEZ6 contribute to physiological and pathological processes in the nervous system are not yet well defined. SEZ6 localizes to the somatodendritic surface of neurons. The SEZ6 ectodomain contains three CUB (complement subcomponent C1r, C1s /sea urchin embryonic growth factor Uegf / bone morphogenetic protein 1) and five complement control protein

(CCP, also referred to as Sushi or short consensus repeat (SCR)) domains. Both CUB and CCP domains are frequently found in proteins of the complement system (Escudero-Esparza, Kalchishkova et al., 2013, Forneris, Wu et al., 2016) and in some proteins, including LEV-10, SOL1/2 and Neto1/2, that bind certain neurotransmitter receptors, such as acetylcholine receptors (AChR) or AMPA (α-amino-3-hydroxy-5-methyl-4-isoxazolepropionic acid) receptors and act as auxiliary subunits that regulate synaptic clustering or gating of neurotransmitter receptors (Gally, Eimer et al., 2004, Gendrel, Rapti et al., 2009, Nakayama & Hama, 2011, Ng, Pitcher et al., 2009, Straub, Hunt et al., 2011, Tang, Pelkey et al., 2011, Wang, Mellem et al., 2012, Zhang, St-Gelais et al., 2009, Zheng, Brockie et al., 2006, Zheng, Mellem et al., 2004). The presence of CUB and CCP domains also in SEZ6 suggests a role for SEZ6 in neuronal protein-protein interactions, but potential interaction partners are not yet known.

Here, we tested the possibility that SEZ6 controls levels of proteins or protein complexes at the neuronal surface. Mass spectrometry analysis of the membrane proteome from SEZ6 knock-out (SEZ6KO) neurons demonstrated a selective reduction of kainate receptor (KAR) subunits 2 and 3 (GluK2 and GluK3) at the cell surface, leading to a lowering of kainate currents in hippocampal brain slices. KARs belong to the family of ionotropic glutamate receptors (iGluRs), which also comprise NMDA (N-methyl-D-aspartate) and AMPA receptors. Mechanistically, we report that the extracellular domain of SEZ6 can bind GluK2 and controls the complex N-glycosylation of GluK2 and/or GluK3, which occurs late in the secretory pathway, as well as the correct transport of GluK2 and/or GluK3 to the plasma membrane. This molecular function of SEZ6 was independent of BACE1 cleavage and, consequently, appears to mediated predominantly by the full-length, but not the cleaved form of SEZ6. Together, these data reveal an unanticipated function for SEZ6 as a specific regulator of the trafficking of KAR subunits GluK2 and GluK3 to the neuronal plasma membrane, thus establishing a new mode of regulation of KAR activity.

Results

SEZ6 controls surface levels of GluK2 and GluK3 in neurons

We used an unbiased mass spectrometry approach and investigated whether loss of SEZ6 affects protein levels at the cell surface of primary neurons. To this aim, we used a modified version of the 'surface-spanning protein enrichment with click sugars' (SUSPECS) method (Herber, Njavro et al., 2018), which biotinylates complex glycosylated, sialylated proteins residing at the surface and late in the secretory pathway. Floxed Sez6 cortical neurons were treated with lentiviral CRE recombinase or GFP to obtain neurons lacking (SEZ6KO) or maintaining SEZ6 (WT), respectively (workflow in Fig. 1A). SEZ6 was consistently detected on the surface of the WT neurons, and not consistently detected in the SEZ6KO neurons, in line with an efficient Cre-mediated SEZ6KO (Fig. 2A and Supplementary Fig. 1). 3209 proteins were detected in 3 out of 3 experiments by the SUSPECS analysis and 571 were glycosylated (Fig. 1B). 40% out of all the proteins detected, and 90% of the glycosylated proteins were classified as membrane proteins according to UniProt keywords (Fig. 1B), proving that our method efficiently enriched for membrane proteins. Proteins were considered as hits if their protein level in SEZ6KO versus WT neurons was lower than log2 ratio(SEZ6KO/WT)=-0.5 (0.7 fold change) or higher than log2 ratio(SEZ6KO/WT)=0.5 (1.4 fold change) and if the p-value of this change was lower than 0.05. This yielded 14 proteins with reduced and 9 proteins with increased abundance in the SEZ6KO neurons. All other proteins did not show quantitative changes between SEZ6KO and WT neurons (Fig. 1C and Supplementary Table 1), demonstrating that loss of SEZ6 selectively affected cell surface levels of only a few neuronal proteins.

Notably, the two pore-forming subunits of kainate receptors, glutamate receptor kainate 2 (gene *Grik2*, protein GluK2) and 3 (gene *Grik3*, protein GluK3), showed the strongest reduction at the cell surface of SEZ6KO neurons with a decrease of 50% and 60%, respectively (Fig. 1C and Supplementary Table 1). Other iGluR subunits were also detected, but not significantly changed (Fig. 1C). This included two subunits of the NMDA receptor subfamily (GluN1, GluN2B) and two AMPA receptor subunits (GluA1, GluA2) (Fig. 1C). Thus, among the detected iGluRs, loss of SEZ6 specifically reduced surface levels of GluK2 and GluK3.

Next, we validated the mass spectrometric results using an independent method based on cell surface biotinylation, which selectively labels proteins only at the cell surface, followed by streptavidin pull-down and immunoblotting (Supplementary Fig. 1). While surface levels of several transmembrane proteins were not affected in SEZ6KO neurons, such as the SEZ6 homolog SEZ6L2 or members of the glutamate receptor family (GluN2B and GluA2), GluK2 and GluK3 were reduced by 50%, which is consistent with the mass spectrometric analysis (Fig. 2A and Fig. 1C). Given that the available antibody does not discriminate between GluK2 and GluK3, the protein band is referred to as GluK2/3 throughout the manuscript, in line with previous publications

(Mennesson, Rydgren et al., 2019, Straub et al., 2011, Zhang et al., 2009). Interestingly, total GluK2/3 protein levels in neuronal lysates were also reduced, but only mildly by about 15% in the SEZ6KO neurons (see later Fig. 4C). Importantly, no difference in the GluK2 and GluK3 mRNA level was found in SEZ6KO neurons (Fig. 2B). Moreover, while mRNA editing at the Q/R site in the channel pore loop of GluK2 is a critical step for controlling cellular protein levels of GluK2 as well as its transport to the cell surface and its degradation (Ball, Atlason et al., 2010, Evans, Gurung et al., 2017), the amount of edited (R) and unedited (Q) mRNA was not altered in the wild-type and SEZ6KO neurons (Fig. 2C). Taken together, these experiments suggest that SEZ6 controls cell surface levels of GluK2/3 at the post-translational level.

SEZ6 controls function of GluK2/3

To test whether the reduced surface levels of GluK2 and GluK3 also result in attenuated kainate receptor signaling, we next recorded kainate-evoked currents in acute hippocampal slices in WT and SEZ6KO mice. We focused on the CA1 region of the hippocampus, where both SEZ6 and GluK2 and/or GluK3 are expressed (Bureau, Bischoff et al., 1999, Kim, Gunnersen et al., 2002, LeinHawrylycz et al., 2007). CA1 pyramidal neurons were whole-cell patch-clamped, and the membrane current was recorded in control ACSF, in the presence of 10 µM kainate for 5 min and after addition of NBQX, an antagonist of both AMPA and kainate receptors (Fig. 3A). Throughout the experiments AMPA receptors were blocked by GYKI53655 in the ACSF. In addition, the activation of NMDA and $GABA_A$ receptors was prevented by the extracellular presence of APV and bicuculline, respectively. Kainate reliably evoked inward currents in both genotypes. However, in the absence of SEZ6 in the SEZ6KO mice the mean charge carried by the kainate-evoked inward currents (calculated as area under the current curves) was reduced by 34% compared to wild type mice (Fig. 3B), consistent with a reduced membrane expression of channel subunits.

GluK2/3 maturation is impaired in SEZ6KO neurons and in vivo in mouse brains

In WT neurons the GluK2/3 immunoreactivity in western blots was seen as two closely co-migrating bands, but in SEZ6KO neurons the upper band appeared reduced and merging with the lower one, suggesting that N-glycosylation of GluK2 and/or GluK3 may be impaired in SEZ6KO neurons (Fig. 4A and Supplementary Fig. 1). In fact, GluK2 and GluK3 have multiple N-glycosylation sites (Parker, Thaysen-Andersen et al., 2013, Vernon, Copits et al., 2017), which are glycosylated to different extents, producing GluK2 and GluK3 forms with more simple, immature glycosylation and with mature glycosylation. GluK2/3 with immature glycans is mostly found within cells, whereas GluK2/3 with mature glycans localizes to a larger extent to the cell surface (Mah, Cornell et al., 2005). Distinction between both sugar modifications is possible with the glycan-removing enzyme endoglycosidase H (EndoH) that cleaves off immature, but not mature N-glycans. To test, whether SEZ6KO affects the glycosylation of GluK2 and/or GluK3, we digested

neuronal protein lysates with EndoH and blotted for the GluK2/3 bands (Fig. 4A). With EndoH, the two bands of GluK2/3 in control conditions were converted to three distinct proteins bands with a lower apparent molecular weight. The lowest band is completely deglycosylated, as shown previously by PNGase F treatment (Nasu-Nishimura, Jaffe et al., 2010). The upper two bands were not completely deglycosylated, demonstrating that they partially contain mature sugar chains, which are not removable by EndoH. SEZ6KO specifically affected the uppermost, EndoH-resistant protein form. Compared to WT, this band had a lower intensity and was shifted to a slightly lower apparent molecular weight, indicating that in the SEZ6KO, GluK2/3 carries less mature glycans (Fig. 4A and model in 4A).

So far, our experiments revealed that SEZ6 modulates mature GluK2 and/or GluK3 glycosylation *in vitro* in primary neurons. To test if maturation of GluK2 and/or GluK3 is also affected *in vivo*, we analyzed their glycosylation pattern in brain homogenates and synaptosomes of wild type and constitutive SEZ6KO adult mice. Similar to our results *in vitro* (Fig. 4A), the upper one of the two GluK2/3 bands under control conditions (no EndoH treatment) was reduced in the SEZ6KO brain and this effect was even more clearly visible after EndoH treatment, where again the uppermost, mature glycoform shifted to a lower apparent molecular weight (Fig. 4B for brain homogenates and Fig. 4E for synaptosomes). Total levels of the GluK2/3 bands were not changed and this was also seen for a control protein, the GluA2 subunit of AMPA receptors (Fig. 4B and D).

Although SEZ6 has two homologs, SEZ6L and SEZ6L2, which have a similar domain structure as SEZ6, there was no effect on mature glycosylation of the GluK2/3 band in SEZ6L and SEZ6L2 single knock-out brain synaptosomes (Fig. 4E). Moreover, the reduced maturation of the GluK2/3 band was not further reduced in synaptosomes from triple-knock-out mice lacking SEZ6 and both of its homologs (Fig. 4E). This demonstrates that specifically SEZ6, and not its homologs, is required for mature glycosylation of GluK2 and/or GluK3.

The relevance of SEZ6 for GluK2/3 maturation was not only seen at very young ages, when SEZ6 expression is high ((Kim et al., 2002, Miyazaki et al., 2006) and Fig. 4F), but also during adulthood (Fig. 4F), demonstrating that the effect of SEZ6 on maturation of GluK2 and/or GluK3 is independent of the developmental stage and that no compensation occurs through other proteins during adulthood. Interestingly, the intensity of the lowest GluK2/3 band was highest during the embryonic stage and decreased sharply after birth (Fig. 4F), but this was independent of SEZ6.

SEZ6 controls HNK-1 glycan modification of GluK2 and/or 3

To identify the SEZ6-dependent changes in glycosylation of GluK2 and/or GluK3, we used a lectin chip microarray (LecChip) that allows characterization of the glycome fingerprint of proteins (Hu & Wong, 2009). Lysates of WT and SEZ6KO neurons were analyzed by a LecChip containing 45 different lectins, which recognize different sugar structures. This analysis revealed a reduction in

glycosylation of GluK2 and/or GluK3 for the lectins PHAE (Phaseolus vulgaris-E) and PHAL (Phaseolus vulgaris-L) (Fig. 5A). These two lectins share the recognition of the oligosaccharide Galβ1-4GlcNAcβ1 as a common motif, a sugar unit commonly involved in complex oligosaccharide formation, including of the human natural killer-1 (HNK-1) epitope (Chou, Ilyas et al., 1986). This is a known glycan modification of GluK2, which affects GluK2 function (Vernon et al., 2017), is found in a few other neuronal proteins, such as GluA2 (Morita, Kakuda et al., 2009) and NCAM-1 (Kruse, Mailhammer et al., 1984) and is generally assumed to control cell adhesion and migration (Morise, Takematsu et al., 2017). To determine, whether loss of SEZ6 indeed reduces modification of the GluK2/3 protein band with the HNK-1 glycan, we immunoprecipitated GluK2/GluK3 from mouse brain extracts and blotted with an anti-HNK-1 antibody ((Stanic, Saldivia et al., 2016) and Fig. 5B). In WT brain extracts, the GluK2/3 band contained the HNK-1 modification, in agreement with a previous report (Vernon et al., 2017). As a control, treatment of immunoprecipitated GluK2/3 protein with the enzyme peptide N-glycosidase F (PNGase), which removes all N-linked sugars, abolished the HNK-1 signal as expected. Importantly, in SEZ6KO brains, the GluK2/3 protein lacked the HNK-1 modification, while the immunoblot signal for HNK-1 in the total brain extract (without immunoprecipitation of GluK2/3 protein) and for the different isoforms of the HNK-1 modified protein NCAM-1 was unaltered (Fig. 5B). Thus, loss of SEZ6 specifically prevents HNK-1 modification of GluK2 and/or GluK3, but not of other proteins in mouse brain. As a further control, global glycome determination of lysates by mass spectrometry did not show significant changes between WT and SEZ6KO neurons (Supplementary Fig. 2), revealing that loss of SEZ6 does not broadly affect N-glycosylation in neurons.

SEZ6 facilitates GluK2 transport within the secretory pathway

So far, our experiments revealed that SEZ6 is required for normal cell surface localization and signaling as well as for correct glycosylation of GluK2 and/or GluK3 with the HNK-1 epitope, which happens in the trans cisterna of the Golgi or in the trans-Golgi network (Kizuka & Oka, 2012). These findings suggest that SEZ6 promotes GluK2 and/or 3 protein trafficking through the secretory pathway.

In order to investigate whether SEZ6 directly affects GluK2 trafficking through the secretory pathway towards the plasma membrane, we used the “retention using selective hooks” (RUSH) system (Fig. 6). Human embryonic kidney 293 (HEK293) cells were chosen as a heterologous system, which do not express endogenous SEZ6 or GluK2 or GluK3, and therefore no competition with endogenous proteins is expected. HEK293 were transfected with a GluK2 construct (SBP-mCherry-GluK2) that is retained in the ER, unless biotin is added to the culture medium, which binds to a streptavidin-KDEL ER anchor and suppresses the interaction with a streptavidin-binding peptide (SBP) at the N-terminus of GluK2. Consequently, GluK2 is released from the artificial anchor from the ER. Thus, release of SBP-mCherry-GluK2 from the ER can be induced in a

synchronous manner (Boncompain, Divoux et al., 2012, Evans et al., 2017). In absence of added biotin, SBP-mCherry-GluK2 was retained in the ER (Fig. 6B, SBP-mCherry-GluK2 is detected in red). 20 min after biotin addition SBP-mCherry-GluK2 largely localized to the Golgi apparatus (Fig. 6B). At 40 min after biotin addition, vesicles containing SBP-mCherry-GluK2 were observed in the cytoplasm of the cells (Fig. 6B and C control mean number of vesicles/cell: 22 ± 13). When SEZ6 (in Fig. 6B detected in green) was co-transfected with SBP-mCherry-GluK2 the number of cytoplasmic vesicles was significantly increased (Fig. 6B and C SEZ6 mean number of vesicles/cell: 36 ± 20) compared to the control transfected cells at the 40 min time point. In contrast, when SEZ6L2 (in Fig. 6B detected in green) was co-transfected with SBP-mCherry-GluK2, the number of vesicles was not significantly different from the control (Fig. 6B and C SEZ6L2 mean number of vesicles/cell: 24 ± 14), proving that also in a heterologous system SEZ6L2 does not influence the trafficking of GluK2. Taken together we conclude that SEZ6 influences GluK2 maturation by controlling its trafficking through the secretory pathway.

The extracellular domain of SEZ6 binds GluK2/3 and is required for mature glycosylation of GluK2/3

To further address the mechanism through which SEZ6 promotes trafficking, glycosylation, surface localization and activity of GluK2 and/or GluK3, we tested which of the several SEZ6 domains is required and whether SEZ6 interacts with GluK2 and/or GluK3.

The SEZ6 ectodomain contains CUB and CCP domains, which may mediate protein-protein interactions, whereas its cytoplasmic domain includes an NPxY motif, which is known to be important for endocytosis of proteins from the cell surface (Bonifacino & Traub, 2003). To investigate which of the protein domains is required for full maturation of GluK2 and/or GluK3, we carried out a domain-deletion analysis of SEZ6. As a control, we used full-length SEZ6 (SEZ6FL) (Fig. 7A). First, one mutant lacked the C-terminal 39 amino acids (SEZ6ΔCyto, amino acids 20-952; amino acids 1-19 are the signal peptide) including the NPxY motif. Second, another mutant was the SEZ6 ectodomain (SEZ6ecto, amino acids 20-909), which has the same amino acid sequence as the soluble SEZ6 (sSEZ6) generated through BACE1 cleavage between leucine906 and aspartate907 of SEZ6 (Pigoni et al., 2016), but contains additional HA and Flag tags. The third mutant was the counterpart to SEZ6ecto, namely the C-terminal fragment (SEZ6CTF, amino acids 907-991) generated by BACE1 cleavage. First, we verified that the constructs were correctly expressed in the SEZ6KO neurons. SEZ6FL displayed the known double band corresponding to the mature form (upper band) and the immature form of the protein (lower band) (Fig. 7B) (Pigoni et al., 2016). SEZ6ΔCyto showed bands of similar molecular weight, but of lower intensity. SEZ6ecto had the expected lower molecular weight than the mature SEZ6FL and was detected in the lysate as the immature form, whereas the mature glycosylated form was efficiently secreted and detected in the conditioned medium of the neurons (Fig. 7C). SEZ6CTF was well expressed at

the expected low molecular weight (24 kDa). SEZ6FL, SEZ6ΔCyto and SEZ6ecto rescued the glycosylation phenotype, as seen by the reappearance of the uppermost GluK2/3 band after EndoH treatment in the SEZ6KO neurons (Fig. 7B), whereas SEZ6CTF did not rescue the maturation of the GluK2/3 protein. Thus, we conclude that the extracellular domain of SEZ6 - either in the membrane-bound or soluble form - is required for the function of SEZ6 in controlling GluK2/3 protein glycosylation. Interestingly, similar observations were made for LEV-10 and SOL-1, where not only the full-length, but also the soluble CUB domain-containing soluble ectodomains rescued surface clustering of neurotransmitter receptors in the corresponding knock-out cells (Gally et al., 2004, Gendrel et al., 2009, Nakayama & Hama, 2011, Zheng et al., 2006).

Within the secretory pathway the ER exit of KARs can be controlled (Contractor, Mulle et al., 2011, Jaskolski, Coussen et al., 2004). Therefore, we used SEZ6∆cyto, but containing a KKXX ER-retention motif (SEZ6∆cytoER) and showed that it was not able to rescue the glycosylation defect of SEZ6KO neurons in contrast to SEZ6∆cyto (Fig. 7D). As expected for the ER localization, SEZ6∆cytoER was only detected as the immature protein band. This experiment demonstrates that SEZ6 affects the post-ER trafficking of the GluK2 and/or 3. This is in line with the RUSH experiment (Fig. 6) which revealed that SEZ6 can promote trafficking of GluK2 in the secretory pathway.

The finding that expression of SEZ6ecto, which corresponds to the physiologically generated BACE1 cleavage fragment of SEZ6 (sSEZ6), rescued the glycosylation phenotype in SEZ6KO neurons, showed that the ectodomain is sufficient to promote GluK2/3 protein maturation. To exclude the possibility that sSEZ6 – generated by BACE1 and found in the extracellular space - might influence GluK2/3 protein maturation indirectly, we also tested whether BACE1 inhibition or deletion, which abolishes sSEZ6 secretion, has an effect. As expected, pharmacological BACE1 inhibition in primary cortical neurons and genetic BACE1 deletion in mouse brain homogenates neither altered GluK2/3 glycosylation nor cell surface levels of the GluK2/3 protein in primary neurons (Supplementary Fig. 3). Thus, we conclude that the requirement of SEZ6 for GluK2/3 protein glycosylation and cell surface localization is independent of BACE1, suggesting that under physiological conditions it is preferentially the full-length form of SEZ6 that controls SEZ6 glycosylation and cell surface levels.

Our findings suggest that the regulation of GluK2 and/or 3 trafficking is mediated by the SEZ6 extracellular domain. To address the possibility of a direct binding of SEZ6 extracellular domain to GluK2 and/or GluK3, we first immunoprecipitated GluK2/3 from mouse brain extract and detected co-immunoprecipitated proteins by mass spectrometry. While the known GluK2/3 interactor Neto2 was detected (Zhang et al., 2009), SEZ6 was not detected (Supplementary Table 2). This suggests that the SEZ6 interaction with GluK2 and/or GluK3 is weaker or shorter-lived than the Neto2-GluK2/3 interaction and not stable enough to be detected in our extract conditions. Thus, to test

whether SEZ6 has the ability to interact with GluK2 and whether such interaction is mediated by the SEZ6 ectodomain, we co-expressed the GluK2a isoform with different SEZ6 mutants in HEK293 cells (Fig. 7E). The SEZ6 mutants containing the extracellular domain (SEZ6FL, SEZ6ΔCyto and SEZ6ecto) co-immunoprecipitated with GluK2a, but SEZ6CTF was not detectable (Fig. 7E). These data demonstrate that SEZ6 is indeed able to form a complex with GluK2 and that the SEZ6 ectodomain is the site of interaction with GluK2.

Discussion

Neurotransmitter receptors have fundamental functions in the nervous system, including for cellular responses to neurotransmission and synaptic plasticity. A fine-tuning of receptor activity is essential for adjusting neurotransmitter signal transduction to the required needs of a cell, organ or whole organism. Here, we identified the CUB and CCP domain-containing protein, SEZ6, as a new regulator of neurotransmission and demonstrate that SEZ6 controls the intracellular trafficking of kainate receptor subunits GluK2 and GluK3 to the cell surface, thereby controlling its glycosylation, cell surface localization and signaling (for a model see Supplementary Fig. 4). This reveals a novel molecular function for the transmembrane protein SEZ6, which is linked to schizophrenia and AD, but is also required for nervous system development, synaptic connectivity and long-term potentiation (LTP) (Gunnersen et al., 2007, Zhu et al., 2018).

The trafficking mechanism of action of SEZ6 on KAR function is surprising. Other CUB and CCP domain-containing proteins such as Neto1, Neto2, SOL-1, LEV-9 and LEV-10 act on iGluRs or AChRs (Nakayama & Hama, 2011). However, they bind stably to their receptors and act as auxiliary receptor subunits that control synaptic receptor localization and its signaling properties, as determined by electrophysiology. For example, Neto1 and Neto2 are known auxiliary KAR subunits (Straub et al., 2011, Tang et al., 2011, Zhang et al., 2009). They bind GluK2 and specifically modulate key functional properties of GluK2, such as inducing slow channel kinetics and high agonist affinity, whereas a potential additional function of Neto1/2 on GluK2 trafficking and synaptic localization remains controversially discussed (Tomita & Castillo, 2012). In contrast to the Neto proteins, SEZ6 does not appear to fulfill the criteria established for auxiliary subunits (Copits & Swanson, 2012, Yan & Tomita, 2012) because our coimmunoprecipitations suggest that the SEZ6 interaction with GluK2 or GluK3 is more transient than the interaction between Neto2 and GluK2. Thus, we propose that SEZ6 is a trafficking factor for GluK2 and/or GluK3 rather than a stably interacting auxiliary subunit, thereby providing an additional layer of regulation of KARs beyond the auxiliary subunits. Interestingly, the SEZ6 homolog SEZ6L2 has recently been shown to bind AMPARs, but not KARs, in transfected cells (Yaguchi, Yabe et al., 2017). Thus, the whole SEZ6 family consisting of SEZ6, SEZ6L and SEZ6L2 may have important, but specific roles in iGluR trafficking.

Transmembrane proteins in the secretory pathway were long thought to traffic by default towards the plasma membrane, but it is now clear that several of them require specific transport helpers, such as iRhom2 for ADAM17, Cornichon for transforming growth factor or ERGIC-53 for certain cathepsins and blood coagulation factors (Dancourt & Barlowe, 2010, Lichtenthaler, 2012). Through its action on the secretory trafficking of GluK2, SEZ6 now joins this growing group of membrane protein transport helpers. The trafficking function of SEZ6 for GluK2 and/or GluK3 is

supported by several findings: firstly, co-expression of SEZ6 with GluK2 promoted trafficking of GluK2 through the secretory pathway, as measured with the RUSH system in HEK293 cells. In addition, the use of an ER-retained SEZ6 construct revealed that SEZ6 specifically controls the post-ER trafficking of GluK2 and/or GluK3. Conversely, loss of SEZ6 reduced neuronal surface levels of GluK2 and/or GluK3 in a post-transcriptional manner without a major effect on total protein levels of GluK2/3 in neurons or mouse brains. Importantly, loss of SEZ6 did not affect cell surface levels of other detected iGluRs and most other transmembrane proteins, revealing a specific effect on GluK2 and/or GluK3 surface localization. Finally, as required for a trafficking factor, SEZ6 bound GluK2 in co-immunoprecipitation experiments and this interaction occurred through its CUB domain-containing ectodomain. Potentially, SEZ6 affects interactions of GluK2 and/or 3 with other proteins, such as protein kinase C and PDZ ligand interactions, that control correct positioning of GluK2 at the plasma membrane(Evans et al., 2017).

Loss of SEZ6 not only reduced trafficking and surface localization of GluK2 and GluK3, but additionally prevented GluK2 and/or GluK3 from carrying the post-translational modification HNK-1, which is a covalently attached sulfated sugar chain consisting of three different sugar molecules, glucuronic acid, galactose and N-acetylglucosamine (HSO3-3GlcAβ1-3Galβ1-4GlcNAc) (Chou et al., 1986). The unique glycostructure that distinguishes HNK-1 from other glycostructures is the terminal sulfated glucuronic acid (Supplementary Fig. 4). HNK-1 has a functional role in cell migration, adhesion and recognition and is an autoantigen in peripheral demyelinating neuropathy (Morise et al., 2017). Addition of the HNK-1 epitope to proteins occurs in the trans cisternae of the Golgi or within the trans-Golgi network (Kizuka & Oka, 2012), but the mechanisms or sequence features that control HNK-1 addition to proteins remain unknown. With our finding that the immunoblot signal intensity for HNK-1 was unaltered in SEZ6KO mouse brains extracts, we conclude that SEZ6 is mechanistically not generally required for HNK-1 modification of proteins, but instead specifically enables HNK-1 modification of GluK2 and/or GluK3. We therefore consider that SEZ6 is either required for transporting GluK2 and 3 to the cellular site of HNK-1 modification or that it facilitates HNK-1 modification of GluK2 and/or GluK3. Whether the lack of the HNK-1 modification in SEZ6KO neurons in turn also contributes to the reduced GluK2/3 surface levels or is independent of the reduced surface levels is not yet clear. However, HNK-1 is generally able to alter protein trafficking, as shown for another iGluR subunit, the AMPAR subunit GluA2. In that case, loss of HNK-1 increased GluA2 endocytosis and reduced cell surface levels of GluA2 in hippocampal neurons (Morita et al., 2009).

Our study shows that SEZ6 is not only required for normal secretory pathway trafficking, cell surface localization and HNK-1 modification of GluK2/3, but also for its signaling. Loss of SEZ6 reduced the amplitude of the kainate current in the ex vivo system of acute hippocampal slices.

The reduced kainate current in SEZ6KO neurons may be a direct consequence of the 50% reduction of GluK2/3 at the cell surface. Additionally, the lack of HNK-1 on GluK2/3 in SEZ6KO neurons may contribute to the reduced kainate current. While it has not yet been investigated whether and how the loss of HNK-1 alters GluK2 and/or GluK3 function, the opposite experiment was done (Vernon et al., 2017). Co-expression of GluK2a or GluK3a with the two HNK-1 synthesizing enzymes in HEK293 cells enabled HNK-1 modification on both GluK2a and GluK3a and resulted in glutamate-evoked currents with slower desensitization kinetics. The mean peak amplitude for the current was not altered for GluK2a but increased three-fold for GluK3a(Vernon et al., 2017). Thus, it appears possible that SEZ6 acts on GluK2/3 function through both mechanisms, i.e. through controlling surface levels and independently through HNK-1 modification of GluK2/3.

SEZ6 is linked to neurological and psychiatric diseases, but the underlying molecular mechanisms are little understood. Genetic variants of SEZ6 are linked to childhood onset schizophrenia (Thr229-Thr231del) (Ambalavanan et al., 2015), intellectual disability (Arg657Gln) (Gilissen et al., 2014) and AD (Arg615His) (Paracchini et al., 2018). These mutations are localized within the SEZ6 ectodomain that interacts with GluK2 and/or GluK3. With our newly established SEZ6 function for surface levels and HNK-1 modification of GluK2 and/or GluK3, it appears possible that these mutations act as loss-of-function mutations and cause reduced KAR activity, which may result in altered synaptic plasticity and LTP (Bortolotto, Clarke et al., 1999, Contractor, Swanson et al., 2001, Pinheiro, Perrais et al., 2007, Sherwood, Amici et al., 2012). Interestingly, besides SEZ6 mutations, also changes in HNK-1 metabolism may contribute to psychiatric diseases. In fact, single nucleotide polymorphisms or chromosome breakpoint translocation sites close to HNK-1 synthesizing enzymes were genetically linked to schizophrenia (Jeffries, Mungall et al., 2003, Kahler, Djurovic et al., 2011).

Not only full-length, but also the soluble SEZ6 ectodomain (sSEZ6) has been linked to disease. While increased sSEZ6 levels in CSF were reported in bipolar, depressive and schizophrenic patients (Maccarrone et al., 2013) and inflammatory pain conditions (Roitman et al., 2019), the opposite was seen in AD, where reduced levels of the sSEZ6 were reported in CSF (Khoonsari, Haggmark et al., 2016). However, it remains unclear whether these changes directly contribute to disease pathogenesis or are merely a consequence of the disease process. sSEZ6 is released from full-length SEZ6 through the action of the protease BACE1 (also known as β-secretase) (Pigoni et al., 2016), which is a key drug target in AD as it catalyzes the first step in the generation of the pathogenic Aβ peptide (Vassar, Kuhn et al., 2014). Our study revealed that the knock-out of BACE1 and the use of BACE inhibitors did not affect glycosylation or cell surface trafficking of GluK2/3. Thus, the action of full-length SEZ6 on GluK2/3 function was independent of BACE1. This is good news for the clinical development of BACE1-targeted inhibitors, as they are not expected to cause side effects by affecting GluK2 and/or GluK3 function. Yet, the BACE1 cleavage products of

SEZ6, sSEZ6 or the C-terminal fragment (SEZ6CTF), may have physiological functions other than full-length SEZ6 and such functions may still be affected by the clinically tested BACE inhibitors. In fact, pharmacological BACE1 inhibition in mice reduced LTP and dendritic spine density in a SEZ6-dependent manner (Zhu et al., 2018). While the underlying molecular mechanisms still need to be elucidated, these experiments imply BACE1 cleavage products in controlling LTP and spine density. Finding different functions for full-length versus soluble SEZ6 is reminiscent of other single-span transmembrane proteins, such as the death receptor DR6 (Colombo, Hsia et al., 2018), the neuronal cell adhesion protein NrCAM (Brummer, Muller et al., 2019) and the B-cell maturation antigen (Laurent, Hoffmann et al., 2015), where the full-length protein and cleavage products have different physiological functions.

In summary, our study identifies the neuronal protein SEZ6 as a novel trafficking protein of KARs that controls activity, localization and glycosylation of the KAR subunits GluK2 and GluK3. This reveals for the first time a molecular function for the transmembrane protein SEZ6, which has fundamental role in the brain, such as for nervous system development, synaptic connectivity and long-term potentiation (Gunnersen et al., 2007, Zhu et al., 2018). Given the genetic link of SEZ6 to psychiatric and neurologic diseases, the new function and mechanism of action for SEZ6 are also of major relevance for understanding these devastating diseases.

Materials and Methods

Materials

The following antibodies were used: monoclonal SEZ6 (Pigoni et al., 2016), polyclonal SEZ6 (Gunnersen et al., 2007), pAb SEZ6L2 (R&D Systems, AF4916), pAb SEZ6L (R&D Systems, AF4804), GluR6/7 (04-921, Millipore. GluK2 and GluK3 antibodies commercially available are not able to discriminate between these two subunits due to their high homology), NMDAR2b (D15B3, Cell Signaling), anti-GluR2 (MAB397, Millipore), 3D5 (kindly provided by Robert Vassar), calnexin (Enzo, Stressgen, Farmingdale, NY, USA, ADI-SPA-860), β-tubulin (T8578, Sigma), β actin (Sigma, A5316), PSD 95 (2507, Cell Signaling), LDLR (R&D Systems, AF2255), NCAM-1 (R&D Systems, AF6070), rat mAb Flag M2 (F1804, Sigma), 5F8 anti-Red (Chromotek), anti- HA.11 (MMS-101P, Covance), HRP coupled anti-mouse and anti-rabbit secondary (DAKO), HRP coupled anti-goat, anti-rat and anti-sheep (Santa Cruz).

The following reagents and media were used: neurobasal medium, HBSS and B27 (Invitrogen), C3 (β-secretase inhibitor IV; Calbiochem, 565788, final concentration 2 μM), DMEM (Gibco), FBS (Thermo Fisher Scientific)

Mouse strains

The following mice were used in this study: wild type (WT) C57BL/6NCrl (Charles River), BACE1-/- (Jackson Laboratory, strain B6.129- Bace1tm1Pcw/J, BACE1KO), SEZ6-/- (SEZ6KO) (Gunnersen et al., 2007), SEZ6 flox/flox (Gunnersen et al., 2007), SEZ6 family triple knockout (TKO) mice lacking SEZ6, SEZ6L and SEZ6L2 (Miyazaki et al., 2006), SEZ6L-/- (SEZ6LKO, bred from SEZ6 family TKO (Miyazaki et al., 2006)) and SEZ6L2-/- (SEZ6L2 KO, bred from SEZ6 family TKO (Miyazaki et al., 2006)). All mice were on a C57BL/6 background and were maintained on a 12/12 h light-dark cycle with food and water *ad libitum.*

Molecular biology

pFUW HA-SLIC-Flagx2-mmSEZ6FL was generated synthetizing full-length *Mus musculus* SEZ6, transcript variant 1 (Uniprot Q7TSK2-1) in pFUW vector, where the insert replaced the original GFP in the pFUGW vector. The signal peptide of SEZ6 was maintained, followed by a short spacer (SLIC) [22], and an HA tag (YPYDVPDYA). A double FLAG tag (DYKDDDDK) was cloned to the C terminus of the protein. The different SEZ6 mutants were similarly synthetized in the pFUW vector and GFP or empty pFUW were used as control. In particular, pFUW HA-SLIC-Flagx2-mmSEZ6Δcyto was generated removing the last 39 amino acids at the C terminus of the protein. The pFUW HA-SLIC-Flagx2-mmSEZ6ecto and pFUW HA-SLIC-Flagx2-mmSEZ6 CTF containing the SEZ6 ectodomain and the SEZ6 C-terminal fragment respectively, were generated according to the BACE1 cleavage site located between leucine906 and aspartate907 (Pigoni et al., 2016). pFUW HA-SLIC-Flagx2-mmSEZ6L2 was generated synthetizing full-length *Mus musculus*

SEZ6L2, transcript variant 1 (Uniprot Q4V9Z5-1) in pFUW vector. For the generation of the SEZ6 retention mutant, the pFUW HA-SLIC-Flagx2-mmSEZ6Δcyto Flagx2 was used as template and the Flagx2 was substituted with the WBP1 retention signal (KKLETFKKTN) (Shikano & Li, 2003).

Isolation of primary cortical neurons

Neuronal cultures were derived from SEZ6 flox/flox and SEZ6KO mice at E15.5/E16.5. Brains from fetuses were prepared and digested with papain (Sigma) for 30 minutes. Tissue was triturated and cortical neurons were separated by sequential passage of the cell suspension through plastic pipettes. Cells were centrifuged for 3 minutes at 800 g, and resuspended in seeding medium (DMEM containing 10% FBS). The cell number was determined and neurons were seeded at a density of 1.5 million cells per milliliter in Poly-D-Lysin (Sigma-Aldrich)-coated plates. In general, neurons were infected at day 2 *in vitro* (DIV) with the exception of the rescue experiment in figure 7 (infection was done at DIV 0 in order to maximize the rescue effect). After 5 days *in vitro* (DIV), neurons were washed with PBS, medium was replaced with fresh neurobasal.and the experiments were carried out at DIV 7.

Cell lysate preparation

In general, supernatants and lysates from neurons were collected at DIV 7 as previously described (Dislich, Wohlrab et al., 2015). In order to detect better the difference in the GluK2/3 glycosylation, Triton lysis buffer (150 mM NaCl, 50 mM Tris pH 7.5, 1% Triton X-100 and protease inhibitor cocktail (Roche) was used. BCA assay (Uptima Interchim, UP95425) was used to quantify protein concentrations and 10–15 µg of total neuronal lysate were used for Western Blot analysis.

Brain homogenization

Brains were isolated from SEZ6KO mice and WT at different age. All brains were homogenized in 20mM HEPES pH 7.4, 150mM NaCl, 0.5% NP-40, 2mM EDTA, 10% Glycerol and incubated on ice for at least 1h. Samples were then centrifuged at maximum speed for 5 minutes in order to remove the membranes. BCA assay (Uptima Interchim, UP95425) was used to quantify protein concentrations and 15–20 µg of total protein were used for Western Blot analysis.

Brain fractionation

Brains were isolated from P7 BACE1 KO mice and WT littermates kindly provided by Prof. Jochen Herms. Samples were processed as previously described (Kuhn, Koroniak et al., 2012) and the concentration of the membrane proteins were quantified with a BCA assay (Uptima Interchim, UP95425). 15–20 µg of total protein were used for Western Blot analysis.

Synaptosomes

Synaptosomes were purified from full mouse brain (without olfactory bulbs and cerebellum) according to Carlin et al. 1980 (Carlin, Grab et al., 1980). Brains were homogenized in 0.32M sucrose, 1mM NaHCO3, 1mM MgCl2 and 0.5 mM CaCl2 and diluted at a final concentration of 10% w/v. Samples were centrifuged at 1400g for 10 min at 4 °C. The supernatants (S1) were transferred to a fresh tube and centrifuged at 13800 g for 10 min at 4 °C. The supernatants (S2) were discarded and pellets (P2) resuspended in 0.32M sucrose, 1mM NaHCO3. Sucrose gradient was set up by slowly over-laying increasing sucrose concentration solutions (0.85M sucrose, 1M sucrose and 1.2M sucrose in water). P2 suspensions were loaded carefully on the sucrose layers and tubes were centrifuged in an ultracentrifuge with swing out rotor at 82.500 g for 2h at 4 °C (max acceleration, but slow deceleration). Synaptosome fractions were collected between layers 1.2M and 1M sucrose, and centrifuged at 13800 g for 15 min at 4 °C. Sucrose was completely removed and pellets (P3) solved in SDT buffer (2% SDS, 100mM Tris, 50mM DTT).

Western blot analysis

Samples were boiled for 5 min at 95 °C in Laemmli buffer and separated on 8% or 12% SDS-polyacrylamide handcast gels or 4-12% MOPS gradient gels (GenScript). PVDF membranes (Millipore) were incubated with primary antibody for 1–2 h at room temperature or at 4 °C overnight. After incubation with secondary antibody at room temperature for 1 h, membranes were developed with ECL prime (GE Healthcare, RPN2232V1).

Deglycosylation assay

10-12 µg of neuronal lysate or brain homogenate were treated with endoglycosidase H (Endo H, New England Biolabs, P0702) or Peptide-N-Glycosidase F (PNGase F, New England Biolabs, P0704) according to the manufacturer's protocol. Afterwards, the samples were separated on 8 % SDS-polyacrylamide gel Western blotting was performed.

Surface biotinylation

Neurons were biotinylated at DIV 7 with EZ-Link™ Sulfo- NHS-Biotin (ThermoFisher, 21217) according to manufacturer's protocol. Quenching was done with ammonium chloride (50 mM) and BSA (1 %) in PBS and lysis with SDS lysis buffer (50 mM Tris-HCl pH 8, 150 mM NaCl, 2 mM EDTA, 1 % SDS). To dilute the samples, RIPA buffer (10 mM Tris-HCl pH 8, 150 mM NaCl, 2 mM EDTA, 1 % Triton, 0.1 % sodium deoxycholate, 0.1 % SDS) was used. After sonication, protein concentrations were quantified and 80 µg of total lysate were incubated with 25 µl of High Capacity Streptavidin Agarose Resin (ThermoFisher, 20361). Samples were incubated rotating 2h at room temperature or overnight at 4 °C. Beads were washed with RIPA buffer and bound proteins were eluted in Laemmli buffer supplemented with 3 mM biotin by boiling at 95 °C. Eluted proteins were separated on 8 % SDS-polyacrylamide gel and Western blot analysis was performed.

RNA extraction and RT-qPCR

RNA was extracted from DIV 7 neurons using the RNeasy Mini Kit (QIAGEN) and Reverse Transcription was performed using the High-Capacity cDNA Reverse Transcription Kit (ThermoFisher) according to manufacturer's protocol. RT-qPCR was carried out using the StepOnePlus real-time PCR system (Life Technologies) and power Sybr Green master mix (Applied Biosystems). Reaction volumes of 20 µl with the following specific primers (0.5 µM) were used (Rangel, Madronal et al., 2009):

Gene	Forward Primer 5'-3'	Reverse Primer 5'-3'
GluA1	CTCGCCCTTGTCGTACCAC	GTCCGCCCTGAGAAATCCAG
GluA2	GTGTCGCCCATCGAAAGTG	AGTAGGCATACTTCCCTTTGGAT
GluK2	ATCGGATATTCGCAAGGAACC	CCATAGGGCCAGATTCCACA
GluK3	AGGTCCTAATGTCACTGACTCTC	GCCATAAAGGGTCCTATCAGAC
GluN2B	GCCATGAACGAGACTGACCC	GCTTCCTGGTCCGTGTCATC
β-Actin	CCCAGAGCAAGAGAGG	GTCCAGACGCAGGAT
GAPDH	AGGTCGGTGTGAACGGATTTG	TGTAGACCATGTAGTTGAGGTCA

Amplification conditions consisted of 15″ denaturation at 95°C; 1 min of annealing and elongation at 60°C for 40 cycles. The results were normalized by the expression levels of *gapdh and βactin*. Data were analyzed by StepOne Software (Applied Biosystems) following the $2^{-\Delta\Delta CT}$ method (Livak & Schmittgen, 2001).

Analysis of GluK2 editing

cDNA extract from DIV 7 neurons (see session RNA extraction and RT-qPCR) was used as template to amplify the M2 region of GluK2. The following primers were used: GluK2 5′-GGTATAATCGACACCCTTGCAACC-3′, GluK2 5′-TGACTCCATTAAGAAAGCATAATCGGA-3′. BbvI (New England Biolabs) digestion was performed according to manufacturer's protocol and was used to determine the level of GluK2 RNA editing (Bernard, Ferhat et al., 1999). The digested product was run on 2% agarose gel, and bands were quantified using NIH ImageJ. To determine the level of editing, was used the formula (intensity of 376 [edited] / intensity of [376 (edited) + 269 (unedited)]) × 100, according to Evans et al. (Evans et al., 2017) . The band at 76 bp was used to determine equal loading.

Inhibitor treatment of neurons

The BACE inhibitor C3 (β-secretase inhibitor IV; Calbiochem, 565788, final concentration 2 µM) was applied to neurons at DIV 5 supplemented to fresh medium. Treatment was prolonged for 48h and lysates collected at DIV 7.

Co-immunoprecipitation

HEK293T were transfected with 1 µg of pcDNA3.6 mycGluR6a(Q) plasmid kindly provided by Prof. Christophe Mulle (Jaskolski, Normand et al., 2005) and 0.5 µg of different SEZ6 and SEZ6L2 constructs (see previous description). 72h later, cells were lysated in 20mM HEPES pH 7.4, 150mM NaCl, 0.5% NP-40, 2mM EDTA, 10% Glycerol and lysates were incubated with protein G agarose beads preconjugated with GluR6/7 antibody (10 µls of antibody and 300 µl of beads were used for 14 samples) O/N at 4 °C. After washing, proteins were eluted in Laemmli Buffer, boiled at 95°C for 5 minutes and loaded on a 4-12% MOPS gradient gel (GenScript). Detection was done with GluR6/7 (04-921, Millipore) and anti- HA.11 (MMS-101P, Covance) antibodies. For the Co-immunoprecipitation followed by mass spectrometry analysis, 50ul of protein G agarose beads per sample were conjugated with 5ul of GluR6/7 antibody or 600ul SEZ6 14E5 hybridoma supernatant o/n, at 4°C, with rotation. Conjugated beads were washed 3 times with PBS and 50 µl of the bis(sulfosuccinimidyl)suberate (BS3) solution (2.5 mM BS3 in PBS) was added and incubated 1 h, RT, rotating. BS3 crosslinked PGS beads were then washed in different solutions: three times with 50 µl of 100 mM glycine pH 2.8, two times with PBS supplemented with 1% Igepal CA-630 (v/v) and finally one time with PBS. After washing, crosslinked beads were incubated with 2mg of brain homogenate in the HEPES NP40 buffer O/N, at 4°C on rotator. Samples were washed three times with HEPES NP40 buffer and eluted in 30 µl of 8% formic acid for 10 min, RT.

Lectin chip microarray (LecChip)

For lectin chip microarray analysis (LecChip), primary neuronal cultures from WT (n = 3) and SEZ6KO mice (n = 4) were first lysed in STET-Buffer (50 mM Tris, pH 7.5, 150 mM NaCl, 2 mM EDTA, 1% Triton-X, PI mix 1:500) and brought to identical protein concentrations (measurement was performed by BCA reagent, Uptima Interchim, UP95425) in TBS to obtain a 0.05 mg/ml solution. LecChip (GlycoTechnica Ltd.) was washed three times with Probing Solution (provided by the manufacturer), and lysates (1 µg/ml) were added to the wells in Probing Solution. Samples were incubated overnight at 18 °C. After incubation, an excess blocker glycoprotein was added to the chip and incubated for 30 min. The Blocking solution was then discarded, and the chip was washed 3 times with 0.1% TBST. Anti GluR6/7 antibody (04-921, Millipore) in blocking solution in TBS was then applied to the chip, and incubated for 1h. After three washes with 0.1% TBST, AF555-labeled goat anti rabbit (Life Technologies) solution in 0.1% TBST was added and incubated for 30 min. Subsequently, the LecChip was washed with TBS and double-distilled water 30 min each. The LecChip was scanned with InnoScan 710 Microarray scanner (Innopsys) and

results were analyzed with CLIQS Array Professional software (TotalLab). Overall, 45 lectin intensities were measured in each sample. An average Pearson correlation coefficient of 0.98 and above was calculated for all samples. Lectin intensities were considered and discoveries were determined using the Original FDR method of Benjamini and Hochberg, with Q = 2%.

Immunoprecipitation and HNK-1 detection

Protein G agarose beads preconjugated with GluR6/7 (1.5 µl of antibody and 40 µl of beads per sample) or NCAM-1 antibody (12.5 µl of antibody and 40 µl of beads per sample) were incubated with 200 ug of total brain homogenates O/N at 4 °C. After washing, proteins were eluted in Laemmli Buffer, boiled at 95°C for 5 minutes and loaded on a 4-12% MOPS gradient gel (GenScript) or 8% gel. Detection was done with HNK-1 1C10 supernatant (Developmental Studies Hybridoma Bank). As control for the specificity of the HNK-1 antibody, the proteins pulled down from two WT samples were digested with PNGase F before elution to remove HNK-1 epitope.

SUSPECS labeling of proteins for mass spectrometry analysis

Surface labeling and processing of the samples were performed as previously described (Herber et al., 2018). Briefly, 40 million primary cortical SEZ6 flox/flox neurons were infected at 2 DIV with iCRE (SEZ6KO neurons) or GFP (control) virus. At 5 DIV medium was replaced with fresh neuronal culture medium supplemented with 50 µM Ac4-ManNAz. At DIV7 biotinylation of glycoproteins at the cell surface was performed via bioorthogonal click chemistry applying 100 µM DBCO-PEG12-biotin (Click-chemistry tools) for 2h at 4 °C. Cells were lysed in STET-lysis buffer (150 mM NaCl, 50 mM Tris (pH 7.5), 2 mM EDTA, 1% Triton X-100) with protease inhibitor, centrifuged and lysates were filtered through a 0.45µM syringe filter (Millipore). Cell lysates of 3 control (GFP) and 3 SEZ6KO (iCRE) were loaded on a polyprep chromatography column (Biorad) containing 300 µL of high capacity streptavidin agarose beads (Thermofisher) and washed with 10 mL 2% SDS in PBS to remove non-specifically bound proteins. Streptavidin-beads were dried completely and proteins were eluted from the beads by boiling 5 min at 95°C in 150 µL Laemmli buffer supplemented with 8 M urea and 3 mM biotin. Samples were separated with 10% SDS-polyacrylamide gel electrophoresis (PAGE) and stained with 0.025% (w/v) Coomassie Brilliant Blue in 10% acetic acid. The gel was destained in 10% acetic acid and each lane was cut into 14 horizontal slices (=14 fractions) at equal height and subjected to tryptic in-gel digestion.

In gel-digestion and peptide purification

In gel digestion and peptide purification were performed as previously described (Shevchenko, Tomas et al., 2006). Briefly, proteins residing in the gel were denatured with 10 mM dithiothreitol (DTT) in 100 mM ammonium bicarbonate (ABC), reduced with 55 mM iodoacetamide (IAA) in 100 mM ABC and proteolytic digestion was performed at 37°C overnight using 150 ng trypsin per

fraction. 40% acetonitrile (ACN) supplemented with 0.1% formic acid was used to extract the peptides. Peptides were dried by vacuum centrifugation, and reconstituted in 0.1% formic acid for proteomic analysis.

LC-MS/MS analysis

Each gel fraction was analyzed on an Easy nLC-1000 (Thermo Sceintific, US), which was coupled online via a nano electrospray source (Thermo Scientific, US) equipped with a PRSO-V1 column oven (Sonation, Germany) to a Velos Pro Orbitrap Mass Spectrometer (Thermo). Peptides were separated on a self-packed C18 column (300 mm × 75µm, ReproSil-Pur 120 C18-AQ, 2.4 µm, Dr. Maisch, Germany) with a binary gradient of water (A) and acetonitrile (B) containing 0.1% formic acid (0 min, 2% B; 3:30 min 5% B; 48:30 min, 25% B; 59:30, 35% B; 64:30, 60% B) at a flow rate of 250 nL/min and column temperature of 50°C. Full MS spectra were acquired in profile mode at a resolution of 30,000 covering a m/z range of 300-2000. The ten most intense peptide ions per full MS scan were chosen for collision induced dissociation (CID) within in the ion trap (isolation width: 2 m/z; normalized collision energy: 35%; activation q: 0.25; activation time: 10 ms). A dynamic exclusion of 40 s was applied for peptide fragmentation. Two technical replicates were acquired per sample.

LC-MS/MS data analysis and statistical evaluation

Database search and label free quantification was performed with the software MaxQuant (version 1.4.1.2, maxquant.org) (Cox & Mann, 2008). Trypsin was defined as protease (cleavage specificity: C-terminal of K and R). Carbamidomethylation of cysteines was defined as fixed modification. Oxidation of methionines and acetylation of protein N-termini were defined as variable modifications. Two missed cleavages were allowed for peptide identification. The first search option was enabled to recalibrate precursor masses using the default values. The data was searched against a mouse database including isoforms (UniProt, download: May 16th, 2014; 51,389 entries). The false discovery rate (FDR) was adjusted to less than 1% for both, peptides and proteins. Common contaminants such as bovine proteins of fetal calf serum and human keratins were excluded. Label-free quantification (LFQ) intensity values were used for relative quantification. At least two ratio counts of razor and unique peptides were required for protein quantification. The LFQ intensities of the technical replicates were averaged and LFQ ratios (SEZ6KO/WT) were calculated separately for each biological replicate. The LFQ ratios were log2 transformed and a one-sample t-test ($\mu 0 = 0$) was applied to identify proteins with a significant abundance difference at the cell surface proteome.

Preparation of acute hippocampal slices

Wild type and SEZ6-/- mice on a C57BL/6 background at postnatal day P15 were used in the experiments. After the mice were deeply anesthetized with CO_2 and decapitated, the brain was immediately removed and immersed in ice-cold slicing solution containing (in mM) 24.7 glucose, 2.48 KCl, 65.47 NaCl, 25.98 $NaHCO_3$, 105 sucrose, 0.5 $CaCl_2$, 7 $MgCl_2$, 1.25 NaH_2PO_4, and 1.7 ascorbic acid (Fluka, Switzerland).The pH value was adjusted with to 7.4 with HCl and stabilized by bubbling with carbogen which contained 95% O_2 and 5% CO_2 and the osmolality was 290-300 mOsm. 300 µm horizontal hippocampal slices were cut in the slicing solution by the use of a vibratome (VT1200S; Leica, Germany). Brain slices were kept in a recovering solution which contained (in mM) 2 $CaCl_2$, 12.5 glucose, 2.5 KCl, 2 $MgCl_2$, 119 NaCl, 26 $NaHCO_3$, 1.25 NaH_2PO_4, 2 thiourea (Sigma, Germany), 5 Na-ascorbate (Sigma), 3 Na-pyruvate (Sigma), and 1 glutathion monoethyl ester (Santa Cruz Biotechnology, USA) at room temperature for at least one hour before the experiment. The pH value of the recovering solution was adjusted to 7.4 with HCl and constantly bubbled with carbogen, and the osmolality was 290 mOsm.

Electrophysiological recordings

After resting in the recovery solution for at least 1 hour, individual hippocampal slices were transferred to the recording chamber, which was constantly perfused at a flow rate of 3 ml/min with artificial cerebrospinal fluid (ACSF) containing (in mM) 2 $CaCl_2$, 20 glucose, 4.5 KCl, 1 $MgCl_2$, 125 NaCl, 26 $NaHCO_3$, and 1.25 NaH_2PO_4 and gassed with 95% O_2 and 5% CO_2 to ensure oxygen saturation and to maintain a pH value of 7.4. 30 µM D-AP5 (Abcam and Tocris, USA), 20 µM GYKI53655 (Tocris), and 10 µM bicuculline (Enzo, USA) were added to the ACSF to block NMDAR-, AMPAR- and $GABA_AR$-mediated synaptic transmission. Somatic whole-cell recordings from CA1 pyramidal neurons were performed with a borosilicate glass pipette with the resistance of ca. 7 MΩ filled with internal solution which contained (in mM) 148 K-gluconate, 10 HEPES, 10 NaCl, 0.5 MgCl2, 4 Mg-ATP, 0.4 Na3-GTP. The pH value of internal solution was adjusted to 7.3 with KOH. Voltage-clamp measurements were carried out using an EPC9/2 patch-clamp amplifier (HEKA, Germany). The membrane potential was held at -70 mV in voltage-clamp mode without liquid junction potential adjustment. Data acquisition and the generation of stimulation protocols were applied by the use of PULSE software (HEKA). Data were collected at 10 kHz and Bessel-filtered at 2.9 kHz and analyzed through Igor 5 software (Wavemetrics, USA).

RUSH Cargo Sorting Assay using Confocal Microscopy

RUSH Cargo Sorting Assay was performed as described previously (Deng, Pakdel et al., 2018). SBP-mCherry-GluK2 construct was kindly provided by Jeremy Henley (Evans et al., 2017). HEK293T cells were cultured on sterile glass slides coated with Poly-D-lysine (Sigma, P6407) in 6-wells. After 24h cells were transfected with 1.2 ug of SBP-mCherry-GluK2 and 50 ng of pFUW HA-SLIC-Flagx2-mmSEZ6FL, pFUW HA-SLIC-Flagx2-mmSEZ6L2 or pFUW HA-SLIC-Flagx2-inactive

iCRE. After 72h, cells were incubated with 40 µM d-Biotin (SUPELCO) in DMEM for 0h, 20 and 40 minutes. As a control, cells without d-Biotin were monitored to confirm retention of the reporter in the ER. After washing with 1x PBS, cells were fixed with 4% paraformaldehyde in PBS for 10 min and prepared for immunofluorescence microscopy. 5F8 anti-Red (Chromotek, dilution 1:300) and anti- HA.11 (MMS-101P, Covance, dilution 1:300) were incubated for at least 3h room temperature or 4 °C overnight. AF488-labeled goat anti mouse (Life Technologies) and AF555-labeled goat anti rat (Life Technologies) secondary antibodies were incubated for 1h at room temperature and Hoechst for 10 minutes at room temperature. Sample images were acquired using a confocal laser-scanning microscope (LSM 780; Carl Zeiss) with 100x magnification (oil objective). To image the complete cell, 10-18 stacks in Z-direction with a step/size of 0.35 µm were recorded of each field of view. For the analysis with ImageJ/Fiji, only cells showing transport of the reporter from the ER to Golgi after Biotin incubation were considered, while cells showing ER signal after Biotin addition were excluded. Furthermore only vesicles of cells expressing the GFP as well as the RUSH-construct were counted.

Glycome analysis

8M guanidine hydrochloride (GuHCl), 1-hydroxybenzotriazole hydrate (HOBt), 50% sodium hydroxide, super DHB matrix (2-hydroxy-5-methoxy-benzoic acid and 2,5-dihydroxybenzoic acid, 1:9), trifluoroacetic acid (TFA), 28-30% ammonium hydroxide solution and lyophilized recombinant PNGase F from Flavobacterium meningosepticum were obtained from Sigma-Aldrich (St. Louis, MO). HPLC SupraGradient acetonitrile (ACN) was obtained from Biosolve (Valkenswaard, The Netherlands). Dithiothreitol (DTT), ethanol and sodium bicarbonate (NaHCO3) were from Merck (Darmstadt, Germany) and 1-ethyl-3-(3-dimethylaminopropyl) carbodiimide (EDC) from Fluorochem (Hadfield, UK). The peptide calibration standard was purchased from Bruker Daltonics (Bremen, Germany). MultiScreen® HTS 96 multiwell plates (pore size 0.45 µm) with high protein-binding membrane (hydrophobic Immobilon-P PVDF membrane) were purchased from Millipore (Amsterdam, The Netherlands), conical 96-well Nunc plates from Thermo Scientific (Roskilde, Denmark). All buffers were prepared using ultra-pure deionized water (MQ) was generated by the Purelab Ultra, maintained at 18.2 MΩ (Veolia Water Technologies Netherlands B.V., Ede, The Netherlands).

Preparation of released N-glycans from cell pellet

N-glycans were released from twelve biological replicates per condition (0.5 × 10 E6 cells each/25 µl) using a 96-well plate PVDF-membrane based N-glycan release protocol as described earlier(Holst, Deuss et al., 2016). Briefly, cell pellets were suspended in MQ and sonicated for 30 min. As controls, Visucon pooled human plasma as well as water blanks were used. Denaturation buffer (5.8 m GuHCl and 5 mM DTT) and 25 µl dissolved cell pellet were onto a preconditioned

HTS 96-well plates with hydrophobic Immobilon-P PVDF membrane and incubated for 30 min at 60 °C. The wells were washed twice with 200 µl mQ with 5 min incubation steps on a horizontal shaker prior to centrifugation and once with 200 µl 100 mM NaHCO3 (1 min, 500 × g). For N-glycan release, 15 µl 100 mm NaHCO3 and 1 mU PNGase F were added per well. After 20 min incubation an additional 15 µl buffer was added. Plates were placed into the incubation device and incubated for overnight at 37 °C. Glycans were recovered into 96-well collection plates by centrifugation (2 min, 1000 × g); eventual residual solution was collected from the membrane and wash 3 times with 40 µl water. Samples were dried for 2 at 45 °C in a vacuum centrifuge and finally dissolved in 25 µl water.

MALDI-TOF (/TOF)-MS(/MS) analysis of released glycans

Prior to MALDI-TOF-MS analysis, sialic acids were stabilized in a linkage-specific way by ethyl esterification and amidation (Reiding, Blank et al., 2014), purified by cotton-HILIC-SPE, and MALDI-TOF-MS analysis was performed on an UltrafleXtreme (Bruker Daltonics) operated under flexControl 3.3 (Build 108; Bruker Daltonics). Ten microliters of the released glycans were added to 50 µL derivatization reagent (250 mM 1-ethyl-3-(3-(dimethylamino)propyl)carbodiimide and 250 mM 1-hydroxybenzotriazole in ethanol) and incubated for 30 min at 37°C at which 10 µL 28-30% ammonium hydroxide is added for amidation. Sixty microliters of ACN were added and derivatized glycans were enriched by cotton hydrophilic-interaction liquid chromatography (HILIC)−solid-phase extraction (SPE) as described before and eluted in 10 µL water (Selman, Hemayatkar et al., 2011). Five µL of the enriched ethyl-esterified glycans was spotted on a MALDI target (MTP AnchorChip 800/384 TF; Bruker Daltonics) together with 1 µL 5 mg/mL super-DHB in 50% ACN and 1 mM NaOH. The spots were dried by air at room temperature. For each spot, a mass spectrum was recorded from m/z 1 000 to 5 000, combining 20 000 shots in a random walk patter at 5 000 Hz and 100 shots per raster spot. Prior to the analysis of the samples, the instrument was calibrated using peptide calibration standard (Bruker Daltonics).

Data processing

For automated relative quantification of the released glycans analyzed by MALDI-TOF-MS, using MassyTools (version 0.1.8.1.) (Jansen, Reiding et al., 2015), the MALDI-TOF-MS files were converted to text files. Spectra were internally calibrated using glycan peaks of known composition signals with a S/N above nine (Supporting Information, ST1), covering the m/z range of the glycans. Integration was performed on targeted peaks for visually determined list of glycans, including at least 95% of the theoretical isotopic pattern. Several quality parameters assess the actual presence of a glycan based on the mass accuracy (between -20 and 20 ppm), the deviation from the theoretical isotopic pattern (below 25%) and the S/N (above nine) of an integrated signal.

Analytes were included for all samples when present in at least two-thirds of one of the biological replicates. Glycan composition (n = 54) signals were normalized to the total signal intensity (Supporting Information, ST2).

Preparation of CoIP samples for mass spectrometry analysis

The protein concentrations of the co-IP samples were estimated using the Pierce 660 nm assay supplemented with the ionic detergent compatibility reagent (Thermo Fisher Scientific, US). A protein amount of 20 µg was subjected to proteolytic digestion using the filter aided sample preparation (FASP) protocol with 30 kDa Vivacon filters (Sartorius, Germany) as previously described (Wisniewski, Zougman et al., 2009). Peptides were purified with self-packed C18 stop and go extraction (STAGE) tips as previously described (Rappsilber, Ishihama et al., 2003).

MS analysis of Co-IP samples

Co-IP samples were analysed on an Easy nLC 1200 nanoHPLC (Thermo Scientific) which was coupled online via a Nanospray Flex Ion Source (Thermo Sientific, US) equipped with a PRSO-V1 column oven (Sonation, Germany) to a Q-Exactive HF mass spectrometer (Thermo Scientific, US). An amount of 1.3 µg of peptides per sample was separated on an in-house packed C18 column (30 cm x 75 µm ID, ReproSil-Pur 120 C18-AQ, 1.9 µm, Dr. Maisch GmbH,Germany) using a binary gradient of water (A) and acetonitrile (B) supplemented with 0.1% formic acid (0 min., 2% B; 3:30 min., 5% B; 137:30 min., 25% B; 168:30 min., 35% B; 182:30 min., 60% B) at 50°C column temperature. A data-dependent acquisition method was used. Full MS scans were acquired at a resolution of 120,000 (m/z range: 300-1400, AGC target: 3E+6). The ten most intense peptide ions per full MS scan were selected for peptide fragmentation (resolution: 15,000, isolation width: 1.6 m/z, AGC target: 1E+5, NCE: 26%). A dynamic exclusion of 120 s was used for peptide fragmentation.

The raw data was analysed with the software Maxquant (maxquant.org, Max-Planck Institute Munich) version 1.5.5.1 (Cox, Hein et al., 2014). The MS data was searched against a reference fasta database of Mus musculus from UniProt (download: March 09th 2017, 16851 entries). Trypsin was defined as protease. Two missed cleavages were allowed for the database search. The option first search was used to recalibrate the peptide masses within a window of 20 ppm. For the main search peptide and peptide fragment mass tolerances were set to 4.5 and 20 ppm, respectively. Carbamidomethylation of cysteine was defined as static modification. Acetylation of the protein N-term as well as oxidation of methionine was set as variable modifications. The false discovery rate for both peptides and proteins was adjusted to less than 1%. The “match between runs” option was enabled with a matching window of 2 min. Label free quantification (LFQ) of proteins required at least two ratio counts of razor or unique peptides. Only razor and unique peptides were used for quantification.

Ethics approval and consent to participate

All animal procedures were performed in accordance with either the European Communities Council Directive (86/609/EEC) or Australian Code of Practice for the Care and Use of Animals for Scientific Purposes. Animal protocols were approved by the Ludwigs-Maximilians-University Munich and the government of Upper Bavaria, or alternatively the Anatomy & Neuroscience, Pathology, Pharmacology, and Physiology Animal Ethics Committee of the University of Melbourne, Australia.

Statistics

In general, data were analysed using Mann-Whitney test and considered significant when p-value was lower than 0.05. At least 6 replicates from 2 biological replicates were considered, as specified for each experiment in the figure legend. In figure 5, discoveries were determined using the FDR method of Benjamini and Hochberg, with Q = 2% and at least 3 mouse brains per genotype were used. When three conditions were compared in figure 6, data from 3 independent experiments were analysed using Kruskal-Wallis. Mass spectrometry data were analysed as described in the previous sessions.

Acknowledgements

We thank Katrin Moschke, Anna Berghofer, Claudia Ihbe and Marek-Jan Czyz for their technical assistance. We thank Rohit Kumar for help with electrophysiology experiments and Hiroshi Takeshima for providing triple SEZ6 KO mice. This work was supported by the Deutsche Forschungsgemeinschaft (German Research Foundation) within the framework of the Munich Cluster for Systems Neurology (EXC 2145 SyNergy) and the research unit FOR2290 and by the Centers of Excellence in Neurodegeneration, Bayerisches Hochschulzentrum für Mittel-, Ost- und Südosteuropa (BAYHOST).). M.A.B. and J.H. are supported by the UK Dementia Research Institute which receives its funding from DRI Ltd, funded by the Medical Research Council, Alzheimer's Society and Alzheimer Research UK. M.A.B. is also funded by a UKRI Future Leaders Fellowship.

References

- Ambalavanan A, Girard SL, Ahn K, Zhou S, Dionne-Laporte A, Spiegelman D, Bourassa CV, Gauthier J, Hamdan FF, Xiong L, Dion PA, Joober R, Rapoport J, Rouleau GA (2015) De novo variants in sporadic cases of childhood onset schizophrenia. European journal of human genetics : EJHG
- Ball SM, Atlason PT, Shittu-Balogun OO, Molnar E (2010) Assembly and intracellular distribution of kainate receptors is determined by RNA editing and subunit composition. Journal of neurochemistry 114: 1805-18
- Bernard A, Ferhat L, Dessi F, Charton G, Represa A, Ben-Ari Y, Khrestchatisky M (1999) Q/R editing of the rat GluR5 and GluR6 kainate receptors in vivo and in vitro: evidence for independent developmental, pathological and cellular regulation. The European journal of neuroscience 11: 604-16
- Boncompain G, Divoux S, Gareil N, de Forges H, Lescure A, Latreche L, Mercanti V, Jollivet F, Raposo G, Perez F (2012) Synchronization of secretory protein traffic in populations of cells. Nature methods 9: 493
- Bonifacino JS, Traub LM (2003) Signals for sorting of transmembrane proteins to endosomes and lysosomes. Annual review of biochemistry 72: 395-447
- Bortolotto ZA, Clarke VR, Delany CM, Parry MC, Smolders I, Vignes M, Ho KH, Miu P, Brinton BT, Fantaske R, Ogden A, Gates M, Ornstein PL, Lodge D, Bleakman D, Collingridge GL (1999) Kainate receptors are involved in synaptic plasticity. Nature 402: 297-301
- Brookmeyer R, Evans DA, Hebert L, Langa KM, Heeringa SG, Plassman BL, Kukull WA (2011) National estimates of the prevalence of Alzheimer's disease in the United States. Alzheimer's & dementia : the journal of the Alzheimer's Association 7: 61-73
- Brummer T, Muller SA, Pan-Montojo F, Yoshida F, Fellgiebel A, Tomita T, Endres K, Lichtenthaler SF (2019) NrCAM is a marker for substrate-selective activation of ADAM10 in Alzheimer's disease. EMBO molecular medicine
- Bureau I, Bischoff S, Heinemann SF, Mulle C (1999) Kainate Receptor-Mediated Responses in the CA1 Field of Wild-Type and GluR6-Deficient Mice. The Journal of Neuroscience 19: 653-663
- Carlin RK, Grab DJ, Cohen RS, Siekevitz P (1980) Isolation and characterization of postsynaptic densities from various brain regions: enrichment of different types of postsynaptic densities. The Journal of cell biology 86: 831-45
- Chou DK, Ilyas AA, Evans JE, Costello C, Quarles RH, Jungalwala FB (1986) Structure of sulfated glucuronyl glycolipids in the nervous system reacting with HNK-1 antibody and some IgM paraproteins in neuropathy. The Journal of biological chemistry 261: 11717-25
- Colombo A, Hsia HE, Wang M, Kuhn PH, Brill MS, Canevazzi P, Feederle R, Taveggia C, Misgeld T, Lichtenthaler SF (2018) Non-cell-autonomous function of DR6 in Schwann cell proliferation. The EMBO journal 37
- Contractor A, Mulle C, Swanson GT (2011) Kainate receptors coming of age: milestones of two decades of research. Trends in neurosciences 34: 154-63
- Contractor A, Swanson G, Heinemann SF (2001) Kainate receptors are involved in short- and long-term plasticity at mossy fiber synapses in the hippocampus. Neuron 29: 209-16
- Copits BA, Swanson GT (2012) Dancing partners at the synapse: auxiliary subunits that shape kainate receptor function. Nat Rev Neurosci 13: 675-86
- Cox J, Hein MY, Luber CA, Paron I, Nagaraj N, Mann M (2014) Accurate proteome-wide label-free quantification by delayed normalization and maximal peptide ratio extraction, termed MaxLFQ. Molecular & cellular proteomics : MCP 13: 2513-26
- Cox J, Mann M (2008) MaxQuant enables high peptide identification rates, individualized p.p.b.-range mass accuracies and proteome-wide protein quantification. Nature biotechnology 26: 1367-72
- Dancourt J, Barlowe C (2010) Protein sorting receptors in the early secretory pathway. Annual review of biochemistry 79: 777-802

- Deng Y, Pakdel M, Blank B, Sundberg EL, Burd CG, von Blume J (2018) Activity of the SPCA1 Calcium Pump Couples Sphingomyelin Synthesis to Sorting of Secretory Proteins in the Trans-Golgi Network. Developmental cell 47: 464-478.e8
- Dislich B, Wohlrab F, Bachhuber T, Muller SA, Kuhn PH, Hogl S, Meyer-Luehmann M, Lichtenthaler SF (2015) Label-free Quantitative Proteomics of Mouse Cerebrospinal Fluid Detects beta-Site APP Cleaving Enzyme (BACE1) Protease Substrates In Vivo. Molecular & cellular proteomics : MCP 14: 2550-63
- Escudero-Esparza A, Kalchishkova N, Kurbasic E, Jiang WG, Blom AM (2013) The novel complement inhibitor human CUB and Sushi multiple domains 1 (CSMD1) protein promotes factor I-mediated degradation of C4b and C3b and inhibits the membrane attack complex assembly. Faseb j 27: 5083-93
- Evans AJ, Gurung S, Wilkinson KA, Stephens DJ, Henley JM (2017) Assembly, Secretory Pathway Trafficking, and Surface Delivery of Kainate Receptors Is Regulated by Neuronal Activity. Cell reports 19: 2613-2626
- Forneris F, Wu J, Xue X, Ricklin D, Lin Z, Sfyroera G, Tzekou A, Volokhina E, Granneman JC, Hauhart R, Bertram P, Liszewski MK, Atkinson JP, Lambris JD, Gros P (2016) Regulators of complement activity mediate inhibitory mechanisms through a common C3b-binding mode. The EMBO journal 35: 1133-1149
- Gally C, Eimer S, Richmond JE, Bessereau JL (2004) A transmembrane protein required for acetylcholine receptor clustering in Caenorhabditis elegans. Nature 431: 578-82
- Gendrel M, Rapti G, Richmond JE, Bessereau JL (2009) A secreted complement-control-related protein ensures acetylcholine receptor clustering. Nature 461: 992-6
- Gilissen C, Hehir-Kwa JY, Thung DT, van de Vorst M, van Bon BW, Willemsen MH, Kwint M, Janssen IM, Hoischen A, Schenck A, Leach R, Klein R, Tearle R, Bo T, Pfundt R, Yntema HG, de Vries BB, Kleefstra T, Brunner HG, Vissers LE et al. (2014) Genome sequencing identifies major causes of severe intellectual disability. Nature 511: 344-7
- Goodman RA, Lochner KA, Thambisetty M, Wingo TS, Posner SF, Ling SM (2017) Prevalence of dementia subtypes in United States Medicare fee-for-service beneficiaries, 2011-2013. Alzheimer's & dementia : the journal of the Alzheimer's Association 13: 28-37
- Gunnersen JM, Kim MH, Fuller SJ, De Silva M, Britto JM, Hammond VE, Davies PJ, Petrou S, Faber ES, Sah P, Tan SS (2007) Sez-6 proteins affect dendritic arborization patterns and excitability of cortical pyramidal neurons. Neuron 56: 621-39
- Herber J, Njavro J, Feederle R, Schepers U, Muller U, Brase S, Muller S, Lichtenthaler SF (2018) Click chemistry-mediated biotinylation reveals a function for the protease BACE1 in modulating the neuronal surface glycoproteome. Molecular & cellular proteomics : MCP
- Herbst R, Nicklin MJ (1997) SEZ-6: promoter selectivity, genomic structure and localized expression in the brain. Brain research Molecular brain research 44: 309-22
- Holst S, Deuss AJ, van Pelt GW, van Vliet SJ, Garcia-Vallejo JJ, Koeleman CA, Deelder AM, Mesker WE, Tollenaar RA, Rombouts Y, Wuhrer M (2016) N-glycosylation Profiling of Colorectal Cancer Cell Lines Reveals Association of Fucosylation with Differentiation and Caudal Type Homebox 1 (CDX1)/Villin mRNA Expression. Molecular & cellular proteomics : MCP 15: 124-40
- Hu S, Wong DT (2009) Lectin microarray. Proteomics Clinical applications 3: 148-54
- Jansen BC, Reiding KR, Bondt A, Hipgrave Ederveen AL, Palmblad M, Falck D, Wuhrer M (2015) MassyTools: A High-Throughput Targeted Data Processing Tool for Relative Quantitation and Quality Control Developed for Glycomic and Glycoproteomic MALDI-MS. Journal of proteome research 14: 5088-98
- Jaskolski F, Coussen F, Nagarajan N, Normand E, Rosenmund C, Mulle C (2004) Subunit composition and alternative splicing regulate membrane delivery of kainate receptors. The Journal of neuroscience : the official journal of the Society for Neuroscience 24: 2506-15
- Jaskolski F, Normand E, Mulle C, Coussen F (2005) Differential trafficking of GluR7 kainate receptor subunit splice variants. The Journal of biological chemistry 280: 22968-76

- Jeffries AR, Mungall AJ, Dawson E, Halls K, Langford CF, Murray RM, Dunham I, Powell JF (2003) beta-1,3-Glucuronyltransferase-1 gene implicated as a candidate for a schizophrenia-like psychosis through molecular analysis of a balanced translocation. Molecular psychiatry 8: 654-63
- Kahler AK, Djurovic S, Rimol LM, Brown AA, Athanasiu L, Jonsson EG, Hansen T, Gustafsson O, Hall H, Giegling I, Muglia P, Cichon S, Rietschel M, Pietilainen OP, Peltonen L, Bramon E, Collier D, St Clair D, Sigurdsson E, Petursson H et al. (2011) Candidate gene analysis of the human natural killer-1 carbohydrate pathway and perineuronal nets in schizophrenia: B3GAT2 is associated with disease risk and cortical surface area. Biological psychiatry 69: 90-6
- Khoonsari PE, Haggmark A, Lonnberg M, Mikus M, Kilander L, Lannfelt L, Bergquist J, Ingelsson M, Nilsson P, Kultima K, Shevchenko G (2016) Analysis of the Cerebrospinal Fluid Proteome in Alzheimer's Disease. PloS one 11: e0150672
- Kim MH, Gunnersen JM, Tan SS (2002) Localized expression of the seizure-related gene SEZ-6 in developing and adult forebrains. Mechanisms of development 118: 171-4
- Kizuka Y, Oka S (2012) Regulated expression and neural functions of human natural killer-1 (HNK-1) carbohydrate. Cellular and molecular life sciences : CMLS 69: 4135-47
- Kruse J, Mailhammer R, Wernecke H, Faissner A, Sommer I, Goridis C, Schachner M (1984) Neural cell adhesion molecules and myelin-associated glycoprotein share a common carbohydrate moiety recognized by monoclonal antibodies L2 and HNK-1. Nature 311: 153-5
- Kuhn PH, Koroniak K, Hogl S, Colombo A, Zeitschel U, Willem M, Volbracht C, Schepers U, Imhof A, Hoffmeister A, Haass C, Rossner S, Brase S, Lichtenthaler SF (2012) Secretome protein enrichment identifies physiological BACE1 protease substrates in neurons. The EMBO journal 31: 3157-68
- Laurent SA, Hoffmann FS, Kuhn PH, Cheng Q, Chu Y, Schmidt-Supprian M, Hauck SM, Schuh E, Krumbholz M, Rubsamen H, Wanngren J, Khademi M, Olsson T, Alexander T, Hiepe F, Pfister HW, Weber F, Jenne D, Wekerle H, Hohlfeld R et al. (2015) gamma-Secretase directly sheds the survival receptor BCMA from plasma cells. Nature communications 6: 7333
- Lein ES, Hawrylycz MJ, Ao N, Ayres M, Bensinger A, Bernard A, Boe AF, Boguski MS, Brockway KS, Byrnes EJ, Chen L, Chen L, Chen TM, Chin MC, Chong J, Crook BE, Czaplinska A, Dang CN, Datta S, Dee NR et al. (2007) Genome-wide atlas of gene expression in the adult mouse brain. Nature 445: 168-76
- Lerma J, Marques JM (2013) Kainate receptors in health and disease. Neuron 80: 292-311
- Lichtenthaler SF (2012) Cell biology. Sheddase gets guidance. Science (New York, NY) 335: 179-80
- Lichtenthaler SF, Lemberg MK, Fluhrer R (2018) Proteolytic ectodomain shedding of membrane proteins in mammals-hardware, concepts, and recent developments. The EMBO journal 37
- Livak KJ, Schmittgen TD (2001) Analysis of relative gene expression data using real-time quantitative PCR and the 2(-Delta Delta C(T)) Method. Methods (San Diego, Calif) 25: 402-8
- Maccarrone G, Ditzen C, Yassouridis A, Rewerts C, Uhr M, Uhlen M, Holsboer F, Turck CW (2013) Psychiatric patient stratification using biosignatures based on cerebrospinal fluid protein expression clusters. Journal of psychiatric research 47: 1572-80
- Mah SJ, Cornell E, Mitchell NA, Fleck MW (2005) Glutamate receptor trafficking: endoplasmic reticulum quality control involves ligand binding and receptor function. The Journal of neuroscience : the official journal of the Society for Neuroscience 25: 2215-25
- Mennesson M, Rydgren E, Lipina T, Sokolowska E, Kulesskaya N, Morello F, Ivakine E, Voikar V, Risbrough V, Partanen J, Hovatta I (2019) Kainate receptor auxiliary subunit NETO2 is required for normal fear expression and extinction. Neuropsychopharmacology : official publication of the American College of Neuropsychopharmacology
- Miyazaki T, Hashimoto K, Uda A, Sakagami H, Nakamura Y, Saito SY, Nishi M, Kume H, Tohgo A, Kaneko I, Kondo H, Fukunaga K, Kano M, Watanabe M, Takeshima H (2006) Disturbance of cerebellar synaptic maturation in mutant mice lacking BSRPs, a novel brain-specific receptor-like protein family. FEBS letters 580: 4057-64
- Morise J, Takematsu H, Oka S (2017) The role of human natural killer-1 (HNK-1) carbohydrate in neuronal plasticity and disease. Biochimica et biophysica acta General subjects 1861: 2455-2461

- Morita I, Kakuda S, Takeuchi Y, Itoh S, Kawasaki N, Kizuka Y, Kawasaki T, Oka S (2009) HNK-1 glyco-epitope regulates the stability of the glutamate receptor subunit GluR2 on the neuronal cell surface. The Journal of biological chemistry 284: 30209-17
- Nakayama M, Hama C (2011) Modulation of neurotransmitter receptors and synaptic differentiation by proteins containing complement-related domains. Neuroscience research 69: 87-92
- Nasu-Nishimura Y, Jaffe H, Isaac JT, Roche KW (2010) Differential regulation of kainate receptor trafficking by phosphorylation of distinct sites on GluR6. The Journal of biological chemistry 285: 2847-56
- Ng D, Pitcher GM, Szilard RK, Sertie A, Kanisek M, Clapcote SJ, Lipina T, Kalia LV, Joo D, McKerlie C, Cortez M, Roder JC, Salter MW, McInnes RR (2009) Neto1 is a novel CUB-domain NMDA receptor-interacting protein required for synaptic plasticity and learning. PLoS biology 7: e41
- Paracchini L, Beltrame L, Boeri L, Fusco F, Caffarra P, Marchini S, Albani D, Forloni G (2018) Exome sequencing in an Italian family with Alzheimer's disease points to a role for seizure-related gene 6 (SEZ6) rare variant R615H. Alzheimer's research & therapy 10: 106
- Parker BL, Thaysen-Andersen M, Solis N, Scott NE, Larsen MR, Graham ME, Packer NH, Cordwell SJ (2013) Site-specific glycan-peptide analysis for determination of N-glycoproteome heterogeneity. Journal of proteome research 12: 5791-800
- Pigoni M, Wanngren J, Kuhn PH, Munro KM, Gunnersen JM, Takeshima H, Feederle R, Voytyuk I, De Strooper B, Levasseur MD, Hrupka BJ, Muller SA, Lichtenthaler SF (2016) Seizure protein 6 and its homolog seizure 6-like protein are physiological substrates of BACE1 in neurons. Molecular neurodegeneration 11: 67
- Pinheiro PS, Perrais D, Coussen F, Barhanin J, Bettler B, Mann JR, Malva JO, Heinemann SF, Mulle C (2007) GluR7 is an essential subunit of presynaptic kainate autoreceptors at hippocampal mossy fiber synapses. Proceedings of the National Academy of Sciences of the United States of America 104: 12181-6
- Rangel A, Madronal N, Gruart A, Gavin R, Llorens F, Sumoy L, Torres JM, Delgado-Garcia JM, Del Rio JA (2009) Regulation of GABA(A) and glutamate receptor expression, synaptic facilitation and long-term potentiation in the hippocampus of prion mutant mice. PloS one 4: e7592
- Rappsilber J, Ishihama Y, Mann M (2003) Stop and go extraction tips for matrix-assisted laser desorption/ionization, nanoelectrospray, and LC/MS sample pretreatment in proteomics. Analytical chemistry 75: 663-70
- Reiding KR, Blank D, Kuijper DM, Deelder AM, Wuhrer M (2014) High-throughput profiling of protein N-glycosylation by MALDI-TOF-MS employing linkage-specific sialic acid esterification. Analytical chemistry 86: 5784-93
- Roitman M, Edgington-Mitchell LE, Mangum J, Ziogas J, Adamides AA, Myles P, Choo-Bunnett H, Bunnett NW, Gunnersen JM (2019) Sez6 levels are elevated in cerebrospinal fluid of patients with inflammatory pain–associated conditions. PAIN Reports 4: e719
- Selman MH, Hemayatkar M, Deelder AM, Wuhrer M (2011) Cotton HILIC SPE microtips for microscale purification and enrichment of glycans and glycopeptides. Analytical chemistry 83: 2492-9
- Sherwood JL, Amici M, Dargan SL, Culley GR, Fitzjohn SM, Jane DE, Collingridge GL, Lodge D, Bortolotto ZA (2012) Differences in kainate receptor involvement in hippocampal mossy fibre long-term potentiation depending on slice orientation. Neurochemistry international 61: 482-9
- Shevchenko A, Tomas H, Havlis J, Olsen JV, Mann M (2006) In-gel digestion for mass spectrometric characterization of proteins and proteomes. Nature protocols 1: 2856-60
- Shikano S, Li M (2003) Membrane receptor trafficking: evidence of proximal and distal zones conferred by two independent endoplasmic reticulum localization signals. Proceedings of the National Academy of Sciences of the United States of America 100: 5783-8
- Stanic K, Saldivia N, Forstera B, Torrejon M, Montecinos H, Caprile T (2016) Expression Patterns of Extracellular Matrix Proteins during Posterior Commissure Development. Frontiers in neuroanatomy 10: 89

- Straub C, Hunt DL, Yamasaki M, Kim KS, Watanabe M, Castillo PE, Tomita S (2011) Distinct functions of kainate receptors in the brain are determined by the auxiliary subunit Neto1. Nature neuroscience 14: 866-73
- Tang M, Pelkey KA, Ng D, Ivakine E, McBain CJ, Salter MW, McInnes RR (2011) Neto1 is an auxiliary subunit of native synaptic kainate receptors. The Journal of neuroscience : the official journal of the Society for Neuroscience 31: 10009-18
- Tomita S, Castillo PE (2012) Neto1 and Neto2: auxiliary subunits that determine key properties of native kainate receptors. The Journal of physiology 590: 2217-23
- Vassar R, Kuhn PH, Haass C, Kennedy ME, Rajendran L, Wong PC, Lichtenthaler SF (2014) Function, therapeutic potential and cell biology of BACE proteases: current status and future prospects. Journal of neurochemistry 130: 4-28
- Vernon CG, Copits BA, Stolz JR, Guzman YF, Swanson GT (2017) N-glycan content modulates kainate receptor functional properties. The Journal of physiology 595: 5913-5930
- Wang R, Mellem JE, Jensen M, Brockie PJ, Walker CS, Hoerndli FJ, Hauth L, Madsen DM, Maricq AV (2012) The SOL-2/Neto auxiliary protein modulates the function of AMPA-subtype ionotropic glutamate receptors. Neuron 75: 838-50
- Wisniewski JR, Zougman A, Nagaraj N, Mann M (2009) Universal sample preparation method for proteome analysis. Nature methods 6: 359-62
- Yaguchi H, Yabe I, Takahashi H, Watanabe M, Nomura T, Kano T, Matsumoto M, Nakayama KI, Watanabe M, Hatakeyama S (2017) Sez6l2 regulates phosphorylation of ADD and neuritogenesis. Biochemical and biophysical research communications 494: 234-241
- Yan D, Tomita S (2012) Defined criteria for auxiliary subunits of glutamate receptors. The Journal of physiology 590: 21-31
- Zhang W, St-Gelais F, Grabner CP, Trinidad JC, Sumioka A, Morimoto-Tomita M, Kim KS, Straub C, Burlingame AL, Howe JR, Tomita S (2009) A transmembrane accessory subunit that modulates kainate-type glutamate receptors. Neuron 61: 385-96
- Zheng Y, Brockie PJ, Mellem JE, Madsen DM, Walker CS, Francis MM, Maricq AV (2006) SOL-1 is an auxiliary subunit that modulates the gating of GLR-1 glutamate receptors in Caenorhabditis elegans. Proceedings of the National Academy of Sciences of the United States of America 103: 1100-5
- Zheng Y, Mellem JE, Brockie PJ, Madsen DM, Maricq AV (2004) SOL-1 is a CUB-domain protein required for GLR-1 glutamate receptor function in C. elegans. Nature 427: 451-7
- Zhu K, Xiang X, Filser S, Marinkovic P, Dorostkar MM, Crux S, Neumann U, Shimshek DR, Rammes G, Haass C, Lichtenthaler SF, Gunnersen JM, Herms J (2018) Beta-Site Amyloid Precursor Protein Cleaving Enzyme 1 Inhibition Impairs Synaptic Plasticity via Seizure Protein 6. Biological psychiatry 83: 428-437

Figure Legends

Figure 1: Loss of SEZ6 selectively changes the levels of GluK2 and GluK3 at the neuronal surface. A) Workflow of the surface analysis performed in SEZ6KO and WT neurons. SEZ6 flox/flox neurons were infected with iCRE (SEZ6KO) and GFP (WT) virus at DIV2 and metabolic labeling was started at DIV5. Surface analysis was performed at DIV7. **B)** Protein classification of the total proteins (3209, left panel) and of the glycoproteins (571, right panel) detected in 3 out of 3 experiments. More than 90% of the glycoproteins detected are classified as membrane proteins, as expected for the surface labeling. **C)** Changes of glycosylated proteins on the cell surface of SEZ6KO neurons compared to WT. The average log2 fold change of SEZ6KO neurons over WT (log2 SEZ6KO/WT) is plotted against the negative log10 of each protein's p-value according to a one-sample t test. Blue labeled dots are considered as hits (including GluK2 and GluK3) and are proteins with a p-value less than 0.05 (neg. log10(0.05)=1.3; horizontal dotted line) and a fold-change to less than -0.5 or more than 0.5 (vertical dotted lines). GluK2 and GluK3 are labeled in pink, GluA1 and GluA2 are indicated with green lines and dots and GluN1 and GluN2B are marked with red lines and dots.

Figure 2: Validation of GluK2/3 reduction on the surface of SEZ6KO neurons by immunoblot. A) SEZ6KO and WT neurons were biotinylated with Sulfo-NHS-Biotin and surface proteins were enriched by streptavidin bead pull-down. The GluK2/3 antibody cannot discriminate the subunits 2 and 3 (Lerma & Marques, 2013), therefore the band is commonly indicated with the labeling GluK2/3. GluK2/3, GluA2 and GluN2B surface levels were quantified, normalized to SEZ6L2 surface levels (negative control) in the same sample (GluK2/3 / SEZ6L2) and divided by the WT levels, with the ratio for WT being set to 1.0 (plot shows mean ± S.E.M., at least 10 replicates in 4 independent biological experiments, Mann-Whitney p-value<0.005). **B)** mRNA levels of GluA1, GluA2, GluK2, GluK3 and GluN2B were quantified in SEZ6KO neurons, normalized to GAPDH and β-actin mRNA in the same sample and compared to the mRNA levels in WT neurons (6 replicates in 2 independent biological experiments). No difference in *GluK2/3* mRNA was detected in SEZ6KO neurons compared to WT. **C)** Editing of GluK2 mRNA was tested in SEZ6KO and WT neurons. The editing value was calculated as (intensity of 376 [edited] / intensity of [376 (edited) + 269 (unedited)]) × 100 and normalized to the band at 76 bp. No difference was detected in SEZ6KO neurons compared to WT (plot shows mean ± S.E.M., 6 replicates in 2 independent biological experiments).

Figure 3: Reduced kainate-evoked inward currents in the absence of SEZ6. (A) *Left*: Current trace resulting from whole-cell voltage-clamp recordings at a holding potential of -70 mV in a CA1 pyramidal neuron in a WT mouse hippocampal slice (P15). The current was recorded in the presence of 10 µM bicuculline, 20 µM GYKI53655 and 30 µM APV in the ACSF. Perfusion of the recording chamber with 10 µM kainate and 100 µM 2,3-dioxo-6-nitro-1,2,3,4-

tetrahydrobenzo[f]quinoxaline-7-sulfonamide (NBQX) are indicated with green and blue bars, respectively. *Right*: Analogous experiment in a SEZ6KO mouse (P15). **(B)** Summary of the experiments in A. Bar graph illustrates mean charge carried by the inward currents (measured as area under the curve, AUC) for the two genotypes at P15 (WT 46.6 ± 0.5 nC (n=10 cells), SEZ6KO 30.8 ± 0.5 nC (n=9 cells), p=0.0375 Mann-Whitney-U-test).

Figure 4: Loss of SEZ6 impairs glycosylation and maturation of GluK2/3. A) In WT neurons, GluK2/3 was seen as two closely comigrating bands, whereas the upper one of lower intensity was missing or running even more closely to the lower band of main intensity in SEZ6KO neurons (schematic representation on the right). When the total lysates of SEZ6KO and WT neurons were digested with endoglycosidase H (EndoH) – which removes immature, but not mature sugars – the two closely comigrating bands were converted to three bands of a lower apparent molecular weight, consistent with full deglycosylation of the lowest band and a partial deglycosylation of the upper two bands (marked in blue, red and green in the right panel). In SEZ6KO neurons the uppermost (light blue) band was missing and a new band of lower apparent molecular weight was seen that was overlapping with the red labeled band and was indicated with the pink asterisk in the SEZ6KO. No difference in the glycosylation of GluA2 was detectable, pointing to a specific effect of SEZ6 on GluK2/3. **B)** The running pattern of GluK2/3 in SEZ6KO and WT brains was compared upon EndoH digestion. Similar to primary neurons, GluK2/3 displayed an immature glycosylation pattern in SEZ6KO brains. **C)** Total GluK2/3 levels were quantified and showed a significant but moderate reduction in SEZ6KO compared to WT neuronal lysates (plot shows mean ± S.E.M., 9 replicates in 3 independent biological experiments, Mann-Whitney p-value<0.005). **D)** No significant change in GluK2/3 total levels was detectable in SEZ6KO and WT adult brains (plot shows mean ± S.E.M., 6 replicates). **E)** Synaptosomes from knock-out (KO) brains of single SEZ6 family members (SEZ6, SEZ6L, SEZ6L2), triple knock-out (TKO) and respective controls (WT and TWT – triple WT) were digested with EndoH. GluK2/3 displayed the immature glycosylation in SEZ6KO and TKO brains, but not in SEZ6L and SEZ6L2 brains, demonstrating non-redundant functions for the SEZ6 family members. **F)** Brain homogenates from SEZ6KO and WT mice at different ages were digested with EndoH. GluK2/3 displayed the immature glycosylation at all developmental stages of SEZ6KO mice, suggesting that no compensation effect is occurring with aging.

Figure 5: Loss of SEZ6 reduces HNK-1 epitope on GluK2/3. A) The glycome fingerprint of GluK2/3 was analyzed by lectin chip microarray (LecChip). Lectin PHAL and PHAE (indicated with asterisks) detected reduced amounts of the oligosaccharide Galβ1-4GlcNAcβ1 on GluK2/3 in SEZ6KO neurons (plot shows mean ± S.E.M., 3 WT replicates and 4 SEZ6KO replicates were used, discoveries were determined using the FDR method of Benjamini and Hochberg, with Q = 2%). **B)** Immunoblot analysis revealed reduction of HNK-1 epitope on GluK2/3 in SEZ6KO brains. *Left panels*: Comparable amounts of GluK2/3 were immunoprecipitated (IP) in WT and SEZ6KO

brains using excess of brain homogenates compared to beads. Anti-HNK-1 antibody was used for detection. HNK-1 band on GluK2/3 was detected only in WT brains but not in SEZ6KO brains (n=6). As a control, HNK-1 modification of NCAM-1 was unaltered, as revealed after IP of NCAM-1 from WT and SEZ6KO brains (n = 3), followed by detection with anti-HNK-1 antibody. Different isoforms of NCAM-1 are annotated with arrowheads (NCAM 180, NCAM 140 and NCAM 120). *Mid panel*: To prove the specificity of the HNK-1 antibody, GluK2/3 was immunoprecipitated and digested with Peptide-N-Glycosidase F (PNGase F), which removes N-linked oligosaccharides. Upon PNGase F digestion, HNK-1 was not detectable in WT brains and the molecular weight of GluK2/3 was reduced. *Right panels*: In total brain homogenates (input), no difference of general HNK-1 epitope or NCAM-1 levels was detected.

Figure 6: SEZ6 facilitates GluK2/3 trafficking through the secretory pathway. A) Schematic representation of the RUSH Cargo Sorting Assay using Confocal Microscopy. HEK293T cells were transfected with the SBP-mCherry-GluK2 plasmid that expresses streptavidin binding peptide (SBP)—mCherry—GluK2 fusion protein and streptavidin-KDEL "anchor" that retains SBP-containing proteins in the ER. Upon addition of biotin in the cell culture medium, SBP-mCherry-GluK2 is released allowing its trafficking through the secretory pathway. **B)** SEZ6, SEZ6L2 and control plasmid (HA-iCRE) were co-transfected with SBP-mCherry-GluK2. Biotin was added to elicit release of SBP-mCherry-GluK2 from the ER (0 min) and cell were fixed at different time points (0, 20 and 40 min). White arrowheads point to Golgi-derived vesicles containing SBP-mCherry-GluK2. In red: SBP-mCherry-GluK2. In green: anti HA antibody detecting HA-iCRE, SEZ6 or SEZ6L2. **C)** The number of vesicles containing SBP-mCherry-GluK2 was determined at each time point. When SEZ6, but not SEZ6L2, was co-transfected, the number of vesicles containing SBP-mCherry-GluK2 was significantly higher compared to the control condition (plot shows mean ± S.D., 3 independent experiments, Kruskal-Wallis p-value < 0.01).

Figure 7: SEZ6 extracellular domain in the secretory pathway rescues GluK2/3 maturation in SEZ6KO neurons and binds to GluK2/3. A) Schematic representation of the constructs used: SEZ6 full length (SEZ6FL), SEZ6 lacking the C-terminal domain (SEZ6Δcyto), SEZ6 ectodomain generated by BACE1 cleavage (SEZ6ecto), SEZ6 C-terminal fragment generated by BACE1 cleavage (SEZ6CTF) and SEZ6 lacking the C-terminal domain but fused to an ER retention signal (SEZ6ΔcytoER). **B)** SEZ6 constitutive KO neurons were transduced with SEZ6 constructs. SEZ6FL and SEZ6Δcyto were detectable as two bands corresponding to mature (higher) and immature (lower) forms of SEZ6. No difference in the apparent molecular weight was detected because the high percentage of the gel used (12%) and the small C-terminal deletion (39 amino acids). SEZ6ecto was present as the immature band in the neuronal lysates and as the mature, secreted band in the conditioned medium **(C)**. SEZ6CTF (with HA and Flag-tags) was detected at the expected low molecular weight. Additionally, the C-terminal fragment generated from SEZ6FL by BACE1 cleavage was detected. Due to its lack of an HA-tag, it had a lower molecular weight

than SEZ6CTF. The C-terminal fragment generated from SEZ6Δcyto upon BACE1 cleavage was not visible because of its low molecular weight. GluK2/3 glycosylation was rescued when SEZ6FL, SEZ6Δcyto and SEZ6ecto were expressed in the neurons, but SEZ6CTF was not able to rescue the phenotype. **D)** Sez6 constitutive KO neurons were transduced with SEZ6ΔcytoER and SEZ6Δcyto. SEZ6ΔcytoER presented only the band corresponding to the immature form of SEZ6, as expected for a protein retained in the ER. SEZ6Δcyto, but not SEZ6ΔcytoER, was able to rescue GluK2/3 glycosylation, showing that SEZ6 localized to the ER is not sufficient to rescue the GluK2/3 glycosylation. **E)** HEK293T cells were co-transfected with a GluK2a plasmid and the SEZ6 constructs. Expression of SEZ6 constructs was analyzed in the total lysates (“Input”) and revealed a similar expression of the different proteins. GluK2a was immunoprcipitated with GluK2/3 antibody and the SEZ6 mutants were detected with the HA.11 antibody (“IP”). SEZ6FL, SEZ6Δcyto and SEZ6ecto, but not SEZ6CTF were co-immunoprecipitated with GluK2a, suggesting that SEZ6 extracellular domain is necessary for GluK2a binding.

Supplementary Figure Legends

Supplementary Fig. 1: Quality control of surface enrichment by Sulfo-NHS-Biotin. SEZ6KO and WT neurons were biotinylated with Sulfo-NHS-Biotin and surface proteins were enriched by streptavidin beads pull-down. Total proteins in the lysates (11 µg, "Total") and surface proteins (60 µg, "Surface") were analyzed by immunoblotting The efficiency of the enrichment is shown by the calnexin depletion, by the absence of immature SEZ6 (black star, Pigoni et al. 2016) and by the absence of a second GluA2 band at a lower molecular weight in the surface pull-down compared to the total lysates.

Supplementary Fig. 2: No changes in the total glycome of SEZ6KO neurons were detected. A general N-glycan analysis was performed using lysates of WT and SEZ6KO neurons. N-glycans were released from the protein extracts (Holst et al., 2016) and subject to MALDI-TOF mass spectrometric analysis. N-acetylneuraminic acids (NeuAc) were subjected to linkage-specific derivatization, allowing stabilization of the sialic acid residues and mass spectrometric distinction of sialic acid linkages on the basis of mass shifts induced by ethyl esterification (α2,6-linkage) and lactonization with sequential amidation (α2,3-linkage). 54 glycan structures were identified and quantified, and none of them showed differences between WT and SEZ6KO neurons (plot shows mean ± S.E.M., 11 WT replicates and 12 SEZ6KO replicates from 2 independent biological experiments were used).

Supplementary Fig 3: BACE1 cleavage does not affect the function of SEZ6 as GluK2/3 regulator. A) WT neurons were treated with the BACE inhibitor C3 or DMSO as control and surface biotinylation with Sulfo-NHS-Biotin was performed. BACE1 inhibition did not only prevent SEZ6ecto formation (Pigoni et al., 2016), but also increased full-length SEZ6 levels at the cell surface compared to the control condition. Even though SEZ6 full length accumulated on the cell surface of BACE-inhibitor treated neurons, no change in GluK2/3 amounts at the cell surface was detected. B) Membrane fraction of WT and BACE1KO brains was digested with EndoH. As expected, SEZ6 full length accumulates in the membrane fraction of BACE1KO brains. No change in GluK2/3 glycosylation or total amount was detected. C) WT and SEZ6KO neurons were treated with the BACE1 inhibitor C3 or DMSO as control and total lysates were analyzed with EndoH digestion. Even though SEZ6 full length accumulates upon BACE inhibition and GluK2/3 presents immature glycosylation in the SEZ6KO neurons, no change of GluK2/3 glycosylation or total amounts was seen when WT neurons were treated with C3. These indicates that both surface localization (A) and glycosylation (B and C) of GluK2/3 are likely to have reached their maximum in WT cells and cannot be enhanced by increased SEZ6 levels, as induced here through BACE1 inhibition.

Supplementary Fig 4: Proposed model for GluK2/3 regulation mediated by SEZ6. SEZ6 interacts with GluK2 in the early secretory pathway (ER) and facilitates its trafficking through the

secretory pathway. While trafficking into the Golgi, GluK2/3 undergoes several sugar modifications, including HNK-1 modification. Once reached the cell surface, SEZ6 and GluK2/3 separate and become independent from each other, explaining why BACE1 cleavage does not affect GluK2/3 maturation. When SEZ6 is not present, GluK2/3 trafficking is impaired and also its function at the cell surface.

Supplementary Table 1: Proteins significantly changed on the cell surface of SEZ6KO neurons compared to WT. Proteins with LFQ intensity lower than log2 ratio (SEZ6KO/WT)=-0.5 (0.71 fold change) or higher than log2 ratio(SEZ6KO/WT)=0.5 (1.4 fold change) and a p-value lower than 0.05 were considered as hits. Proteins are sorted according to their fold change ("Ratio") and their p-values is reported ("p-value"). Membrane ("Membrane"), soluble ("Soluble") and proteins with unknown classification ("Unknown") were detected, according to Uniprot.

Supplementary Table 2: Proteins co-immunoprecipitated with GluK2/3 in endogenous conditions. GluK2/3 and SEZ6 as control were immunoprecipitated in WT brain homogenates (n=6). Proteins co-immunoprecipitated with GluK2/3 in more than 4 out of 6 replicates and detected in less than 2 out of 6 controls, are reported in the table. Proteins are sorted according to their average LFQ intensity, showing at the top of the table the proteins giving a stronger signal. Neto2 was co-immunoprecipitated with GluK2/3 in endogenous conditions, but SEZ6 was not detectable ("NaN").

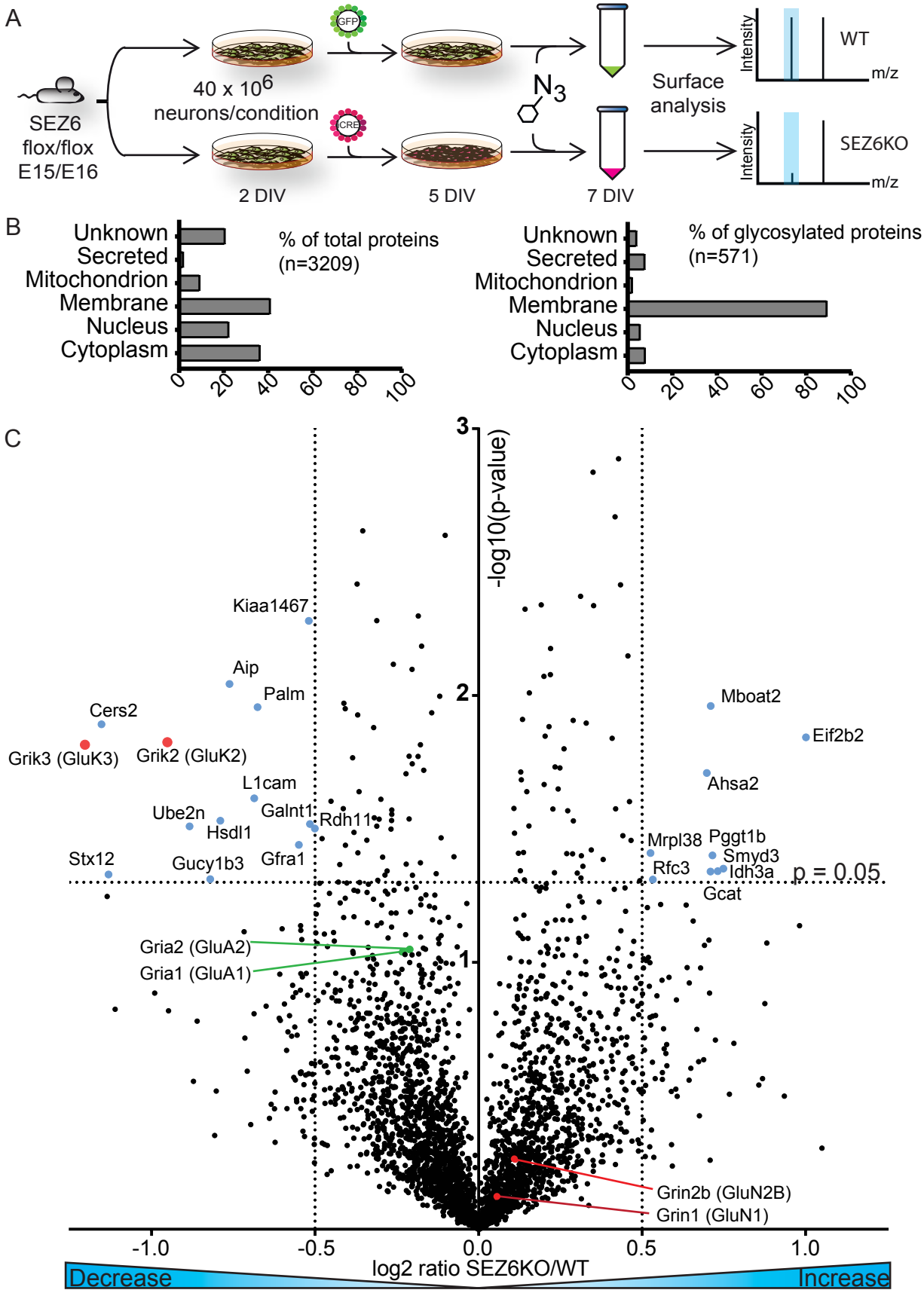
A
SEZ6
flox/flox
E15/E16
40 x 10^6
neurons/condition
GFP
CRE
2 DIV
5 DIV
N3
7 DIV
Surface
analysis
Intensity
WT
m/z
SEZ6KO
B
Unknown
Secreted
Mitochondrion
Membrane
Nucleus
Cytoplasm
% of total proteins
(n=3209)
% of glycosylated proteins
(n=571)
0
20
40
60
80
100
C
-log10(p-value)
3
2
1
Kiaa1467
Aip
Palm
Cers2
Grik3 (GluK3)
Grik2 (GluK2)
L1cam
Ube2n
Galnt1
Rdh11
Hsdl1
Gfra1
Stx12
Gucy1b3
Gria2 (GluA2)
Gria1 (GluA1)
Mboat2
Eif2b2
Ahsa2
Mrpl38
Pggt1b
Smyd3
Rfc3
Idh3a
Gcat
p = 0.05
Grin2b (GluN2B)
Grin1 (GluN1)
-1.0
-0.5
0.0
0.5
1.0
log2 ratio SEZ6KO/WT
Decrease
Increase

Figure 1

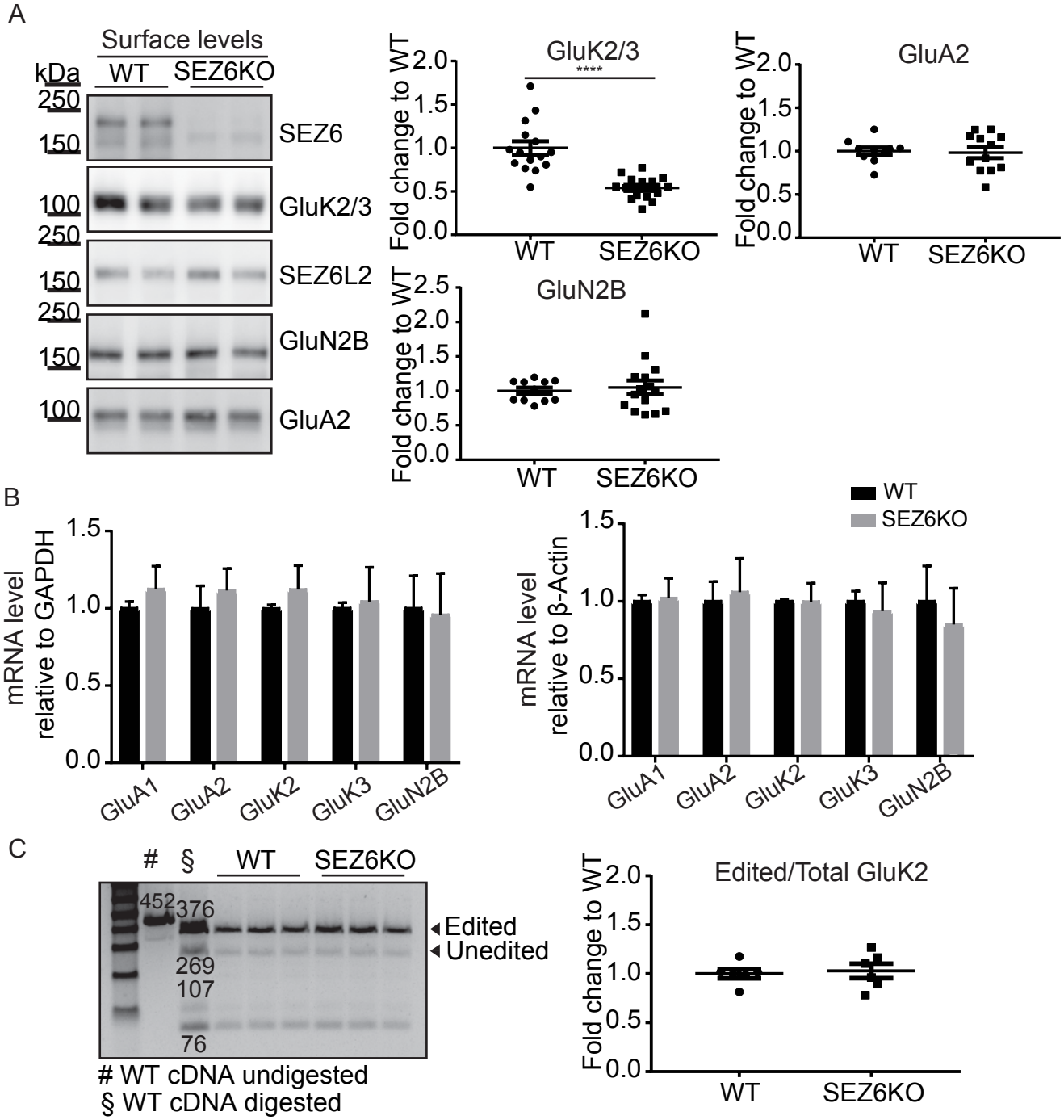
A
Surface levels
kDa
WT
SEZ6KO
250
150
100
250
150
250
150
100
SEZ6
GluK2/3
SEZ6L2
GluN2B
GluA2
GluK2/3
****
Fold change to WT
2.0
1.5
1.0
0.5
0.0
WT
SEZ6KO
GluA2
GluN2B
2.5
B
mRNA level relative to GAPDH
mRNA level relative to β-Actin
WT
SEZ6KO
GluA1
GluA2
GluK2
GluK3
GluN2B
C
#
§
452
376
269
107
76
Edited
Unedited
WT cDNA undigested
§ WT cDNA digested
Edited/Total GluK2

Figure 2

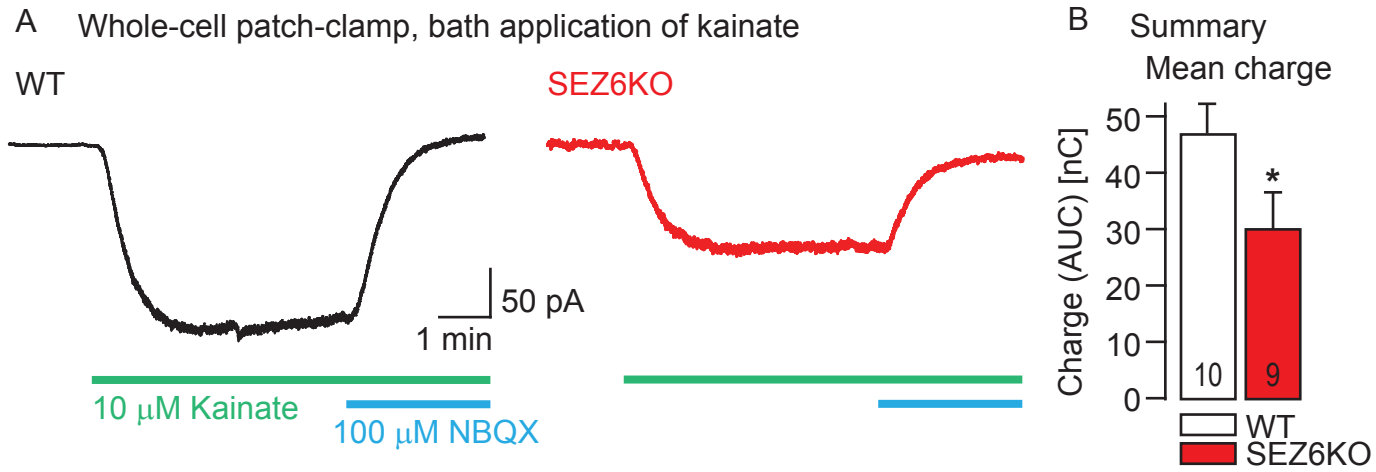
A
Whole-cell patch-clamp, bath application of kainate
WT
SEZ6KO
50 pA
1 min
10 μM Kainate
100 μM NBQX
B
Summary
Mean charge
Charge (AUC) [nC]
50
40
30
20
10
0
10
9
*
WT
SEZ6KO

Figure 3

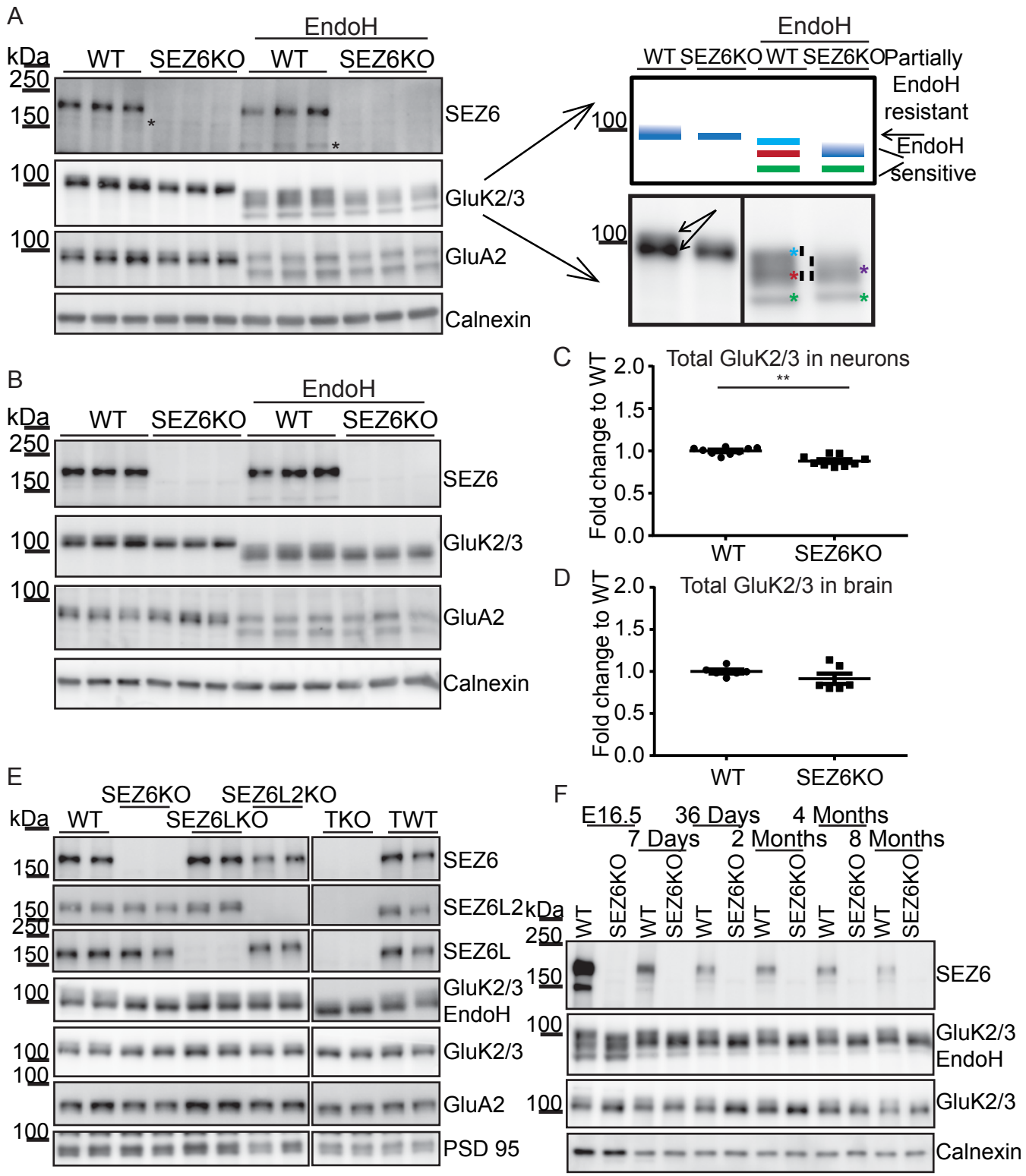
A
EndoH
kDa
WT
SEZ6KO
WT
SEZ6KO
250
150
100
100
SEZ6
GluK2/3
GluA2
Calnexin
EndoH
WT SEZ6KO WT SEZ6KO
Partially EndoH resistant
EndoH sensitive
100
100
B
EndoH
kDa
WT
SEZ6KO
WT
SEZ6KO
250
150
100
100
SEZ6
GluK2/3
GluA2
Calnexin
C
Total GluK2/3 in neurons
**
Fold change to WT
2.0
1.5
1.0
0.5
0.0
WT
SEZ6KO
D
Total GluK2/3 in brain
Fold change to WT
2.0
1.5
1.0
0.5
0.0
WT
SEZ6KO
E
SEZ6KO
SEZ6L2KO
kDa
WT
SEZ6LKO
TKO
TWT
150
150
250
150
100
100
100
100
SEZ6
SEZ6L2
SEZ6L
GluK2/3
EndoH
GluK2/3
GluA2
PSD 95
F
E16.5
36 Days
4 Months
7 Days
2 Months
8 Months
WT
SEZ6KO
kDa
250
150
100
100
SEZ6
GluK2/3
EndoH
GluK2/3
Calnexin

Figure 4

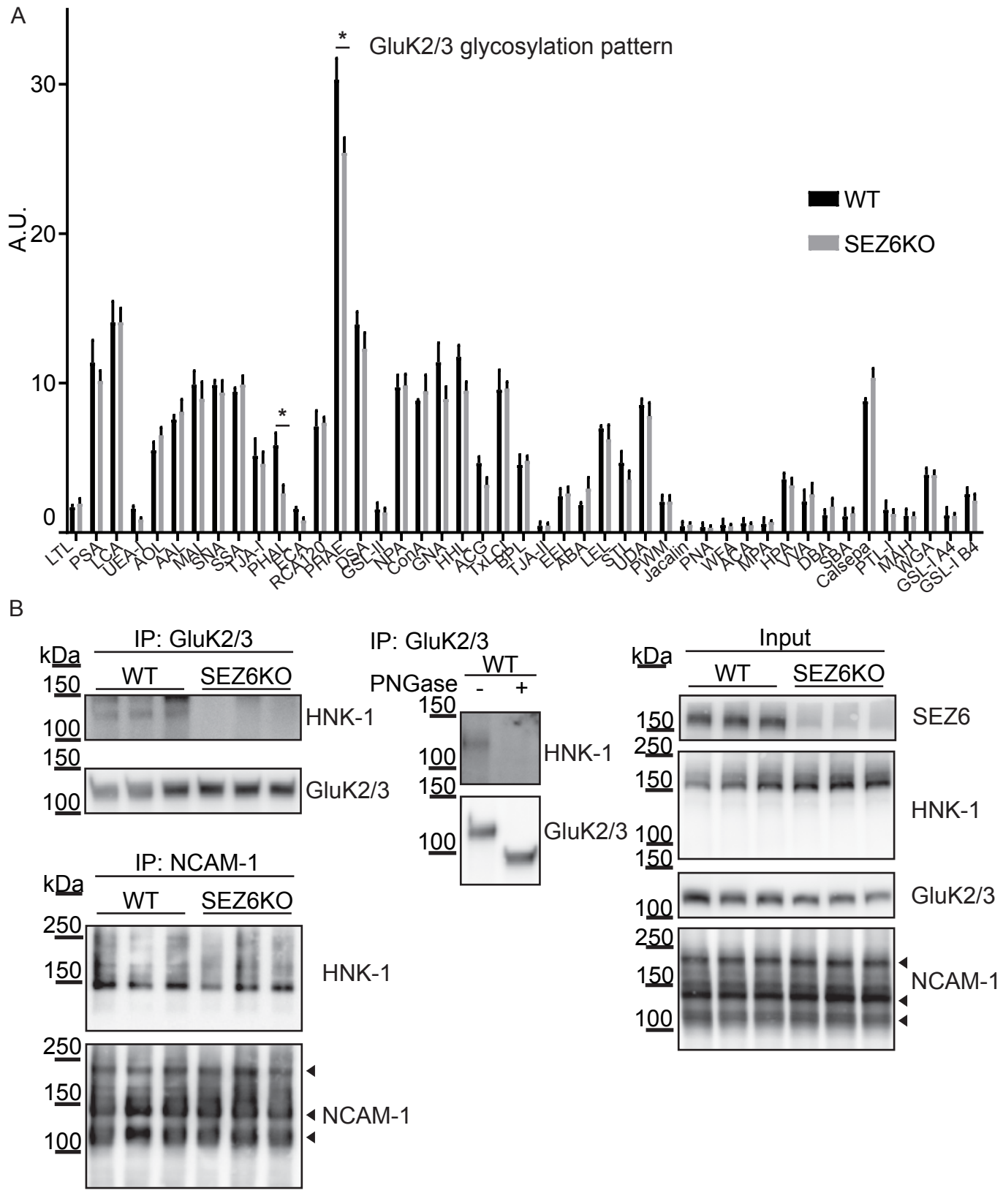
A
GluK2/3 glycosylation pattern
A.U.
30
20
10
0
WT
SEZ6KO
*
*
LTL
PSA
LCA
UEA-I
AOL
AAL
MAL
SNA
SSA
TJA-I
PHAL
ECA
RCA120
PHAE
DSA
GSL-II
NPA
ConA
GNA
HHL
ACG
TxLCI
BPL
TJA-II
EEL
ABA
LEL
STL
UDA
PWM
Jacalin
PNA
WFA
ACA
MPA
HPA
VVA
DBA
SBA
Calsepa
PTL-I
MAH
WGA
GSL-I A4
GSL-I B4
B
IP: GluK2/3
kDa
WT
SEZ6KO
150
100
HNK-1
150
100
GluK2/3
IP: NCAM-1
kDa
WT
SEZ6KO
250
150
HNK-1
250
150
100
NCAM-1
IP: GluK2/3
WT
PNGase
-
+
150
100
HNK-1
150
100
GluK2/3
Input
kDa
WT
SEZ6KO
150
SEZ6
250
150
HNK-1
100
150
GluK2/3
100
250
150
NCAM-1
100

Figure 5

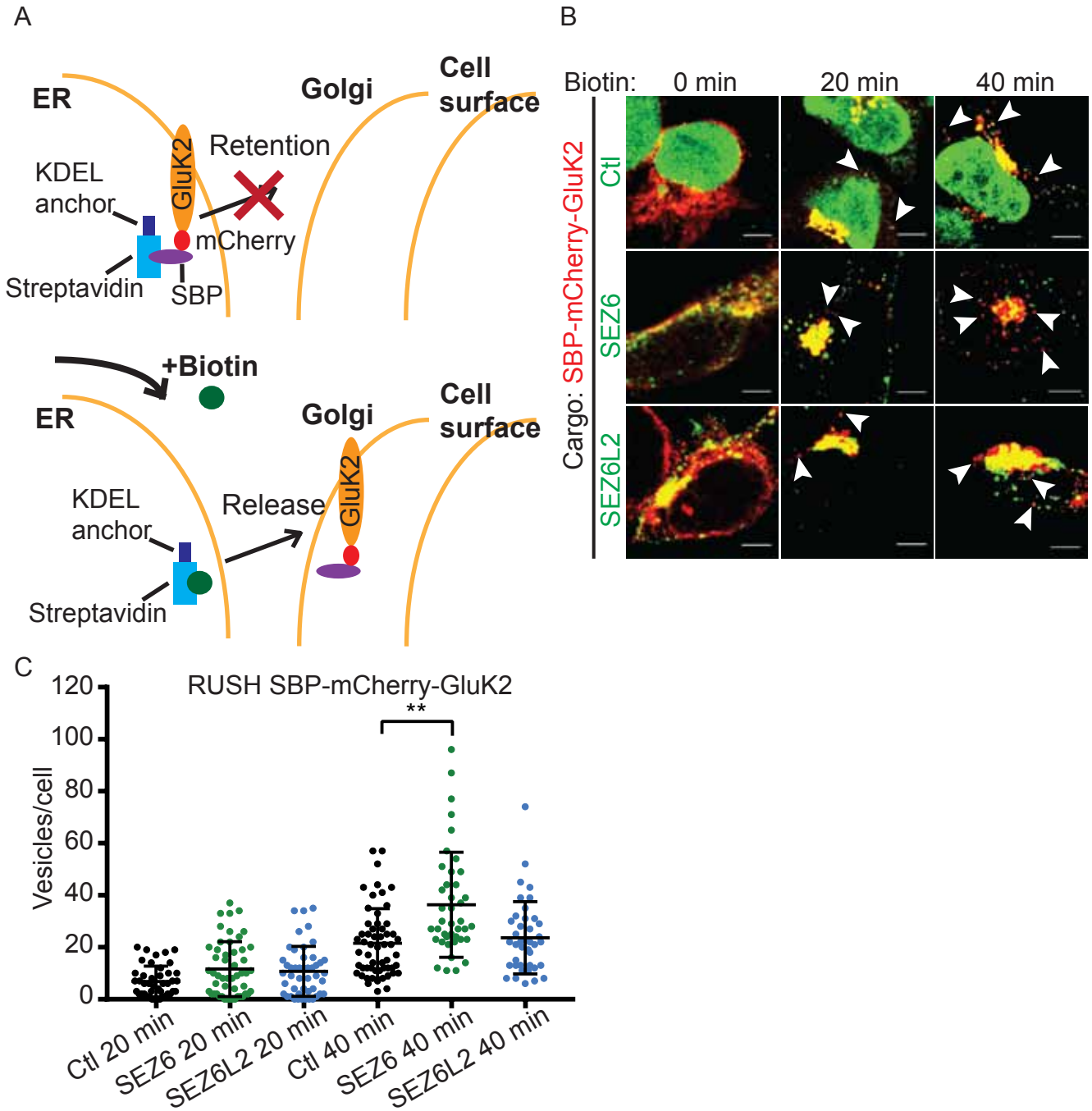
A
ER
Golgi
Cell surface
GluK2
Retention
KDEL anchor
mCherry
Streptavidin
SBP
+Biotin
ER
Golgi
Cell surface
KDEL anchor
Release
GluK2
Streptavidin
B
Biotin:
0 min
20 min
40 min
Cargo: SBP-mCherry-GluK2
Ctl
SEZ6
SEZ6L2
C
RUSH SBP-mCherry-GluK2
Vesicles/cell
120
100
80
60
40
20
0
**
Ctl 20 min
SEZ6 20 min
SEZ6L2 20 min
Ctl 40 min
SEZ6 40 min
SEZ6L2 40 min

Figure 6

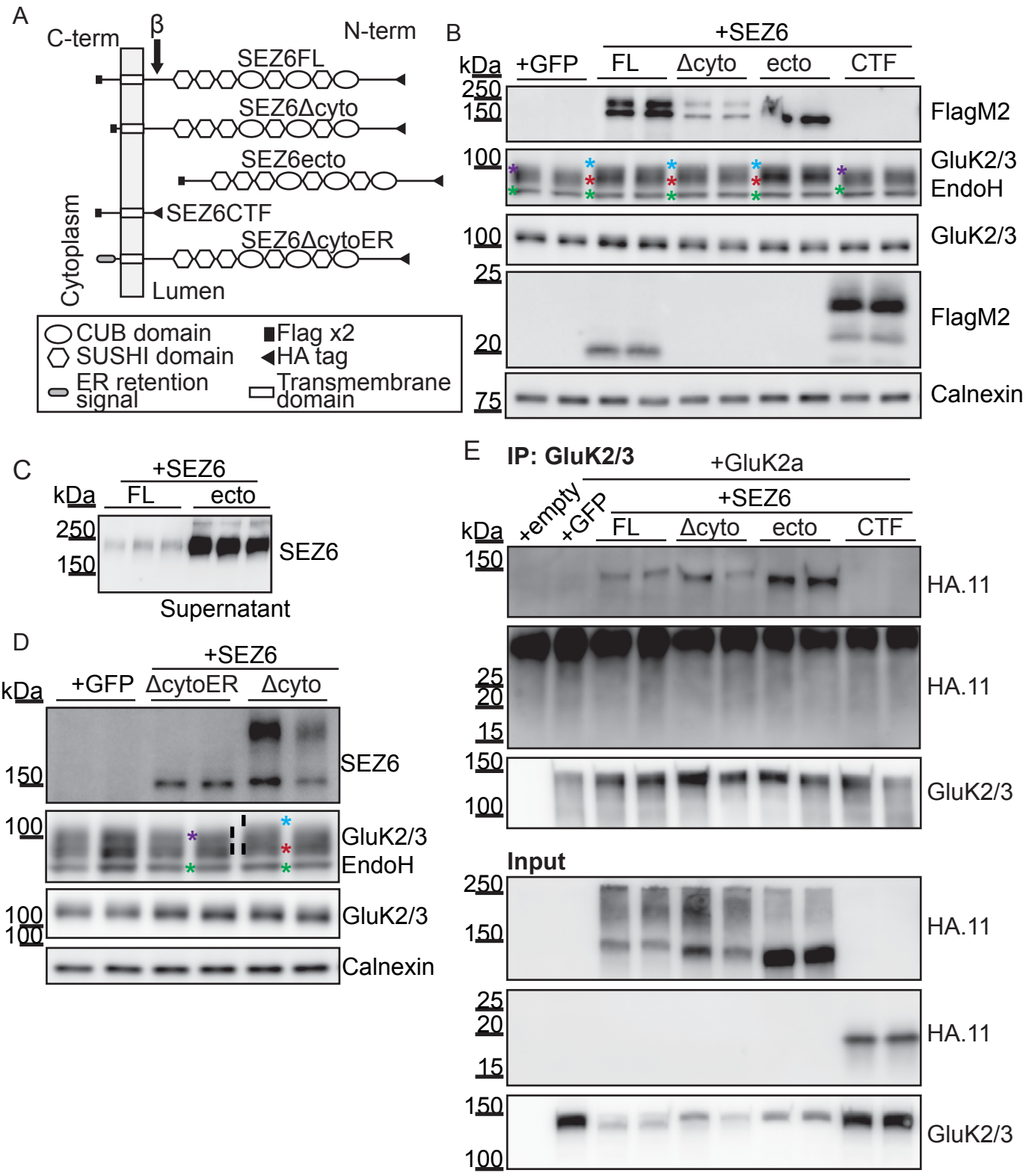
A
C-term
β
N-term
SEZ6FL
SEZ6Δcyto
SEZ6ecto
SEZ6CTF
SEZ6ΔcytoER
Cytoplasm
Lumen
CUB domain
SUSHI domain
ER retention signal
Flag x2
HA tag
Transmembrane domain
B
+SEZ6
kDa
+GFP
FL
Δcyto
ecto
CTF
250
150
100
25
20
75
FlagM2
GluK2/3 EndoH
GluK2/3
FlagM2
Calnexin
C
+SEZ6
kDa
FL
ecto
250
150
SEZ6
Supernatant
D
+SEZ6
kDa
+GFP
ΔcytoER
Δcyto
150
100
100
100
SEZ6
GluK2/3 EndoH
GluK2/3
Calnexin
E
IP: GluK2/3
+GluK2a
+SEZ6
kDa
+empty
+GFP
FL
Δcyto
ecto
CTF
150
25
20
15
150
100
HA.11
HA.11
GluK2/3
Input
250
150
25
20
15
150
100
HA.11
HA.11
GluK2/3

Figure 7

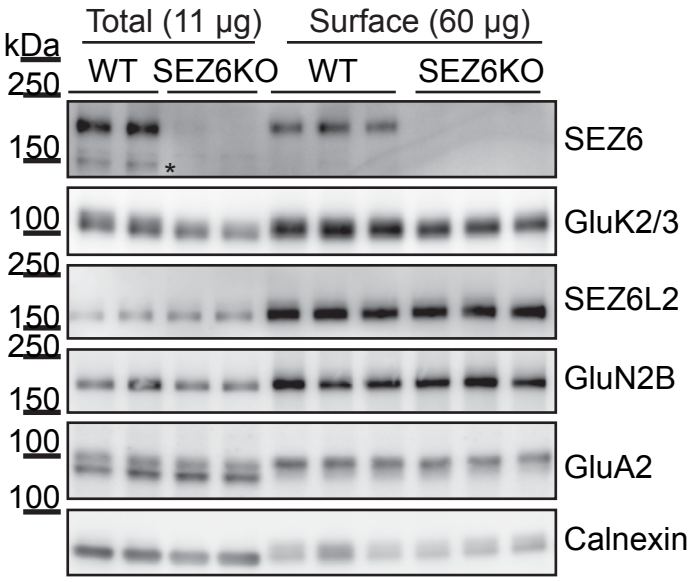

Supplementary 1

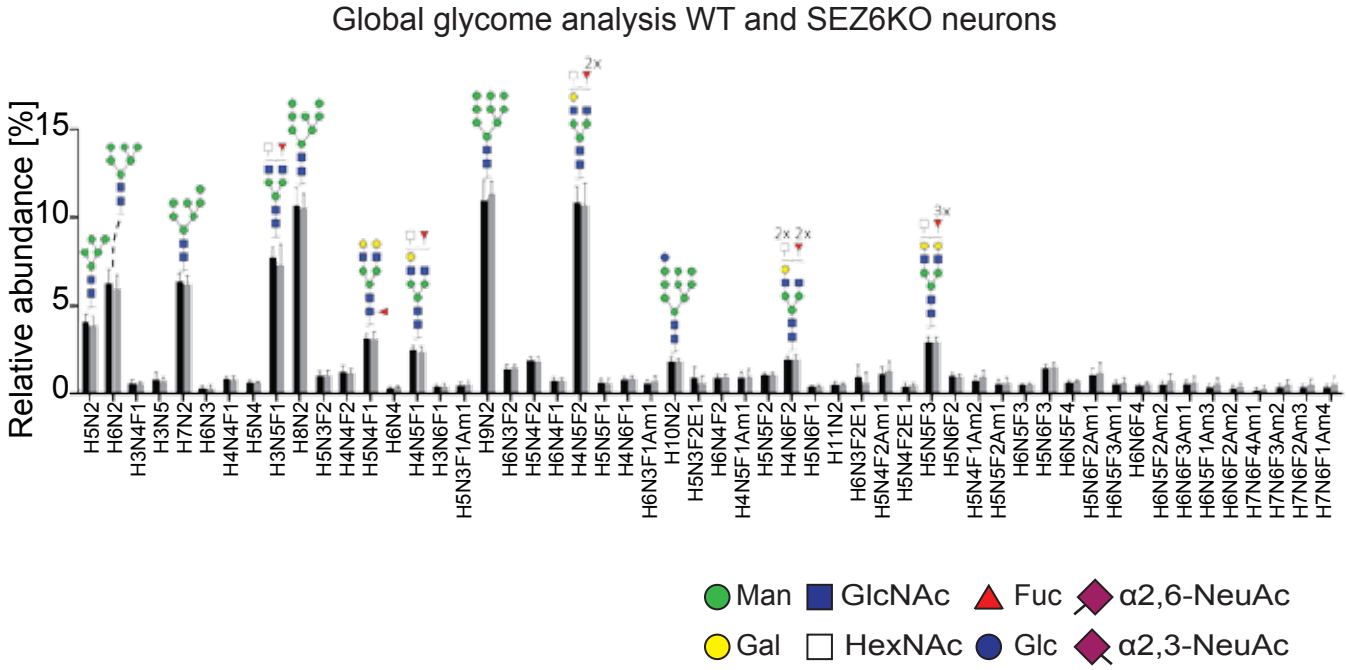

Supplementary 2

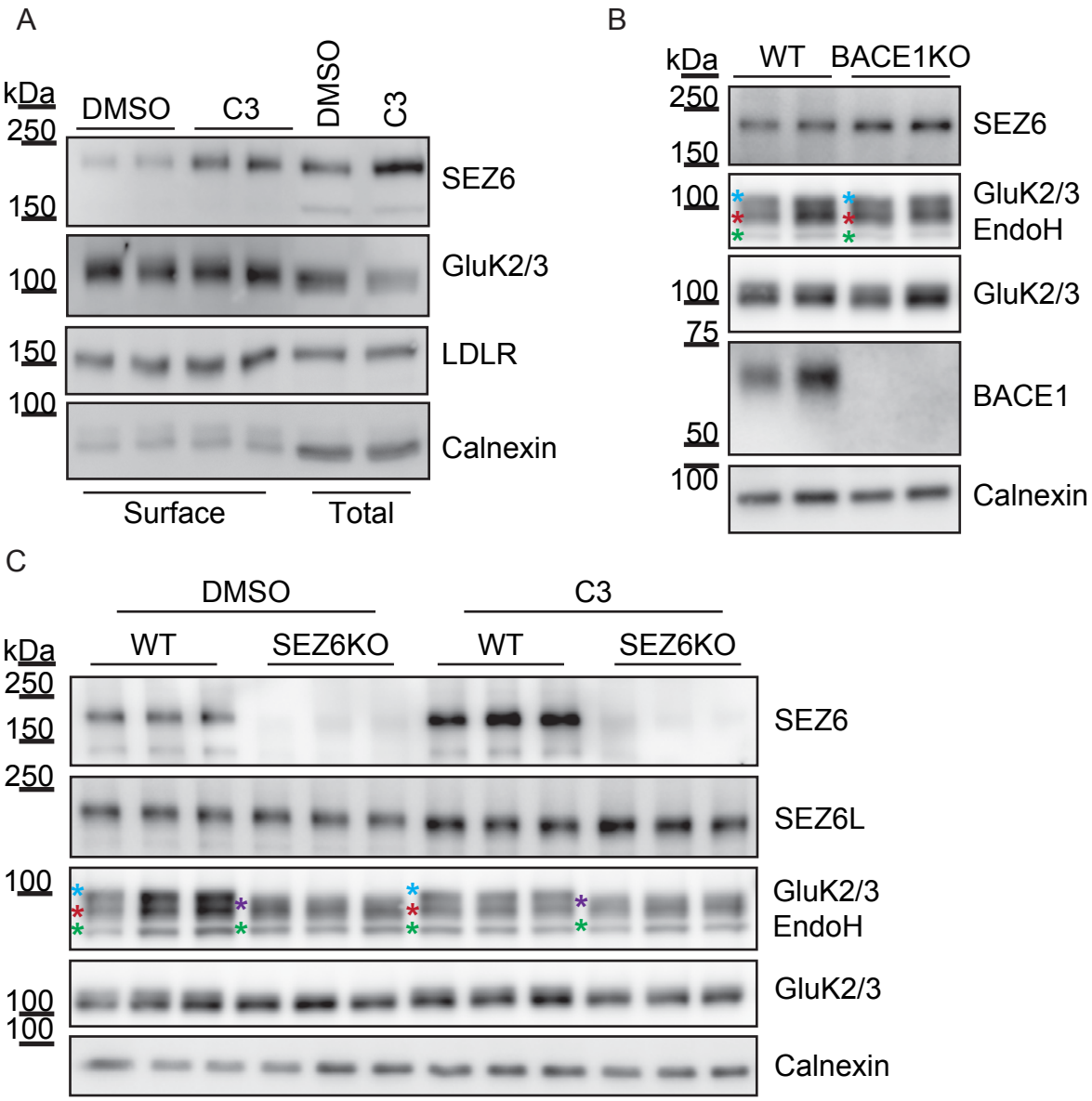

Supplementary 3

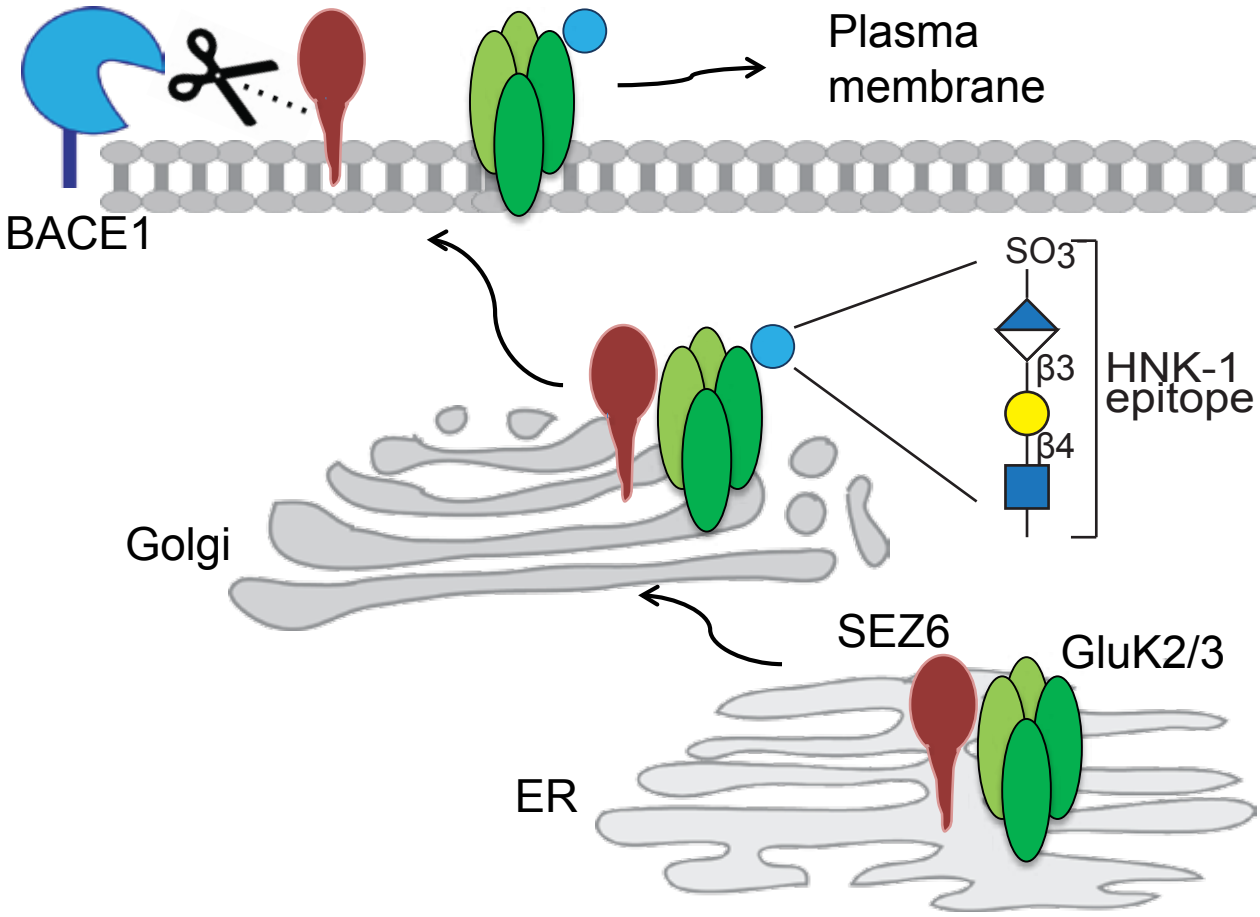

Supplementary 4

Supplementary Table 1

Protein IDs	Gene names	Protein names	Ratio	p-value	Protein type
B1AS29	Grik3/ GluK3	Glutamate receptor ionotropic. kainate 3	0.43	0.02	Membrane
D3YTM0	Cers2	Ceramide synthase 2	0.45	0.01	Soluble
Q9ER00	Stx12	Syntaxin-12	0.46	0.05	Membrane
P39087	Grik2/ GluK2	Glutamate receptor ionotropic. kainate 2	0.52	0.01	Membrane
P61089	Ube2n	Ubiquitin-conjugating enzyme E2 N	0.54	0.03	Soluble
O54865	Gucy1b 3	Guanylate cyclase soluble subunit beta-1	0.57	0.05	Soluble
Q8BTX9	Hsdl1	Inactive hydroxysteroid dehydrogenase-like protein 1	0.58	0.03	Soluble
O08915	Aip	AH receptor-interacting protein	0.59	0.01	Soluble
P11627	L1cam	Neural cell adhesion molecule L1	0.62	0.02	Membrane
Q9Z0P4-2	Palm	Paralemmin-1	0.63	0.01	Membrane
P97785-2	Gfra1	GDNF family receptor alpha-1	0.68	0.04	Membrane
Q8BYI8	Kiaa1467	Uncharacterized protein KIAA1467	0.70	0.01	Membrane
O08912	Galnt1	Polypeptide N-acetylgalactosaminyltransferase 1	0.70	0.03	Membrane
Q9R1R8	Rdh11	Retinol dehydrogenase 11	0.71	0.03	Unknown

Protein IDs	Gene names	Protein names	Ratio	p-value	Protein Type
Q99LD9	Eif2b2	Translation initiation factor eIF-2B subunit beta	2.00	0.01	Unknown
Q9CWR2	Smyd3	Histone-lysine N-methyltransferase SMYD3	1.68	0.04	Soluble
Q9D6R2	Idh3a	Isocitrate dehydrogenase [NAD] subunit alpha. mitochondrial	1.66	0.05	Soluble
Q8BUY9	Pggt1b	Geranylgeranyl transferase type-1 subunit beta	1.64	0.04	Unknown
Q8R3I2-3	Mboat2	Lysophospholipid acyltransferase 2	1.64	0.01	Membrane
O88986	Gcat	2-amino-3-ketobutyrate coenzyme A ligase. mitochondrial	1.64	0.05	Soluble
F6S1R2	Ahsa2	Activator of 90 kDa heat shock protein ATPase homolog 2	1.62	0.02	Unknown
Q8R323	Rfc3	Replication factor C subunit 3	1.45	0.05	Soluble
Q8K2M0-2	Mrpl38	39S ribosomal protein L38. mitochondrial	1.44	0.04	Soluble

Supplementary Table 2

Protein IDs	Gene names	Protein names	Average LFQ intensity[#]
B1AS29	Grik3/ GluK3	Glutamate receptor ionotropic, kainate 3	31,97
P39087	Grik2/ GluK2	Glutamate receptor ionotropic, kainate 2	31,64
Q61626	Grik5/ GluK5	Glutamate receptor ionotropic, kainate 5	28,25
P47757-2	Capzb	F-actin-capping protein subunit beta	25,30
E9Q171	Nfasc	Neurofascin	25,23
Q8BMF5	Grik4	Glutamate receptor ionotropic, kainate 4	24,79
O09061	Psmb1	Proteasome subunit beta type-1	24,57
P47708	Rph3a	Rabphilin-3A	24,05
Q60692	Psmb6	Proteasome subunit beta type-6	23,95
Q3U2G2	Hspa4	Heat shock 70 kDa protein 4	23,87
Q8BNJ6	Neto2	Neuropilin and tolloid-like protein 2	23,76
P35486	Pdha1	Pyruvate dehydrogenase E1 component subunit alpha, somatic form, mitochondrial	23,73
P59016	Vps33b	Vacuolar protein sorting-associated protein 33B	22,12
Q7TSK2	Sez6	Seizure protein 6	NaN

[#]log2 scale

Further answer to reviewer's comment:

Specific Comments on Section 2.2:
Figure 5 – Does the PNGase treatment affect GluK2/3 band shift in the Sez6 KO neurons?

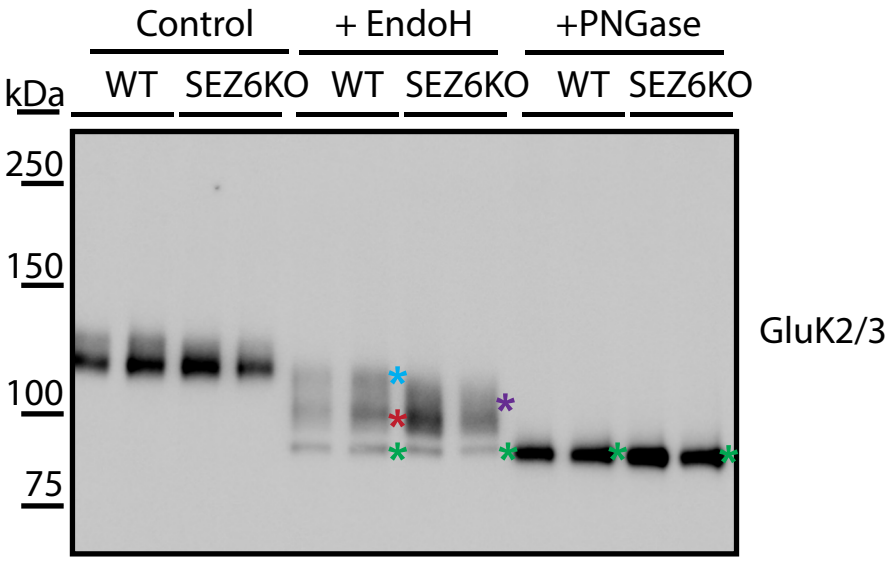

Comment on figure 5: Loss of SEZ6 affects EndoH sensitivity of GluK2/3. In the control neuronal lysates ("Control") WT condition, GluK2/3 was seen as two closely comigrating bands. In the control neuronal lysates SEZ6KO condition, the upper band of lower intensity was missing or running even more closely to the lower band of main intensity. When the total lysates of SEZ6KO and WT neurons were digested with endoglycosidase H ("+EndoH") – which removes immature, but not mature sugars – the two closely comigrating bands were converted to three bands of a lower apparent molecular weight, consistent with full deglycosylation of the lowest band (marked in green) and a partial deglycosylation of the upper two bands (marked in light blue and red). In SEZ6KO neurons the uppermost (light blue) band was missing. A new band of lower apparent molecular weight, partially overlapping with the red labeled band was detected (indicated with the purple asterisk). When both WT and SEZ6KO neuronal lysates were treated with PNGase ("+PNGase") – which removes also mature sugars – no difference in the glycosylation of GluK2/3 was detected (green marks).

3. Discussion and future perspectives

BACE1 is the initial enzyme that cleaves APP to generate the AD-related pathological Aβ peptide and is therefore considered as an appealing therapeutic target for AD [24,25]. Several BACE1 inhibitors have been generated and tested both in preclinical and clinical trials (phase 2 and 3). Unfortunately, most of the clinical trials for BACE inhibitor have been stopped in the last years due to the lack of efficacy and presence of undesired side effects in BACE-inhibitors treated patients. In line with these evidences in humans, BACE1KO mice and mice treated with BACE1 inhibitors also display pathological phenotypes (see introduction), and some of them have been connected to the loss of cleavage of BACE1 substrates other than APP. Therefore, it would be extremely important to understand if, similarly to mice, the side effects reported in human are also due to a loss of cleavage of BACE1 substrates. To this aim, the first step is the identification of physiological BACE1 substrates, followed by their biochemical and functional characterization.

3.1 SEZ6 processing and its biological functions in neurons

Several BACE1 substrates have been identified and, among these, SEZ6 and the other family member SEZ6L are the BACE1 substrates with the strongest reduction of their shed ectodomains in conditioned medium of BACE1 inhibited murine neurons [52]. Here, I showed that both soluble SEZ6 (sSEZ6) and soluble SEZ6L (sSEZ6L) are dramatically reduced when BACE activity is abolished either upon treatment of primary cortical neurons with BACE inhibitor or genetic knock-out of BACE1 *in vivo* [126]. In addition, the full length form of both SEZ6 (+80%) and SEZ6L (+60%), accumulated on the cell surface of neurons when BACE1 was not active. The accumulation of these proteins was also reproduced in an independent unbiased cell surface proteome study of BACE1 inhibited neurons [127].

Similar to APP and SEZ6L [55,128], the CTF of SEZ6 was further cleaved by γ-secretase and degraded most likely shorted afterwards since it was not detectable if γ-secretase was not inhibited. However, whether SEZ6 function is mediated by the full length form of the protein or by the cleavage products (sSEZ6 or SEZ6-CTF) is

still under debate. Considering the strong alterations occurring in SEZ6 shedding as a consequence of BACE1 loss of cleavage, we can speculate that the accumulation of full length SEZ6 (SEZ6FL) on the cell surface might lead to a gain of function. On the other hand, the loss of cleavage products might lead to a loss of SEZ6 function. Indeed, Zhu *et al.* identified an important function of SEZ6 in maintaining normal dendritic spine dynamics and proved that the reduction of spine density measured in BACE inhibitor treated mice is most likely due to the accumulation of SEZ6FL or the reduction in SEZ6-CTF [37].

On the other hand, the novel function of SEZ6 as a modulator of kainate receptor 2 (GluK2) and 3 (GluK3), which I discovered in this study, seems not to be influenced by BACE1 cleavage but rather depends on SEZ6FL. The trafficking as well as the glycosylation of Gluk2 and 3 were altered in SEZ6KO neurons which reduced the cell surface levels of both kainate receptors by 50%. Therefore, inhibition or absence of BACE1, which leads to an increased abundance of SEZ6 on the cell surface, might also result in elevated cell surface levels or differences in glycosylation of Gluk2/3. However, I showed that in BACE inhibitor treated neurons and BACE1KO mice no alteration in GluK2/3 glycosylation or surface abundance was detectable. Furthermore, no accumulation of GluK2/3 on the cell surface of neurons treated with BACE inhibitor was reported by Herber *et al*. [127]. Even if the effect of an induction of BACE1 activity has still to be tested, these evidences point in the direction that BACE1 activity does not influence SEZ6 to function as a regulator of GluK2/3 trafficking.

Additionally, Gunnersen *et al.* showed that overexpression of SEZ6 isoform III (similar, but not identical to sSEZ6 generated by BACE1 cleavage) has a probranching activity and enhances the number of neurites but reduces their length [57]. In the opposite direction, overexpression of ectopic Sez-6 t II (full length SEZ6) decreases neurite number and negatively influences dendritic arborization under basal conditions [57]. This indicates that BACE inhibitor treated neurons, where SEZ6 full length accumulates and sSEZ6 is absent, would display a marked reduction in neurite number. Unfortunately, validating this hypothesis might be complicated considering that also some other BACE1 substrates, among these CHL1 [129] and APP [130-132], are involved in neurite branching.

Conclusively, these evidences suggest that SEZ6 has multiple functions which are partially independent of SEZ6 processing, including trafficking of GluK2/3. On the other hand, additional functions like spine density promotion are modulated by BACE1 activity and its loss of activity leads to side effects due to loss of cleavage of SEZ6.

3.2 sSEZ6 and sSEZ6L as biomarkers for BACE activity and companion diagnostics

Having the possibility to monitor SEZ6 shedding in murine models and ultimately in patients treated with BACE1 inhibitors, would be a powerful way not only to prevent the side effects due to absent or reduced cleavage of SEZ6 itself, but also more in general to modulate BACE1 activity without completely abolishing it. To test if sSEZ6 might be a good biomarker, I measured sSEZ6 and sSEZ6L levels in the CSF of WT and BACE1KO mice. The ectodomains were clearly detectable both via mass spectrometry and Western Blotting and the ectodomains of both proteins were dramatically reduced to less than 10% in the CSF of BACE1KO mice. Since it was reported that *in vitro* SEZ6 proteins can be cleaved also by BACE2, the protein homologous of BACE1 [126,55], I also analyzed the CSF of BACE2KO mice. This experiment showed that sSEZ6 levels in BACE2KO mice are equal to those detected in the WT mice, indicating that sSEZ6 detectable in the CSF of mice is a product of BACE1 cleavage [126].

Although my results strongly suggest sSEZ6 as a highly potent biomarker for BACE1 activity, the detection of sSEZ6 was so far done via mass spectrometry and Western blot, which cannot be used as high throughput readout methods. Additionally, with the final goal of using sSEZ6/sSEZ6L as biomarkers for BACE1 activity on routinely basis both for research and clinical purposes, the detection method has to be reproducible, operator independent, and does not have to require special equipment such as a mass spectrometer. For this purpose, we have chosen the very sensitive immunoassay-based Meso Scale Discovery Platform (MSD) which is suitable for large scale clinical testing. This method combines the specificity and sensitivity of antibodies similarly to a standard ELISA method and the stability of electrochemiluminescence (ECL) as a detection technique in contrast to the colorimetric reaction employed by conventional ELISA. The MSD method usually

covers a broader dynamic range than standard ELISAs and also requires less sample volume due to its improved sensitivity [133]. In order to optimize a MSD platform for the detection of sSEZ6 in the CSF of mice, specific monoclonal antibodies were generated by immunizing rats with SEZ6 ectodomain overexpressed and purified from HEK293T cells [126]. The specificity and sensitivity of these newly generated clones was proved using SEZ6KO mouse brain lysates similarly to Pigoni *et al.* [126]. The next step, will be to test different combinations of monoclonal antibodies produced in house and commercially available, identify a combination of clones that are not only able to specifically detect sSEZ6, but also able to monitor a dose-dependent reduction of sSEZ6 in brain lysates and CSF of rodents treated with BACE inhibitors. Additionally, it will be important to generate, screen and test monoclonal antibodies against human sSEZ6, in order to optimize an MSD assay specifically detecting sSEZ6 in human body fluids. When the optimization phase will be completed, the human sSEZ6 MSD might be used to monitor SEZ6 processing in a more reproducible, quicker and operator-independent manner in patients.

Ideally, an appealing biomarker should be easily accessible in order to maximize the compliance of the patients; therefore it will be important to measure sSEZ6 and sSEZ6L levels in mouse plasma samples. Considering the expression pattern of SEZ6 and BACE1, both quite highly expressed in the nervous system and particularly in neurons but not in other body tissues [9,134], I speculate that sSEZ6 will be probably not detectable in murine plasma. On the other hand, SEZ6L has a broader distribution and it is expressed in other body tissues in addition to the CNS, for example in pancreatic cells and lungs [49,57]. BACE2 also shows a broader expression pattern compare to BACE1. BACE2 expression in the brain is limited to a subset of neurons but it is expressed in different glia cells [135], and plays an important role in melanosome biogenesis [136]. Additionally, BACE2 is expressed in pancreatic β cells [137], where we and other groups proved that it can cleave SEZ6L [55]. Therefore, it is highly probable that sSEZ6L will be detected in plasma but it will be important to clarify if its levels are also influenced by BACE2 cleavage.

In the last decade, the idea of complete BACE1 inhibition in order to abolish Aβ production has been changed in favor of a partial and rather preventive inhibition of BACE1. The idea is strongly supported by the evidence that the Icelandic mutation (A673T) in the APP gene, which is protective against Alzheimer's disease and

cognitive decline, reduces approximately 40% of Aβ production for the entire lifespan of the person [23]. Therefore, the ideal treatment should target a 50% to 20% reduction of Aβ production but should be started several years before plaque formation and the onset of symptoms. This approach should reduce the side effects due to the loss of cleavage of BACE1 substrates, prevent or delay AD-related symptoms and the onset of disease [138-140].

Monitoring sSEZ6 as a companion diagnostic biomarker for BACE1 activity could be used to identify a safe range of BACE inhibition that lowers Aβ production avoiding the side effects due to loss of cleavage of SEZ6. Since also other BACE1 substrates can contribute to mechanism-based side effects, it would be desirable to use a panel of different markers like CHL1, or neuregulin-1. In the long run and in the prospective of personalized medicine, sSEZ6 and other BACE1 substrates might be useful to monitor the efficacy of a BACE inhibition in each treated patient in order to individually adjust the dose of inhibitor according to instant response and tolerability of the drug.

Last, the connection between pathological phenotypes described in patients treated with BACE inhibitors and loss of cleavage of BACE substrates remains a point that has to be further investigated. Indeed, some patients treated with different BACE inhibitors displayed some mild memory deficits, psychiatric symptoms and tendency to fall and get injuries [43]. Given that loss of processing of Neuregulin-1 in BACE1KO mice leads to hypomyelination and loss of muscle spindles [38,44-46], it is possible that loss of Neuregulin-1 cleavage contributes to the undesired motor side effects seen in some patients treated with BACE inhibitors. Similarly, SEZ6 function is connected to dendritic spine density and synapsis maintenance, and several evidences connect SEZ6 with psychiatric diseases, suggesting that psychiatric symptoms occurring in BACE inhibitor treated patients might be due to a loss of cleavage of SEZ6. Having the human SEZ6 MSD will allow to measure sSEZ6 levels in a reliable manner in the subgroup of patients who displayed side effects and compare them to those who do not show any symptoms. This human sSEZ6 MSD detection platform will help to better understand the cause of the side effects and to define a tolerable degree of BACE1 inhibition.

3.3 SEZ6 as a regulator of ionotropic kainate receptors 2 and 3

3.3.1 Cell surface analysis of SEZ6KO cortical neurons

Even if SEZ6 knock-out (SEZ6KO) mice have been generated and described more than ten years ago [57], and they display alterations in the morphology and functionality of the neurons as well as behavioral deficits, the molecular function of SEZ6 and the mechanisms that lead to those phenotypes are still largely unknown. The structure of SEZ6, rich in CUB and SCR domains involved in protein-protein interaction [141,142], and the localization of SEZ6 at the cell surface [126], point in the direction of an involvement in cell-cell adhesion or cell communication.

In order to study the cell surface composition of SEZ6KO neurons and compare it to the WT condition in an unbiased manner, I performed a mass spectrometry analysis based on the SUSPECS method recently published in our laboratory [127]. Primary cortical neurons were fed with tetra-acetylated N-azidomannosamine, a click chemistry-suitable azido-modified mannose derivative that is metabolically incorporated in the newly synthetized glycosylated proteins during their maturation in the ER and Golgi. After two days of metabolic labeling the cells were biotinylated with dibenzylcyclooctyne (DBCO)-biotin, a membrane not-permeable compound, which reacts with the azido group of the glycoprotein, facilitating covalent biotinylation of the glycoproteins present at the cell surface. Biotinylated proteins were enriched with streptavidin agarose and analyzed by mass spectrometry using label-free protein quantification. Since it is known that SEZ6KO neurons present a reduced number of dendritic spines and diminished punctate staining for postsynaptic density, I performed the surface analysis at an early developmental stage of the primary cortical neurons (DIV 7), in order to avoid that specific effects may be masked by a general reduction in synaptic proteins.

As expected, no overall drastic changes were detected comparing the cell surface proteome of SEZ6KO and WT neurons. Nevertheless, some changes in protein abundances point towards a selective function of SEZ6 in protein trafficking or maturation of specific proteins. Noteworthy, the ionotropic kainate receptors 2 (GluK2) and 3 (GluK3) showed an abundance reduction of roughly 50% on the cell surface of SEZ6KO neurons. The other subunits of the ionotropic kainate receptors

(GluK1, KA1 and KA2) were not detected in our analysis. In contrast, other glutamate receptors such as α-amino-3-hydroxy-5-methylisoxazole-4-propionic acid (AMPA) and N-methyl-D-aspartate (NMDA) receptors were detected but not significantly changed on the cell surface of the neurons. Even if we cannot exclude that all kainate receptor subunits were affected by SEZ6 loss, this analysis proves that the GluK2 and GluK3 reduction is a specific effect and does not affect the levels of all ionotropic glutamate receptors at the cell surface.

Other proteins significantly reduced on the cell surface of SEZ6KO neurons were Ceramide synthase 2 (-50%) and Syntaxin-12 (-50%). CERS2 is mainly expressed in oligodendrocites and is involved in sphingolipids biosynthesis. Sphingolipids are involved in various neuronal events. For example, inhibition of shingolipid synthesis through blockage of ceramide synthase in Purkinje cells leads to elongated but less-branched dendrites [143] and disrupts axonal outgrowth in cultured hippocampal neurons [144]. Even if a connection between the altered branching of SEZ6KO neurons and alterations in Ceramide synthase might be possible, it remains difficult to explain the physiological significance of CERS2 on the neuronal cell-surface and this was not further investigated in this study.

Little is known about Syntaxin-12 (STX-12), a part that it is mainly expressed in endosomes and seems to act as t-SNARE, a protein present on organelle membrane which interacts with v-SNAREs present on transport vesicles and allows targeting, docking, and fusion of the right vesicles to the right membrane [145]. Considering the similarity of STX-12 with the other family member Syntaxin-13 (STX-13), a role in controlling the intracellular fate of AMPA receptors and the endosomal sorting of the GriA2 subunit towards recycling and membrane targeting was proposed [146]. The family member STX-13 is in fact known to localize in the endosomes and be important in membrane fusion events during the recycling of plasma membrane proteins [147]. In particular, it was reported that syntaxin 13 binds GRASP-1, an important component of the molecular machinery that regulates the directions of endosomal trafficking in neurons, and this interaction is required for GluA2 recycling [148,149].

Considering that the structure of SEZ6 is rich in CUB domains and there are multiple evidences in literature supporting the role of CUB containing proteins in

neurotransmitter receptors regulation [79-84], the relationship between SEZ6 and GluK2/3 was further investigated.

3.3.2 SEZ6 as a regulator of GluK2/3

Here, I provide multiple evidences proving that SEZ6 is a regulator of kainate receptors trafficking. First, GluK2/3 levels are reduced on the surface of SEZ6KO neurons in a specific manner. Second, in a heterologous system (RUSH), the co-expression of SEZ6 with GluK2a enhances the number of GluK2a-positive secretory vesicles. Additionally, GluK2/3 in the SEZ6KO neurons and mouse brains are more sensitive to EndoH and carry less HNK-1 epitope, therefore their maturation status is less advanced in the absence of SEZ6, which can be linked to its reduced cell surface abundance. On the other side, when the total GluK2/3 protein level was tested, just a milder reduction was detected in the SEZ6KO neurons. This mild reduction might be a consequence of a compensatory, increased degradation of GluK2/3 occurring upon accumulation of immature GluK2/3 in the ER. It was in fact reported that mutant forms of GluRs, which lead to misfolded or misassembled complexes, are retained in the ER and probably eliminated by the endoplasmic reticulum-associated degradation (ERAD) system [150,151]. Taken all together, these evidences show that SEZ6 regulates the maturation and trafficking of GluK2/3 and just partially its total levels.

Considering the high homology between SEZ6 and the other family members, a redundant functionality was hypothesized for SEZ6L and SEZ6L2. Therefore, I considered GluK2/3 maturation in mouse KO for the other SEZ6 family members and found that GluK2/3 maturation is not impaired in SEZ6LKO and SEZ6L2KO mice. This evidence might suggest different functions for the three family members. Another possibility that has to be considered is that SEZ6L and SEZ6L2 mediate a SEZ6-similar function but in different areas of the brain or at different age of the mice. The situation where members of the same protein family modulate the same glutamate receptors but in different brain areas and in a different manner, was already reported for the NETO family. NETO1 and NETO2 are both known to bind and regulate GluK2/3, but GluK2/3 binds preferentially to Neto2 in the cerebral cortex, and Neto1, but not Neto2, is required for the synaptic abundance of KARs [85,86,81]. An alternative scenario is that different members of the SEZ6 family are

specifically involved in the regulation of different glutamate receptors. Similarly, NETO1 also regulates NMDARs [83] but no involvement of NETO2 in NMDARs regulation was proved yet.

3.3.3 SEZ6 as a regulator of GluK2/3 glycosylation

It is known that glycosylation changes on KARs can modulate their function and cellular localization [152,153]. Therefore, I further investigated which sugars are specifically changed on GluK2/3 in SEZ6KO neurons. Using an unbiased approach (Lectin Chip analysis) followed by a validation via Western Blotting, I showed that the sulfated trisaccharide human natural killer-1 (HNK-1) epitope is specifically reduced on GluK2/3 in SEZ6KO neurons and mouse brain. In addition, I showed that no general reduction of HNK-1 was detected in the full SEZ6KO proteome or on NCAM, another protein known to carry the HNK-1 sugar.

HNK-1 is mainly expressed in the nervous system but, despite its broad expression in the brain, is only carried by certain kinds of molecules, indicating that its biosynthesis in the Golgi is tightly regulated. In the nervous system only few HNK-1-carrying proteins have been identified which include NCAM and L1 [154], adhesion proteins belonging to the Ig-superfamily, and a specific glutamate receptor subunit, GluA2 [153]. The fact that no general changes of HNK-1 were detected in the entire proteome of SEZ6KO neurons and that other proteins known to carry HNK-1 epitope, such as NCAM and GluA2, were detected but not changed on the cell surface of SEZ6KO neurons, strongly suggest that the reduction of HNK-1 is a specific effect occurring on GluK2/3.

Worth mentioning, the HNK-1 carbohydrate epitope was already identified on Gluk2/3 [152], but the impact of HNK-1 on the function of endogenous GluK2/3 is not characterized yet. In the case of GluA2, a reduction of HNK-1 on the receptor reduces the GluA2 interaction with N-cadherin, GluA2 stability on the cell surface [153] and might influence GluA2 spine-promoting activity [155,156]. Similarly, I speculate that the HNK-1 reduction on GluK2/3 might affect its stability on the cell surface and be the cause of the reduced amount of GluK2/3 on the cell surface in SEZ6KO neurons. On the other hand, the HNK-1 reduction on GluK2/3 might simply

be a further confirmation that in the absence of SEZ6, GluK2/3 does not reach the Golgi compartment where GlcAT-P, the glucuronyltransferase responsible for the HNK-1 biosynthesis, is active. In order to further investigate this possibility, it would be meaningful to compare the GluK2/3 maturation in GlcAT-PKO and SEZ6KO neurons and study if the two conditions phenocopy each other. In general, considering all the evidences provided in this thesis, it is more likely that SEZ6 is involved in GluK2/3 trafficking to the Golgi where GlcAT-P is active.

3.3.4 SEZ6 regulates GluK2/3 via CUB domains

Several CUB domain-containing proteins have been identified as regulators of ionotropic acetylcholine receptors and ionotropic glutamate receptors [79-86], and often their function and interaction with the receptors are mediated by the CUB domains [84,83,82]. Consistently with these findings, SEZ6 full length, and SEZ6 lacking the C-terminal tail were able to rescue the maturation of GluK2/3 when reintroduced in SEZ6KO neurons. In addition, similarly to soluble SOL-1 [84], SEZ6 ectodomain expressed in *cis* was also sufficient to rescue the maturation of GluK2/3. The same is not true for SEZ6 CTF, indicating that SEZ6 extracellular region, containing the CUB domains, is necessary and sufficient to mediate the SEZ6 function as a regulator of GluK2/3 maturation. Similarly, when the same mutants were tested for the interaction with GluK2a in HEK293T cells overexpressing both SEZ6 and GluK2a, no interaction between GluK2a and SEZ6 CTF was detectable but the other SEZ6 mutants were consistently co-immunoprecipitated with GluK2a. These evidences do not exclude that the SCR domains play a role in the regulation of GluK2/3 but, together with the previously mentioned literature, strongly point in the direction that the CUB domain of SEZ6 are important for the binding and regulation of GluK2/3.

Even if I could reproduce the interaction between GluK2/3 and NETO2 in endogenous conditions [81], I was not able to show a direct interaction between SEZ6 and GluK2/3 in neurons or in brains. Indeed, for other CUB domain-containing proteins, it was also not possible to show a direct interaction with the regulated receptor in endogenous conditions, but only in overexpressed conditions [80]. The inability of detecting the endogenous interaction might be attributed to different factors. For example, the total amount of proteins present in the tissue and the

percentage of them that are involved in the interaction might be very low. Additionally, the strength of the interaction and the type of detergent used to solubilize the transmembrane proteins are critical factors to be considered. Conclusively, a transient interaction, maybe restricted to certain subcellular compartments, like the SEZ6 and GluK2/3 interaction seems to be, will be particularly difficult to detect.

3.3.5 Can SEZ6 be considered an auxiliary subunit for GluK2/3?

The CUB domain-containing proteins previously mentioned are also considered as auxiliary subunits of the receptors that they regulate. Auxiliary subunits are, according to the classification proposed by Yan and Tomita 2012 [157], non-pore-forming subunit directly and stably interacting with a pore-forming subunit. Auxiliary subunits are able to modulate channel properties and/or to traffic it in heterologous cells. Additionally, their necessity for the correct expression and maintenance of channel properties and/or localization of the receptor has to be proven *in vivo*.

This raises the question: can SEZ6 be considered an auxiliary subunit for GluK2/3?

First, that SEZ6 regulates the surface amounts and maturation of GluK2/3 was proven in different systems and manners. I not only showed that GluK2/3 is reduced on the cell surface of SEZ6KO neurons with two independent methods, but I also proved through the analysis of GluK2/3 glycosylation, that the maturation of the receptor is impaired. Second, using the RUSH system, I showed that SEZ6 facilitates the trafficking and exportation of GluK2/3 in a heterologous system. Third, similarly to SOL-1, I was able to prove a direct interaction between SEZ6 and GluK2 in overexpressing conditions and providing evidences that the SEZ6 CUB domains are most likely to mediate the interaction with GluK2a and are important for GluK2/3 trafficking and maturation. Fourth, I showed that the impaired glycosylation of GluK2/3 is an early event occurring already in the brain of embryos, but the effect is not rescued postnatally or during aging of the mice, indicating the relevance of SEZ6 function *in vivo* and at all developmental stages of the murine brain. Finally, I showed that the SEZ6 mutant, which is retained in the ER and not present in the Golgi does not rescue GluK2/3 maturation, pointing in the direction that SEZ6 does not only

regulate the exit of GluK2/3 from the ER but is also involved in the trafficking to the Golgi.

On the other hand, I was not able to prove a direct and stable interaction between SEZ6 and GluK2 in endogenous conditions and I did not validate the hypothesis that SEZ6 is a non-pore forming subunit by itself. Additionally, the electrophysiological analysis that was done shows that SEZ6KO hippocampal slices are less sensitive to KA stimulation. Nevertheless, this is most likely a consequence of a reduced number of receptors at the cell surface, but does not provide information about the channel properties of GluK2/3. If SEZ6, similarly to NETO1 and NETO2 [81,85], also modulates kinetic parameters of kainate receptors and if this modulation occurs also *in vivo* has to be further investigated.

Taken all together, these evidences strongly point in the direction of a novel function of SEZ6 as an auxiliary subunit for GluK2/3. Nevertheless, since some important aspects mentioned in the definition of auxiliary subunits are not fulfilled by SEZ6 yet, and further investigations are required, I consider premature to include SEZ6 in the family of the auxiliary subunits of kainate receptors.

3.3.6 SEZ6 and kainate receptors in disease

Even if multiple studies have linked SEZ6 mutations to psychiatric disturbances and neurodevelopmental disorders, the mechanism behind these associations was not investigated. Considering the novel function of SEZ6 discovered in this thesis and the well-established role of kainate receptors in brain development, it would be extremely important to investigate how changes in SEZ6-mediated GluK2/3 regulation affect the brain development. For example, it would be interesting to check if the *de novo* variant of SEZ6 sequence associated with Childhood-onset schizophrenia (COS) described by Ambalavanan *et al.* leads to reduced expression of SEZ6 and if it also correlates with alteration in GluK2/3 maturation. Interestingly, Tucholski *et al.* reported that KARs glycosylation is altered and GluK2/3 is more sensitive to EndoH digestion in schizophrenia patients [115]. Therefore, a larger cohort of schizophrenia patients should be considered to investigate if the impaired glycosylation of GluK2/3 indeed correlates with reduced SEZ6 levels.

Moreover, a few studies connect SEZ6 alterations with neurodegenerative diseases. Recently, the rare variant R615H of SEZ6 was found in the members of a large Italian family suffering of late onset AD carrying no typical FAD-linked mutations [76]. Since the mutation maps on the second CUB domain present in SEZ6 extracellular region, it would be interesting to investigate if it affects the function of SEZ6 as regulator of GluK2/3 and the binding between these two proteins. Additionally, reduced levels of SEZ6 ectodomain have been detected in the CSF of AD patients compared to healthy controls [75]. If it can be confirmed that reduced levels of SEZ6 correlate with impair maturation of GluK2/3 in the postmortem brain of AD patients, it would be tempting to speculate an involvement of SEZ6 in the glutamate receptor and synaptic dysfunction occurring in early stages of AD.

Considering the important functions of SEZ6 and KARs during brain development and the evidences associating these proteins to developmental disorders, the function of SEZ6 as a KARs regulator discovered in this thesis might potentially represent a regulatory mechanism involved in the determination of developmental disorders. Future studies are required to investigate if this novel mechanism represents also a potential therapeutic target for the treatment of psychiatric disorders.

To conclude, since BACE1 is one of the main drug targets for the treatment of AD, the loss of cleavage of its substrates represents one major drawback and an issue that needs to be overcome before BACE inhibitor might be used on routinely bases in patients. If on one hand I show that SEZ6 cleavage is completely dependent by BACE1, I also prove that at least some of SEZ6 functions do not depend by BACE1 activity. Therefore, these findings represent double positive news for the BACE inhibitors. First, it might be predicted that no side effects due to altered GluK2/3 trafficking and altered excitatory synaptic transmission will occur in patients treated with BACE inhibitors, making this approach safer. Second, the fact that SEZ6 is cleaved only by BACE1 makes it a valuable biomarker to monitor specifically and sensitively BACE1 activity in patients, representing in the long term an additional step forward in the direction of personalized medicine.

References

1. Mega MS, Cummings JL, Fiorello T, Gornbein J (1996) The spectrum of behavioral changes in Alzheimer's disease. Neurology 46 (1):130-135
2. Ferri CP, Prince M, Brayne C, Brodaty H, Fratiglioni L, Ganguli M, Hall K, Hasegawa K, Hendrie H, Huang Y, Jorm A, Mathers C, Menezes PR, Rimmer E, Scazufca M (2005) Global prevalence of dementia: a Delphi consensus study. Lancet (London, England) 366 (9503):2112-2117. doi:10.1016/s0140-6736(05)67889-0
3. Prince M, Bryce R, Albanese E, Wimo A, Ribeiro W, Ferri CP (2013) The global prevalence of dementia: a systematic review and metaanalysis. Alzheimer's & dementia : the journal of the Alzheimer's Association 9 (1):63-75.e62. doi:10.1016/j.jalz.2012.11.007
4. Brookmeyer R, Evans DA, Hebert L, Langa KM, Heeringa SG, Plassman BL, Kukull WA (2011) National estimates of the prevalence of Alzheimer's disease in the United States. Alzheimer's & dementia : the journal of the Alzheimer's Association 7 (1):61-73. doi:10.1016/j.jalz.2010.11.007
5. Goodman RA, Lochner KA, Thambisetty M, Wingo TS, Posner SF, Ling SM (2017) Prevalence of dementia subtypes in United States Medicare fee-for-service beneficiaries, 2011-2013. Alzheimer's & dementia : the journal of the Alzheimer's Association 13 (1):28-37. doi:10.1016/j.jalz.2016.04.002
6. 2016 Alzheimer's disease facts and figures (2016). Alzheimer's & dementia : the journal of the Alzheimer's Association 12 (4):459-509
7. Hurd MD, Martorell P, Delavande A, Mullen KJ, Langa KM (2013) Monetary costs of dementia in the United States. The New England journal of medicine 368 (14):1326-1334. doi:10.1056/NEJMsa1204629
8. Braak H, Del Tredici-Braak K (2015) Alzheimer's Disease, Neural Basis of. In: Wright JD (ed) International Encyclopedia of the Social & Behavioral Sciences (Second Edition). Elsevier, Oxford, pp 591-596. doi:https://doi.org/10.1016/B978-0-08-097086-8.55001-6
9. Vassar R, Bennett BD, Babu-Khan S, Kahn S, Mendiaz EA, Denis P, Teplow DB, Ross S, Amarante P, Loeloff R, Luo Y, Fisher S, Fuller J, Edenson S, Lile J, Jarosinski MA, Biere AL, Curran E, Burgess T, Louis JC, Collins F, Treanor J, Rogers G, Citron M (1999) Beta-secretase cleavage of Alzheimer's amyloid precursor protein by the transmembrane aspartic protease BACE. Science (New York, NY) 286 (5440):735-741
10. Haass C, Kaether C, Thinakaran G, Sisodia S (2012) Trafficking and proteolytic processing of APP. Cold Spring Harbor perspectives in medicine 2 (5):a006270. doi:10.1101/cshperspect.a006270
11. Haass C, Selkoe DJ (2007) Soluble protein oligomers in neurodegeneration: lessons from the Alzheimer's amyloid beta-peptide. Nature reviews Molecular cell biology 8 (2):101-112. doi:10.1038/nrm2101
12. Tsai J, Grutzendler J, Duff K, Gan WB (2004) Fibrillar amyloid deposition leads to local synaptic abnormalities and breakage of neuronal branches. Nature neuroscience 7 (11):1181-1183. doi:10.1038/nn1335
13. Hardy J, Allsop D (1991) Amyloid deposition as the central event in the aetiology of Alzheimer's disease. Trends in pharmacological sciences 12 (10):383-388
14. Kirkitadze MD, Bitan G, Teplow DB (2002) Paradigm shifts in Alzheimer's disease and other neurodegenerative disorders: the emerging role of oligomeric assemblies. Journal of neuroscience research 69 (5):567-577. doi:10.1002/jnr.10328
15. Zhao LN, Long H, Mu Y, Chew LY (2012) The toxicity of amyloid beta oligomers. International journal of molecular sciences 13 (6):7303-7327. doi:10.3390/ijms13067303
16. Lee CY, Landreth GE (2010) The role of microglia in amyloid clearance from the AD brain. Journal of neural transmission (Vienna, Austria : 1996) 117 (8):949-960. doi:10.1007/s00702-010-0433-4
17. Fukumoto H, Cheung BS, Hyman BT, Irizarry MC (2002) Beta-secretase protein and activity are increased in the neocortex in Alzheimer disease. Archives of neurology 59 (9):1381-1389
18. Holsinger RM, McLean CA, Beyreuther K, Masters CL, Evin G (2002) Increased expression of the amyloid precursor beta-secretase in Alzheimer's disease. Annals of neurology 51 (6):783-786. doi:10.1002/ana.10208
19. Yang LB, Lindholm K, Yan R, Citron M, Xia W, Yang XL, Beach T, Sue L, Wong P, Price D, Li R, Shen Y (2003) Elevated beta-secretase expression and enzymatic activity detected in sporadic Alzheimer disease. Nature medicine 9 (1):3-4. doi:10.1038/nm0103-3

20. Vassar R, Kovacs DM, Yan R, Wong PC (2009) The beta-secretase enzyme BACE in health and Alzheimer's disease: regulation, cell biology, function, and therapeutic potential. The Journal of neuroscience : the official journal of the Society for Neuroscience 29 (41):12787-12794. doi:10.1523/jneurosci.3657-09.2009
21. Mullan M, Crawford F, Axelman K, Houlden H, Lilius L, Winblad B, Lannfelt L (1992) A pathogenic mutation for probable Alzheimer's disease in the APP gene at the N-terminus of beta-amyloid. Nature genetics 1 (5):345-347. doi:10.1038/ng0892-345
22. Citron M, Oltersdorf T, Haass C, McConlogue L, Hung AY, Seubert P, Vigo-Pelfrey C, Lieberburg I, Selkoe DJ (1992) Mutation of the beta-amyloid precursor protein in familial Alzheimer's disease increases beta-protein production. Nature 360 (6405):672-674. doi:10.1038/360672a0
23. Jonsson T, Atwal JK, Steinberg S, Snaedal J, Jonsson PV, Bjornsson S, Stefansson H, Sulem P, Gudbjartsson D, Maloney J, Hoyte K, Gustafson A, Liu Y, Lu Y, Bhangale T, Graham RR, Huttenlocher J, Bjornsdottir G, Andreassen OA, Jonsson EG, Palotie A, Behrens TW, Magnusson OT, Kong A, Thorsteinsdottir U, Watts RJ, Stefansson K (2012) A mutation in APP protects against Alzheimer's disease and age-related cognitive decline. Nature 488
24. Vassar R, Kuhn PH, Haass C, Kennedy ME, Rajendran L, Wong PC, Lichtenthaler SF (2014) Function, therapeutic potential and cell biology of BACE proteases: current status and future prospects. Journal of neurochemistry 130 (1):4-28. doi:10.1111/jnc.12715
25. Yan R, Vassar R (2014) Targeting the beta secretase BACE1 for Alzheimer's disease therapy. The Lancet Neurology 13 (3):319-329. doi:10.1016/s1474-4422(13)70276-x
26. Alexander R, Budd S, Russell M, Kugler A, Cebers G, Ye N, Olsson T, Burdette D, Maltby J, Paraskos J, Elsby K, Han D, Goldwater R, Ereshefsky L (2014) AZD3293 A novel BACE1 inhibitor: safety, tolerability, and effects on plasma and CSF Aβ peptides following single- and multiple-dose administration. Neurobiology of aging 35:S2. doi:https://doi.org/10.1016/j.neurobiolaging.2014.01.033
27. Asai M, Hattori C, Iwata N, Saido TC, Sasagawa N, Szabo B, Hashimoto Y, Maruyama K, Tanuma S, Kiso Y, Ishiura S (2006) The novel beta-secretase inhibitor KMI-429 reduces amyloid beta peptide production in amyloid precursor protein transgenic and wild-type mice. Journal of neurochemistry 96 (2):533-540. doi:10.1111/j.1471-4159.2005.03576.x
28. Bernier F, Sato Y, Matijevic M, Desmond H, McGrath S, Burns L, Kaplow JM, Albala B (2013) Clinical study of E2609, a novel BACE1 inhibitor, demonstrates target engagement and inhibition of BACE1 activity in CSF. Alzheimer's & Dementia 9 (4, Supplement):P886. doi:https://doi.org/10.1016/j.jalz.2013.08.244
29. Forman M, Palcza J, Tseng J, Leempoels J, Ramael S, Han D, Jhee S, Ereshefsky L, Tanen M, Laterza O, Dockendorf M, Krishna G, Ma L, Wagner J, Troyer M (2012) The novel BACE inhibitor MK-8931 dramatically lowers cerebrospinal fluid Aβ peptides in healthy subjects following single- and multiple-dose administration. Alzheimer's & Dementia 8 (4, Supplement):P704. doi:https://doi.org/10.1016/j.jalz.2012.05.1900
30. Kennedy ME, Stamford AW, Chen X, Cox K, Cumming JN, Dockendorf MF, Egan M, Ereshefsky L, Hodgson RA, Hyde LA, Jhee S, Kleijn HJ, Kuvelkar R, Li W, Mattson BA, Mei H, Palcza J, Scott JD, Tanen M, Troyer MD, Tseng JL, Stone JA, Parker EM, Forman MS (2016) The BACE1 inhibitor verubecestat (MK-8931) reduces CNS beta-amyloid in animal models and in Alzheimer's disease patients. Science translational medicine 8 (363):363ra150. doi:10.1126/scitranslmed.aad9704
31. Lai R, Albala B, Kaplow JM, Aluri J, Yen M, Satlin A (2012) First-in-human study of E2609, a novel BACE1 inhibitor, demonstrates prolonged reductions in plasma beta-amyloid levels after single dosing. Alzheimer's & Dementia 8 (4, Supplement):P96. doi:https://doi.org/10.1016/j.jalz.2012.05.237
32. May PC, Dean RA, Lowe SL, Martenyi F, Sheehan SM, Boggs LN, Monk SA, Mathes BM, Mergott DJ, Watson BM, Stout SL, Timm DE, Smith Labell E, Gonzales CR, Nakano M, Jhee SS, Yen M, Ereshefsky L, Lindstrom TD, Calligaro DO, Cocke PJ, Greg Hall D, Friedrich S, Citron M, Audia JE (2011) Robust central reduction of amyloid-beta in humans with an orally available, non-peptidic beta-secretase inhibitor. The Journal of neuroscience : the official journal of the Society for Neuroscience 31 (46):16507-16516. doi:10.1523/jneurosci.3647-11.2011
33. Willis B, Martenyi F, Dean R, Lowe S, Nakano M, Monk S, Gonzales C, Mergott D, Daugherty L, Citron M, May P (2012) Central BACE1 inhibition by LY2886721 produces opposing effects on APP processing as reflected by cerebrospinal fluid sAPPalpha and sAPPbeta. Alzheimer's & Dementia 8 (4, Supplement):P582. doi:https://doi.org/10.1016/j.jalz.2012.05.1584
34. May PC, Willis BA, Lowe SL, Dean RA, Monk SA, Cocke PJ, Audia JE, Boggs LN, Borders AR, Brier RA, Calligaro DO, Day TA, Ereshefsky L, Erickson JA, Gevorkyan H, Gonzales CR, James DE, Jhee SS, Komjathy SF, Li L, Lindstrom TD, Mathes BM, Martenyi F, Sheehan SM,

Stout SL, Timm DE, Vaught GM, Watson BM, Winneroski LL, Yang Z, Mergott DJ (2015) The potent BACE1 inhibitor LY2886721 elicits robust central Abeta pharmacodynamic responses in mice, dogs, and humans. The Journal of neuroscience : the official journal of the Society for Neuroscience 35 (3):1199-1210. doi:10.1523/jneurosci.4129-14.2015
35. Kamikubo Y, Takasugi N, Niisato K, Hashimoto Y, Sakurai T (2017) Consecutive Analysis of BACE1 Function on Developing and Developed Neuronal Cells. Journal of Alzheimer's disease : JAD 56 (2):641-653. doi:10.3233/jad-160806
36. Filser S, Ovsepian SV, Masana M, Blazquez-Llorca L, Brandt Elvang A, Volbracht C, Muller MB, Jung CK, Herms J (2015) Pharmacological inhibition of BACE1 impairs synaptic plasticity and cognitive functions. Biological psychiatry 77 (8):729-739. doi:10.1016/j.biopsych.2014.10.013
37. Zhu K, Xiang X, Filser S, Marinkovic P, Dorostkar MM, Crux S, Neumann U, Shimshek DR, Rammes G, Haass C, Lichtenthaler SF, Gunnersen JM, Herms J (2018) Beta-Site Amyloid Precursor Protein Cleaving Enzyme 1 Inhibition Impairs Synaptic Plasticity via Seizure Protein 6. Biological psychiatry 83 (5):428-437. doi:10.1016/j.biopsych.2016.12.023
38. Cheret C, Willem M, Fricker FR, Wende H, Wulf-Goldenberg A, Tahirovic S, Nave KA, Saftig P, Haass C, Garratt AN, Bennett DL, Birchmeier C (2013) Bace1 and Neuregulin-1 cooperate to control formation and maintenance of muscle spindles. The EMBO journal 32 (14):2015-2028. doi:10.1038/emboj.2013.146
39. Savonenko AV, Melnikova T, Laird FM, Stewart KA, Price DL, Wong PC (2008) Alteration of BACE1-dependent NRG1/ErbB4 signaling and schizophrenia-like phenotypes in BACE1-null mice. Proceedings of the National Academy of Sciences of the United States of America 105 (14):5585-5590. doi:10.1073/pnas.0710373105
40. Kobayashi D, Zeller M, Cole T, Buttini M, McConlogue L, Sinha S, Freedman S, Morris RG, Chen KS (2008) BACE1 gene deletion: impact on behavioral function in a model of Alzheimer's disease. Neurobiology of aging 29 (6):861-873. doi:10.1016/j.neurobiolaging.2007.01.002
41. Laird FM, Cai H, Savonenko AV, Farah MH, He K, Melnikova T, Wen H, Chiang HC, Xu G, Koliatsos VE, Borchelt DR, Price DL, Lee HK, Wong PC (2005) BACE1, a major determinant of selective vulnerability of the brain to amyloid-beta amyloidogenesis, is essential for cognitive, emotional, and synaptic functions. The Journal of neuroscience : the official journal of the Society for Neuroscience 25 (50):11693-11709. doi:10.1523/jneurosci.2766-05.2005
42. Wang H, Song L, Laird F, Wong PC, Lee HK (2008) BACE1 knock-outs display deficits in activity-dependent potentiation of synaptic transmission at mossy fiber to CA3 synapses in the hippocampus. The Journal of neuroscience : the official journal of the Society for Neuroscience 28 (35):8677-8681. doi:10.1523/jneurosci.2440-08.2008
43. Egan MF, Kost J, Tariot PN, Aisen PS, Cummings JL, Vellas B, Sur C, Mukai Y, Voss T, Furtek C, Mahoney E, Harper Mozley L, Vandenberghe R, Mo Y, Michelson D (2018) Randomized Trial of Verubecestat for Mild-to-Moderate Alzheimer's Disease. The New England journal of medicine 378 (18):1691-1703. doi:10.1056/NEJMoa1706441
44. Willem M, Garratt AN, Novak B, Citron M, Kaufmann S, Rittger A, DeStrooper B, Saftig P, Birchmeier C, Haass C (2006) Control of peripheral nerve myelination by the beta-secretase BACE1. Science (New York, NY) 314 (5799):664-666. doi:10.1126/science.1132341
45. Hu X, Hicks CW, He W, Wong P, Macklin WB, Trapp BD, Yan R (2006) Bace1 modulates myelination in the central and peripheral nervous system. Nature neuroscience 9 (12):1520-1525. doi:10.1038/nn1797
46. Fleck D, van Bebber F, Colombo A, Galante C, Schwenk BM, Rabe L, Hampel H, Novak B, Kremmer E, Tahirovic S, Edbauer D, Lichtenthaler SF, Schmid B, Willem M, Haass C (2013) Dual cleavage of neuregulin 1 type III by BACE1 and ADAM17 liberates its EGF-like domain and allows paracrine signaling. The Journal of neuroscience : the official journal of the Society for Neuroscience 33 (18):7856-7869. doi:10.1523/jneurosci.3372-12.2013
47. Hitt B, Riordan S, Kukreja L, Eimer W, Rajapaksha T, Vassar R (2012) Beta-site amyloid precursor protein (APP) cleaving enzyme 1 (BACE1) deficient mice exhibit a close homolog of L1 (CHL1) loss-of-function phenotype involving axon guidance defects. The Journal of biological chemistry 287
48. Wong HK, Sakurai T, Oyama F, Kaneko K, Wada K, Miyazaki H, Kurosawa M, De Strooper B, Saftig P, Nukina N (2005) beta Subunits of voltage-gated sodium channels are novel substrates of beta-site amyloid precursor protein-cleaving enzyme (BACE1) and gamma-secretase. The Journal of biological chemistry 280 (24):23009-23017. doi:10.1074/jbc.M414648200
49. Kim DY, Carey BW, Wang H, Ingano LA, Binshtok AM, Wertz MH, Pettingell WH, He P, Lee VM, Woolf CJ, Kovacs DM (2007) BACE1 regulates voltage-gated sodium channels and neuronal activity. Nat Cell Biol 9

50. Barao S, Moechars D, Lichtenthaler SF, De Strooper B (2016) BACE1 Physiological Functions May Limit Its Use as Therapeutic Target for Alzheimer's Disease. Trends in neurosciences 39 (3):158-169. doi:10.1016/j.tins.2016.01.003
51. Hemming ML, Elias JE, Gygi SP, Selkoe DJ (2009) Identification of beta-secretase (BACE1) substrates using quantitative proteomics. PloS one 4 (12):e8477-e8477. doi:10.1371/journal.pone.0008477
52. Kuhn PH, Koroniak K, Hogl S, Colombo A, Zeitschel U, Willem M, Volbracht C, Schepers U, Imhof A, Hoffmeister A, Haass C, Rossner S, Brase S, Lichtenthaler SF (2012) Secretome protein enrichment identifies physiological BACE1 protease substrates in neurons. The EMBO journal 31 (14):3157-3168. doi:10.1038/emboj.2012.173
53. Dislich B, Wohlrab F, Bachhuber T, Muller SA, Kuhn PH, Hogl S, Meyer-Luehmann M, Lichtenthaler SF (2015) Label-free Quantitative Proteomics of Mouse Cerebrospinal Fluid Detects beta-Site APP Cleaving Enzyme (BACE1) Protease Substrates In Vivo. Molecular & cellular proteomics : MCP 14 (10):2550-2563. doi:10.1074/mcp.M114.041533
54. Zhou L, Barao S, Laga M, Bockstael K, Borgers M, Gijsen H, Annaert W, Moechars D, Mercken M, Gevaer K, De Strooper B (2012) The neural cell adhesion molecules L1 and CHL1 are cleaved by BACE1 protease in vivo. The Journal of biological chemistry 287
55. Stutzer I, Selevsek N, Esterhazy D, Schmidt A, Aebersold R, Stoffel M (2013) Systematic proteomic analysis identifies beta-site amyloid precursor protein cleaving enzyme 2 and 1 (BACE2 and BACE1) substrates in pancreatic beta-cells. The Journal of biological chemistry 288 (15):10536-10547. doi:10.1074/jbc.M112.444703
56. Boonen M, Staudt C, Gilis F, Oorschot V, Klumperman J, Jadot M (2016) Cathepsin D and its newly identified transport receptor SEZ6L2 can modulate neurite outgrowth. Journal of cell science 129 (3):557-568. doi:10.1242/jcs.179374
57. Gunnersen JM, Kim MH, Fuller SJ, De Silva M, Britto JM, Hammond VE, Davies PJ, Petrou S, Faber ES, Sah P, Tan SS (2007) Sez-6 proteins affect dendritic arborization patterns and excitability of cortical pyramidal neurons. Neuron 56 (4):621-639. doi:10.1016/j.neuron.2007.09.018
58. Wakana S, Sugaya E, Naramoto F, Yokote N, Maruyama C, Jin W, Ohguchi H, Tsuda T, Sugaya A, Kajiwara K (2000) Gene mapping of SEZ group genes and determination of pentylenetetrazol susceptible quantitative trait loci in the mouse chromosome. Brain research 857 (1-2):286-290
59. Miyazaki T, Hashimoto K, Uda A, Sakagami H, Nakamura Y, Saito SY, Nishi M, Kume H, Tohgo A, Kaneko I, Kondo H, Fukunaga K, Kano M, Watanabe M, Takeshima H (2006) Disturbance of cerebellar synaptic maturation in mutant mice lacking BSRPs, a novel brain-specific receptor-like protein family. FEBS letters 580 (17):4057-4064. doi:10.1016/j.febslet.2006.06.043
60. Bonifacino JS, Traub LM (2003) Signals for sorting of transmembrane proteins to endosomes and lysosomes. Annual review of biochemistry 72:395-447. doi:10.1146/annurev.biochem.72.121801.161800
61. Kim MH, Gunnersen JM, Tan SS (2002) Localized expression of the seizure-related gene SEZ-6 in developing and adult forebrains. Mechanisms of development 118 (1-2):171-174
62. Gunnersen JM, Augustine C, Spirkoska V, Kim M, Brown M, Tan SS (2002) Global analysis of gene expression patterns in developing mouse neocortex using serial analysis of gene expression. Molecular and cellular neurosciences 19 (4):560-573. doi:10.1006/mcne.2001.1098
63. Herbst R, Nicklin MJ (1997) SEZ-6: promoter selectivity, genomic structure and localized expression in the brain. Brain research Molecular brain research 44 (2):309-322
64. Gorlov IP, Meyer P, Liloglou T, Myles J, Boettger MB, Cassidy A, Girard L, Minna JD, Fischer R, Duffy S, Spitz MR, Haeussinger K, Kammerer S, Cantor C, Dierkesmann R, Field JK, Amos CI (2007) Seizure 6-like (SEZ6L) gene and risk for lung cancer. Cancer research 67 (17):8406-8411. doi:10.1158/0008-5472.can-06-4784
65. Causevic M, Dominko K, Malnar M, Vidatic L, Cermak S, Pigoni M, Kuhn PH, Colombo A, Havas D, Flunkert S, McDonald J, Gunnersen JM, Hutter-Paier B, Tahirovic S, Windisch M, Krainc D, Lichtenthaler SF, Hecimovic S (2018) BACE1-cleavage of Sez6 and Sez6L is elevated in Niemann-Pick type C disease mouse brains. PloS one 13 (7):e0200344. doi:10.1371/journal.pone.0200344
66. Ishikawa N, Daigo Y, Takano A, Taniwaki M, Kato T, Tanaka S, Yasui W, Takeshima Y, Inai K, Nishimura H, Tsuchiya E, Kohno N, Nakamura Y (2006) Characterization of SEZ6L2 cell-surface protein as a novel prognostic marker for lung cancer. Cancer science 97 (8):737-745. doi:10.1111/j.1349-7006.2006.00258.x

67. Ambalavanan A, Girard SL, Ahn K, Zhou S, Dionne-Laporte A, Spiegelman D, Bourassa CV, Gauthier J, Hamdan FF, Xiong L, Dion PA, Joober R, Rapoport J, Rouleau GA (2015) De novo variants in sporadic cases of childhood onset schizophrenia. European journal of human genetics : EJHG. doi:10.1038/ejhg.2015.218
68. Maccarrone G, Ditzen C, Yassouridis A, Rewerts C, Uhr M, Uhlen M, Holsboer F, Turck CW (2013) Psychiatric patient stratification using biosignatures based on cerebrospinal fluid protein expression clusters. Journal of psychiatric research 47 (11):1572-1580. doi:10.1016/j.jpsychires.2013.07.021
69. Gilissen C, Hehir-Kwa JY, Thung DT, van de Vorst M, van Bon BW, Willemsen MH, Kwint M, Janssen IM, Hoischen A, Schenck A, Leach R, Klein R, Tearle R, Bo T, Pfundt R, Yntema HG, de Vries BB, Kleefstra T, Brunner HG, Vissers LE, Veltman JA (2014) Genome sequencing identifies major causes of severe intellectual disability. Nature 511 (7509):344-347. doi:10.1038/nature13394
70. Mulley JC, Iona X, Hodgson B, Heron SE, Berkovic SF, Scheffer IE, Dibbens LM (2011) The Role of Seizure-Related SEZ6 as a Susceptibility Gene in Febrile Seizures. Neurology research international 2011:917565. doi:10.1155/2011/917565
71. Yu ZL, Jiang JM, Wu DH, Xie HJ, Jiang JJ, Zhou L, Peng L, Bao GS (2007) Febrile seizures are associated with mutation of seizure-related (SEZ) 6, a brain-specific gene. Journal of neuroscience research 85 (1):166-172. doi:10.1002/jnr.21103
72. Xu C, Mullersman JE, Wang L, Bin Su B, Mao C, Posada Y, Camarillo C, Mao Y, Escamilla MA, Wang KS (2013) Polymorphisms in seizure 6-like gene are associated with bipolar disorder I: evidence of gene x gender interaction. Journal of affective disorders 145 (1):95-99. doi:10.1016/j.jad.2012.07.017
73. Marshall CR, Noor A, Vincent JB, Lionel AC, Feuk L, Skaug J, Shago M, Moessner R, Pinto D, Ren Y, Thiruvahindrapduram B, Fiebig A, Schreiber S, Friedman J, Ketelaars CE, Vos YJ, Ficicioglu C, Kirkpatrick S, Nicolson R, Sloman L, Summers A, Gibbons CA, Teebi A, Chitayat D, Weksberg R, Thompson A, Vardy C, Crosbie V, Luscombe S, Baatjes R, Zwaigenbaum L, Roberts W, Fernandez B, Szatmari P, Scherer SW (2008) Structural variation of chromosomes in autism spectrum disorder. American journal of human genetics 82 (2):477-488. doi:10.1016/j.ajhg.2007.12.009
74. Kumar RA, Marshall CR, Badner JA, Babatz TD, Mukamel Z, Aldinger KA, Sudi J, Brune CW, Goh G, Karamohamed S, Sutcliffe JS, Cook EH, Geschwind DH, Dobyns WB, Scherer SW, Christian SL (2009) Association and mutation analyses of 16p11.2 autism candidate genes. PloS one 4 (2):e4582. doi:10.1371/journal.pone.0004582
75. Khoonsari PE, Haggmark A, Lonnberg M, Mikus M, Kilander L, Lannfelt L, Bergquist J, Ingelsson M, Nilsson P, Kultima K, Shevchenko G (2016) Analysis of the Cerebrospinal Fluid Proteome in Alzheimer's Disease. PloS one 11 (3):e0150672. doi:10.1371/journal.pone.0150672
76. Paracchini L, Beltrame L, Boeri L, Fusco F, Caffarra P, Marchini S, Albani D, Forloni G (2018) Exome sequencing in an Italian family with Alzheimer's disease points to a role for seizure-related gene 6 (SEZ6) rare variant R615H. Alzheimer's research & therapy 10 (1):106. doi:10.1186/s13195-018-0435-2
77. Anderson GR, Galfin T, Xu W, Aoto J, Malenka RC, Sudhof TC (2012) Candidate autism gene screen identifies critical role for cell-adhesion molecule CASPR2 in dendritic arborization and spine development. Proceedings of the National Academy of Sciences of the United States of America 109 (44):18120-18125. doi:10.1073/pnas.1216398109
78. Lin HH, Stacey M, Saxby C, Knott V, Chaudhry Y, Evans D, Gordon S, McKnight AJ, Handford P, Lea S (2001) Molecular analysis of the epidermal growth factor-like short consensus repeat domain-mediated protein-protein interactions: dissection of the CD97-CD55 complex. The Journal of biological chemistry 276 (26):24160-24169. doi:10.1074/jbc.M101770200
79. Wang R, Mellem JE, Jensen M, Brockie PJ, Walker CS, Hoerndli FJ, Hauth L, Madsen DM, Maricq AV (2012) The SOL-2/Neto auxiliary protein modulates the function of AMPA-subtype ionotropic glutamate receptors. Neuron 75 (5):838-850. doi:10.1016/j.neuron.2012.06.038
80. Zheng Y, Mellem JE, Brockie PJ, Madsen DM, Maricq AV (2004) SOL-1 is a CUB-domain protein required for GLR-1 glutamate receptor function in C. elegans. Nature 427 (6973):451-457. doi:10.1038/nature02244
81. Zhang W, St-Gelais F, Grabner CP, Trinidad JC, Sumioka A, Morimoto-Tomita M, Kim KS, Straub C, Burlingame AL, Howe JR, Tomita S (2009) A transmembrane accessory subunit that modulates kainate-type glutamate receptors. Neuron 61 (3):385-396. doi:10.1016/j.neuron.2008.12.014

82. Gally C, Eimer S, Richmond JE, Bessereau JL (2004) A transmembrane protein required for acetylcholine receptor clustering in Caenorhabditis elegans. Nature 431 (7008):578-582. doi:10.1038/nature02893
83. Ng D, Pitcher GM, Szilard RK, Sertie A, Kanisek M, Clapcote SJ, Lipina T, Kalia LV, Joo D, McKerlie C, Cortez M, Roder JC, Salter MW, McInnes RR (2009) Neto1 is a novel CUB-domain NMDA receptor-interacting protein required for synaptic plasticity and learning. PLoS biology 7 (2):e41. doi:10.1371/journal.pbio.1000041
84. Zheng Y, Brockie PJ, Mellem JE, Madsen DM, Walker CS, Francis MM, Maricq AV (2006) SOL-1 is an auxiliary subunit that modulates the gating of GLR-1 glutamate receptors in Caenorhabditis elegans. Proceedings of the National Academy of Sciences of the United States of America 103 (4):1100-1105. doi:10.1073/pnas.0504612103
85. Straub C, Hunt DL, Yamasaki M, Kim KS, Watanabe M, Castillo PE, Tomita S (2011) Distinct functions of kainate receptors in the brain are determined by the auxiliary subunit Neto1. Nature neuroscience 14 (7):866-873. doi:10.1038/nn.2837
86. Tang M, Pelkey KA, Ng D, Ivakine E, McBain CJ, Salter MW, McInnes RR (2011) Neto1 is an auxiliary subunit of native synaptic kainate receptors. The Journal of neuroscience : the official journal of the Society for Neuroscience 31 (27):10009-10018. doi:10.1523/jneurosci.6617-10.2011
87. Yaguchi H, Yabe I, Takahashi H, Watanabe M, Nomura T, Kano T, Matsumoto M, Nakayama KI, Watanabe M, Hatakeyama S (2017) Sez6l2 regulates phosphorylation of ADD and neuritogenesis. Biochemical and biophysical research communications 494 (1-2):234-241. doi:10.1016/j.bbrc.2017.10.047
88. Lodge D (2009) The history of the pharmacology and cloning of ionotropic glutamate receptors and the development of idiosyncratic nomenclature. Neuropharmacology 56 (1):6-21. doi:10.1016/j.neuropharm.2008.08.006
89. Hollmann M, Maron C, Heinemann S (1994) N-glycosylation site tagging suggests a three transmembrane domain topology for the glutamate receptor GluR1. Neuron 13 (6):1331-1343
90. Bennett JA, Dingledine R (1995) Topology profile for a glutamate receptor: three transmembrane domains and a channel-lining reentrant membrane loop. Neuron 14 (2):373-384
91. Pahl S, Tapken D, Haering SC, Hollmann M (2014) Trafficking of kainate receptors. Membranes 4 (3):565-595. doi:10.3390/membranes4030565
92. Jaskolski F, Coussen F, Nagarajan N, Normand E, Rosenmund C, Mulle C (2004) Subunit composition and alternative splicing regulate membrane delivery of kainate receptors. The Journal of neuroscience : the official journal of the Society for Neuroscience 24 (10):2506-2515. doi:10.1523/jneurosci.5116-03.2004
93. Jaskolski F, Normand E, Mulle C, Coussen F (2005) Differential trafficking of GluR7 kainate receptor subunit splice variants. The Journal of biological chemistry 280 (24):22968-22976. doi:10.1074/jbc.M413166200
94. Gallyas F, Jr., Ball SM, Molnar E (2003) Assembly and cell surface expression of KA-2 subunit-containing kainate receptors. Journal of neurochemistry 86 (6):1414-1427
95. Ball SM, Atlason PT, Shittu-Balogun OO, Molnar E (2010) Assembly and intracellular distribution of kainate receptors is determined by RNA editing and subunit composition. Journal of neurochemistry 114 (6):1805-1818. doi:10.1111/j.1471-4159.2010.06895.x
96. Mah SJ, Cornell E, Mitchell NA, Fleck MW (2005) Glutamate receptor trafficking: endoplasmic reticulum quality control involves ligand binding and receptor function. The Journal of neuroscience : the official journal of the Society for Neuroscience 25 (9):2215-2225. doi:10.1523/jneurosci.4573-04.2005
97. Valluru L, Xu J, Zhu Y, Yan S, Contractor A, Swanson GT (2005) Ligand binding is a critical requirement for plasma membrane expression of heteromeric kainate receptors. The Journal of biological chemistry 280 (7):6085-6093. doi:10.1074/jbc.M411549200
98. Pickering DS, Taverna FA, Salter MW, Hampson DR (1995) Palmitoylation of the GluR6 kainate receptor. Proceedings of the National Academy of Sciences of the United States of America 92 (26):12090-12094
99. Hirbec H, Francis JC, Lauri SE, Braithwaite SP, Coussen F, Mulle C, Dev KK, Coutinho V, Meyer G, Isaac JT, Collingridge GL, Henley JM (2003) Rapid and differential regulation of AMPA and kainate receptors at hippocampal mossy fibre synapses by PICK1 and GRIP. Neuron 37 (4):625-638
100. Wang LY, Taverna FA, Huang XP, MacDonald JF, Hampson DR (1993) Phosphorylation and modulation of a kainate receptor (GluR6) by cAMP-dependent protein kinase. Science (New York, NY) 259 (5098):1173-1175

101. Martin S, Nishimune A, Mellor JR, Henley JM (2007) SUMOylation regulates kainate-receptor-mediated synaptic transmission. Nature 447 (7142):321-325. doi:10.1038/nature05736
102. Garcia EP, Mehta S, Blair LA, Wells DG, Shang J, Fukushima T, Fallon JR, Garner CC, Marshall J (1998) SAP90 binds and clusters kainate receptors causing incomplete desensitization. Neuron 21 (4):727-739
103. Bowie D, Garcia EP, Marshall J, Traynelis SF, Lange GD (2003) Allosteric regulation and spatial distribution of kainate receptors bound to ancillary proteins. The Journal of physiology 547 (Pt 2):373-385. doi:10.1113/jphysiol.2002.033076
104. Tang M, Ivakine E, Mahadevan V, Salter MW, McInnes RR (2012) Neto2 interacts with the scaffolding protein GRIP and regulates synaptic abundance of kainate receptors. PloS one 7 (12):e51433. doi:10.1371/journal.pone.0051433
105. Laezza F, Wilding TJ, Sequeira S, Coussen F, Zhang XZ, Hill-Robinson R, Mulle C, Huettner JE, Craig AM (2007) KRIP6: a novel BTB/kelch protein regulating function of kainate receptors. Molecular and cellular neurosciences 34 (4):539-550. doi:10.1016/j.mcn.2006.12.003
106. Salinas GD, Blair LA, Needleman LA, Gonzales JD, Chen Y, Li M, Singer JD, Marshall J (2006) Actinfilin is a Cul3 substrate adaptor, linking GluR6 kainate receptor subunits to the ubiquitin-proteasome pathway. The Journal of biological chemistry 281 (52):40164-40173. doi:10.1074/jbc.M608194200
107. Lerma J, Marques JM (2013) Kainate receptors in health and disease. Neuron 80 (2):292-311. doi:10.1016/j.neuron.2013.09.045
108. Tashiro A, Dunaevsky A, Blazeski R, Mason CA, Yuste R (2003) Bidirectional regulation of hippocampal mossy fiber filopodial motility by kainate receptors: a two-step model of synaptogenesis. Neuron 38 (5):773-784
109. Benes FM, Todtenkopf MS, Kostoulakos P (2001) GluR5,6,7 subunit immunoreactivity on apical pyramidal cell dendrites in hippocampus of schizophrenics and manic depressives. Hippocampus 11 (5):482-491. doi:10.1002/hipo.1065
110. Porter RH, Eastwood SL, Harrison PJ (1997) Distribution of kainate receptor subunit mRNAs in human hippocampus, neocortex and cerebellum, and bilateral reduction of hippocampal GluR6 and KA2 transcripts in schizophrenia. Brain research 751 (2):217-231
111. Scarr E, Beneyto M, Meador-Woodruff JH, Dean B (2005) Cortical glutamatergic markers in schizophrenia. Neuropsychopharmacology : official publication of the American College of Neuropsychopharmacology 30 (8):1521-1531. doi:10.1038/sj.npp.1300758
112. Garey LJ, Von Bussmann KA, Hirsch SR (2006) Decreased numerical density of kainate receptor-positive neurons in the orbitofrontal cortex of chronic schizophrenics. Experimental Brain Research 173 (2):234-242. doi:10.1007/s00221-006-0396-8
113. Beneyto M, Kristiansen LV, Oni-Orisan A, McCullumsmith RE, Meador-Woodruff JH (2007) Abnormal glutamate receptor expression in the medial temporal lobe in schizophrenia and mood disorders. Neuropsychopharmacology : official publication of the American College of Neuropsychopharmacology 32 (9):1888-1902. doi:10.1038/sj.npp.1301312
114. Dracheva S, Byne W, Chin B, Haroutunian V (2008) Ionotropic glutamate receptor mRNA expression in the human thalamus: absence of change in schizophrenia. Brain research 1214:23-34. doi:10.1016/j.brainres.2008.03.039
115. Tucholski J, Simmons MS, Pinner AL, McMillan LD, Haroutunian V, Meador-Woodruff JH (2013) N-linked glycosylation of cortical N-methyl-D-aspartate and kainate receptor subunits in schizophrenia. Neuroreport 24 (12):688-691. doi:10.1097/WNR.0b013e328363bd8a
116. Motazacker MM, Rost BR, Hucho T, Garshasbi M, Kahrizi K, Ullmann R, Abedini SS, Nieh SE, Amini SH, Goswami C, Tzschach A, Jensen LR, Schmitz D, Ropers HH, Najmabadi H, Kuss AW (2007) A defect in the ionotropic glutamate receptor 6 gene (GRIK2) is associated with autosomal recessive mental retardation. American journal of human genetics 81 (4):792-798. doi:10.1086/521275
117. Shaltiel G, Maeng S, Malkesman O, Pearson B, Schloesser RJ, Tragon T, Rogawski M, Gasior M, Luckenbaugh D, Chen G, Manji HK (2008) Evidence for the involvement of the kainate receptor subunit GluR6 (GRIK2) in mediating behavioral displays related to behavioral symptoms of mania. Molecular psychiatry 13 (9):858-872. doi:10.1038/mp.2008.20
118. Lanore F, Labrousse VF, Szabo Z, Normand E, Blanchet C, Mulle C (2012) Deficits in morphofunctional maturation of hippocampal mossy fiber synapses in a mouse model of intellectual disability. The Journal of neuroscience : the official journal of the Society for Neuroscience 32 (49):17882-17893. doi:10.1523/jneurosci.2049-12.2012
119. Schiffer HH, Heinemann SF (2007) Association of the human kainate receptor GluR7 gene (GRIK3) with recurrent major depressive disorder. American journal of medical genetics Part

B, Neuropsychiatric genetics : the official publication of the International Society of Psychiatric Genetics 144b (1):20-26. doi:10.1002/ajmg.b.30374
120. Wilson GM, Flibotte S, Chopra V, Melnyk BL, Honer WG, Holt RA (2006) DNA copy-number analysis in bipolar disorder and schizophrenia reveals aberrations in genes involved in glutamate signaling. Hum Mol Genet 15 (5):743-749. doi:10.1093/hmg/ddi489
121. Begni S, Popoli M, Moraschi S, Bignotti S, Tura GB, Gennarelli M (2002) Association between the ionotropic glutamate receptor kainate 3 (GRIK3) ser310ala polymorphism and schizophrenia. Molecular psychiatry 7 (4):416-418. doi:10.1038/sj.mp.4000987
122. Ahmad Y, Bhatia MS, Mediratta PK, Sharma KK, Negi H, Chosdol K, Sinha S (2009) Association between the ionotropic glutamate receptor kainate3 (GRIK3) Ser310Ala polymorphism and schizophrenia in the Indian population. The world journal of biological psychiatry : the official journal of the World Federation of Societies of Biological Psychiatry 10 (4):330-333. doi:10.3109/15622970802688044
123. Mulle C, Sailer A, Perez-Otano I, Dickinson-Anson H, Castillo PE, Bureau I, Maron C, Gage FH, Mann JR, Bettler B, Heinemann SF (1998) Altered synaptic physiology and reduced susceptibility to kainate-induced seizures in GluR6-deficient mice. Nature 392 (6676):601-605. doi:10.1038/33408
124. Smolders I, Bortolotto ZA, Clarke VR, Warre R, Khan GM, O'Neill MJ, Ornstein PL, Bleakman D, Ogden A, Weiss B, Stables JP, Ho KH, Ebinger G, Collingridge GL, Lodge D, Michotte Y (2002) Antagonists of GLU(K5)-containing kainate receptors prevent pilocarpine-induced limbic seizures. Nature neuroscience 5 (8):796-804. doi:10.1038/nn880
125. Sander T, Hildmann T, Kretz R, Furst R, Sailer U, Bauer G, Schmitz B, Beck-Mannagetta G, Wienker TF, Janz D (1997) Allelic association of juvenile absence epilepsy with a GluR5 kainate receptor gene (GRIK1) polymorphism. American journal of medical genetics 74 (4):416-421
126. Pigoni M, Wanngren J, Kuhn PH, Munro KM, Gunnersen JM, Takeshima H, Feederle R, Voytyuk I, De Strooper B, Levasseur MD, Hrupka BJ, Muller SA, Lichtenthaler SF (2016) Seizure protein 6 and its homolog seizure 6-like protein are physiological substrates of BACE1 in neurons. Molecular neurodegeneration 11 (1):67. doi:10.1186/s13024-016-0134-z
127. Herber J, Njavro J, Feederle R, Schepers U, Muller U, Brase S, Muller S, Lichtenthaler SF (2018) Click chemistry-mediated biotinylation reveals a function for the protease BACE1 in modulating the neuronal surface glycoproteome. Molecular & cellular proteomics : MCP. doi:10.1074/mcp.RA118.000608
128. Scheuner D, Eckman C, Jensen M, Song X, Citron M, Suzuki N, Bird TD, Hardy J, Hutton M, Kukull W, Larson E, Levy-Lahad E, Viitanen M, Peskind E, Poorkaj P, Schellenberg G, Tanzi R, Wasco W, Lannfelt L, Selkoe D, Younkin S (1996) Secreted amyloid beta-protein similar to that in the senile plaques of Alzheimer's disease is increased in vivo by the presenilin 1 and 2 and APP mutations linked to familial Alzheimer's disease. Nature medicine 2 (8):864-870
129. Barao S, Gartner A, Leyva-Diaz E, Demyanenko G, Munck S, Vanhoutvin T, Zhou L, Schachner M, Lopez-Bendito G, Maness PF, De Strooper B (2015) Antagonistic Effects of BACE1 and APH1B-gamma-Secretase Control Axonal Guidance by Regulating Growth Cone Collapse. Cell reports 12 (9):1367-1376. doi:10.1016/j.celrep.2015.07.059
130. Perez RG, Zheng H, Van der Ploeg LH, Koo EH (1997) The beta-amyloid precursor protein of Alzheimer's disease enhances neuron viability and modulates neuronal polarity. The Journal of neuroscience : the official journal of the Society for Neuroscience 17 (24):9407-9414
131. Wallace WC, Akar CA, Lyons WE (1997) Amyloid precursor protein potentiates the neurotrophic activity of NGF. Brain research Molecular brain research 52 (2):201-212
132. Ikin AF, Sabo SL, Lanier LM, Buxbaum JD (2007) A macromolecular complex involving the amyloid precursor protein (APP) and the cytosolic adapter FE65 is a negative regulator of axon branching. Molecular and cellular neurosciences 35 (1):57-63. doi:10.1016/j.mcn.2007.02.003
133. Oh ES, Mielke MM, Rosenberg PB, Jain A, Fedarko NS, Lyketsos CG, Mehta PD (2010) Comparison of conventional ELISA with electrochemiluminescence technology for detection of amyloid-beta in plasma. Journal of Alzheimer's disease : JAD 21 (3):769-773. doi:10.3233/jad-2010-100456
134. Bigl M, Apelt J, Luschekina EA, Lange-Dohna C, Roßner S, Schliebs R (2000) Expression of β-secretase mRNA in transgenic Tg2576 mouse brain with Alzheimer plaque pathology. Neuroscience letters 292 (2):107-110. doi:https://doi.org/10.1016/S0304-3940(00)01452-X
135. Iryna Voytyuk1, Stephan A Mueller3,4, Julia Herber3,4, An Snellinx1,2, Dieder Moechars5, Geert van Loo6,7 ,, Stefan F Lichtenthaler3, 8,9, Bart De Strooper1,2,9,10 BACE2 distribution in major brain cell types and identification of novel substrates.

136. Rochin L, Hurbain I, Serneels L, Fort C, Watt B, Leblanc P, Marks MS, De Strooper B, Raposo G, van Niel G (2013) BACE2 processes PMEL to form the melanosome amyloid matrix in pigment cells. Proceedings of the National Academy of Sciences of the United States of America 110
137. Esterhazy D, Stutzer I, Wang H, Rechsteiner MP, Beauchamp J, Dobeli H, Hilpert H, Matile H, Prummer M, Schmidt A, Lieske N, Boehm B, Marselli L, Bosco D, Kerr-Conte J, Aebersold R, Spinas GA, Moch H, Migliorini C, Stoffel M (2011) Bace2 is a beta cell-enriched protease that regulates pancreatic beta cell function and mass. Cell Metab 14
138. Kimura R, Devi L, Ohno M (2010) Partial reduction of BACE1 improves synaptic plasticity, recent and remote memories in Alzheimer's disease transgenic mice. Journal of neurochemistry 113 (1):248-261. doi:10.1111/j.1471-4159.2010.06608.x
139. McConlogue L, Buttini M, Anderson JP, Brigham EF, Chen KS, Freedman SB, Games D, Johnson-Wood K, Lee M, Zeller M, Liu W, Motter R, Sinha S (2007) Partial reduction of BACE1 has dramatic effects on Alzheimer plaque and synaptic pathology in APP Transgenic Mice. The Journal of biological chemistry 282
140. Vassar R (2014) BACE1 inhibitor drugs in clinical trials for Alzheimer's disease. Alzheimer's research & therapy 6 (9):89. doi:10.1186/s13195-014-0089-7
141. Nakayama M, Hama C (2011) Modulation of neurotransmitter receptors and synaptic differentiation by proteins containing complement-related domains. Neuroscience research 69 (2):87-92. doi:10.1016/j.neures.2010.11.006
142. Escudero-Esparza A, Kalchishkova N, Kurbasic E, Jiang WG, Blom AM (2013) The novel complement inhibitor human CUB and Sushi multiple domains 1 (CSMD1) protein promotes factor I-mediated degradation of C4b and C3b and inhibits the membrane attack complex assembly. Faseb j 27 (12):5083-5093. doi:10.1096/fj.13-230706
143. Furuya S, Ono K, Hirabayashi Y (1995) Sphingolipid biosynthesis is necessary for dendrite growth and survival of cerebellar Purkinje cells in culture. Journal of neurochemistry 65 (4):1551-1561
144. Harel R, Futerman AH (1993) Inhibition of sphingolipid synthesis affects axonal outgrowth in cultured hippocampal neurons. The Journal of biological chemistry 268 (19):14476-14481
145. Tang BL, Tan AE, Lim LK, Lee SS, Low DY, Hong W (1998) Syntaxin 12, a member of the syntaxin family localized to the endosome. The Journal of biological chemistry 273 (12):6944-6950
146. Jung JJ, Inamdar SM, Tiwari A, Choudhury A (2012) Regulation of intracellular membrane trafficking and cell dynamics by syntaxin-6. Bioscience reports 32 (4):383-391. doi:10.1042/bsr20120006
147. Prekeris R, Klumperman J, Chen YA, Scheller RH (1998) Syntaxin 13 Mediates Cycling of Plasma Membrane Proteins via Tubulovesicular Recycling Endosomes. The Journal of cell biology 143 (4):957-971. doi:10.1083/jcb.143.4.957
148. Hoogenraad CC, Popa I, Futai K, Martinez-Sanchez E, Wulf PS, van Vlijmen T, Dortland BR, Oorschot V, Govers R, Monti M, Heck AJ, Sheng M, Klumperman J, Rehmann H, Jaarsma D, Kapitein LC, van der Sluijs P (2010) Neuron specific Rab4 effector GRASP-1 coordinates membrane specialization and maturation of recycling endosomes. PLoS biology 8 (1):e1000283. doi:10.1371/journal.pbio.1000283
149. Steiner P, Sarria JC, Glauser L, Magnin S, Catsicas S, Hirling H (2002) Modulation of receptor cycling by neuron-enriched endosomal protein of 21 kD. The Journal of cell biology 157 (7):1197-1209. doi:10.1083/jcb.200202022
150. Vandenberghe W, Bredt DS (2004) Early events in glutamate receptor trafficking. Current Opinion in Cell Biology 16 (2):134-139. doi:https://doi.org/10.1016/j.ceb.2004.01.003
151. Vivithanaporn P, Lash LL, Marszalec W, Swanson GT (2007) Critical Roles for the M3–S2 Transduction Linker Domain in Kainate Receptor Assembly and Postassembly Trafficking. The Journal of Neuroscience 27 (39):10423-10433. doi:10.1523/jneurosci.2674-07.2007
152. Vernon CG, Copits BA, Stolz JR, Guzman YF, Swanson GT (2017) N-glycan content modulates kainate receptor functional properties. The Journal of physiology 595 (17):5913-5930. doi:10.1113/jp274790
153. Morita I, Kakuda S, Takeuchi Y, Itoh S, Kawasaki N, Kizuka Y, Kawasaki T, Oka S (2009) HNK-1 glyco-epitope regulates the stability of the glutamate receptor subunit GluR2 on the neuronal cell surface. The Journal of biological chemistry 284 (44):30209-30217. doi:10.1074/jbc.M109.024208
154. Kruse J, Mailhammer R, Wernecke H, Faissner A, Sommer I, Goridis C, Schachner M (1984) Neural cell adhesion molecules and myelin-associated glycoprotein share a common

carbohydrate moiety recognized by monoclonal antibodies L2 and HNK-1. Nature 311 (5982):153-155
155. Saglietti L, Dequidt C, Kamieniarz K, Rousset MC, Valnegri P, Thoumine O, Beretta F, Fagni L, Choquet D, Sala C, Sheng M, Passafaro M (2007) Extracellular interactions between GluR2 and N-cadherin in spine regulation. Neuron 54 (3):461-477. doi:10.1016/j.neuron.2007.04.012
156. Morita I, Kakuda S, Takeuchi Y, Kawasaki T, Oka S (2009) HNK-1 (human natural killer-1) glyco-epitope is essential for normal spine morphogenesis in developing hippocampal neurons. Neuroscience 164 (4):1685-1694. doi:10.1016/j.neuroscience.2009.09.065
157. Yan D, Tomita S (2012) Defined criteria for auxiliary subunits of glutamate receptors. The Journal of physiology 590 (1):21-31. doi:10.1113/jphysiol.2011.213868

List of publications

Martina Pigoni, Jana Hartmann, Jasenka Njavro, Merav D Shmueli, Stephan A Müller, Peer-Hendrik Kuhn, Pan Gao, Mai Ly Tran, Birgit Blank, Agnes L. Hipgrave Ederveen, Julia Von Blume, Christophe Mulle, Jenny M Gunnersen, Manfred Wuhrer, Gerhard Rammes, Marc Aurel Busche, Thomas Koeglsperger and Stefan F Lichtenthaler. Seizure protein 6 controls glycosylation, trafficking and function of kainate receptor subunits GluK2 and GluK3. Under revision

Scilabra, S. D., **Pigoni, M.**, Pravatá, V., Schätzl, T., Müller, S. A., Troeberg, L., Lichtenthaler, S. F. (2018) Increased TIMP-3 expression alters the cellular secretome through dual inhibition of the metalloprotease ADAM10 and ligand-binding of the LRP-1 receptor. Sci Rep. doi: 10.1038/s41598-018-32910-4.

Causevic, M., Dominko, K., Malnar, M., Vidatic, L., Cermak, S., **Pigoni, M.**, Kuhn, P.H., Colombo, A., Havas, D., Flunkert, S., McDonald, J., Gunnersen, J.M., Hutter-Paier, B., Tahirovic, S., Windisch, M., Krainc, D., Lichtenthaler, S.F., Hecimovic, S. (2018) BACE1-cleavage of Sez6 and Sez6L is elevated in Niemann-Pick type C disease mouse brains. PLoS One. doi: 10.1371/journal.pone.0200344.

Brummer, T., **Pigoni, M.**, Rossello, A., Wang, H., Noy, P. J., Tomlinson, M. G., Blobel, C. P., Lichtenthaler, S. F. (2018) The Metalloprotease A Disintegrin and Metalloprotease 10' (ADAM10) undergoes rapid, post-lysis autocatalytic degradation. FASEB J. doi: 10.1096/fj.201700823RR

Pigoni, M., Wanngren, J., Kuhn, P. H., Munro, K. M., Gunnersen, J. M., Takeshima, H., Lichtenthaler, S. F. (2016). Seizure protein 6 and its homolog seizure 6-like protein are physiological substrates of BACE1 in neurons. Mol Neurodegener, 11(1): 67. doi:10.1186/s13024-016-0134-z

Pigoni, M., Gunnersen, J. M., & Lichtenthaler, S. F. (2016). Seizure-6 proteins highlight BACE1 functions in neurobiology. Oncotarget. doi:10.18632/oncotarget.13801 (Comment article)

Munro, K. M., Nash, A., **Pigoni, M**., Lichtenthaler, S. F., & Gunnersen, J. M. (2016). Functions of the Alzheimer's Disease Protease BACE1 at the Synapse in the Central Nervous System. J Mol Neurosci, 60(3): 305-315. doi:10.1007/s12031-016-0800-1 (Review article)

Scilabra, S. D., Yamamoto, K., **Pigoni, M.**, Sakamoto, K., Müller, S. A., Papadopoulou, A., Kadomatsu, K. (2016). Dissecting the interaction between tissue inhibitor of metalloproteinases-3 (TIMP-3) and low density lipoprotein receptor-related protein-1 (LRP-1): Development of a "TRAP" to increase levels of TIMP-3 in the tissue. Matrix Biol. doi:10.1016/j.matbio.2016.07.004

Affidavit

Eidesstattliche Versicherung/Affidavit

Hiermit versichere ich an Eides statt, dass ich die vorliegende Dissertation FUNCTION AND DIAGNOSTIC POTENTIAL OF THE SEZ6 PROTEIN FAMILY - NOVEL SUBSTRATES OF THE ALZHEIMER PROTEASE BACE1 selbstständig angefertigt habe, mich außer der angegebenen keiner weiteren Hilfsmittel bedient und alle Erkenntnisse, die aus dem Schrifttum ganz oder annähernd übernommen sind, als solche kenntlich gemacht und nach ihrer Herkunft unter Bezeichnung der Fundstelle einzeln nachgewiesen habe.

I hereby confirm that the dissertation FUNCTION AND DIAGNOSTIC POTENTIAL OF THE SEZ6 PROTEIN FAMILY - NOVEL SUBSTRATES OF THE ALZHEIMER PROTEASE BACE1 is the result of my own work and that I have only used sources or materials listed and specified in the dissertation.

München, den 10.04.2019 Unterschrift signature

Martina Pigoni

Declaration of author contributions

1) Seizure protein 6 and its homolog seizure 6-like protein are physiological substrates of BACE1 in neurons

Martina Pigoni, Johanna Wanngren, Peer-Hendrik Kuhn, Kathryn M. Munro, Jenny M. Gunnersen, Hiroshi Takeshima, Regina Feederle, Iryna Voytyuk, Bart De Strooper, Mikail D. Levasseur, Brian J. Hrupka, Stephan A. Müller and Stefan F. Lichtenthaler

Author´contributions

MP performed the experiments in HEK293T cells, in neurons and in mouse brain *ex-vivo*

JW contributed to perform part of the experiments in MIN6 cells

PHK, SAM performed the mass spectrometry analysis

KMM performed all immunohistochemical staining

IV collected CSF from mice

MDL performed part of the experiments in MIN6 cells

JMG, BDS, BJH supervised the analysis and participated in the drafting of the manuscript.

HT and RF provided reagents

SFL designed the study and wrote the manuscript.

All authors read and approved the final manuscript.

2) Seizure protein 6 controls glycosylation, trafficking and function of kainate receptor subunits GluK2 and GluK3

Martina Pigoni, Jana Hartmann, Jasenka Njavro, Merav D Shmueli, Stephan A Müller, Peer-Hendrik Kuhn, Pan Gao, Mai Ly Tran, Birgit Blank, Agnes L. Hipgrave Ederveen, Julia Von Blume, Christophe Mulle, Jenny M Gunnersen, Manfred Wuhrer, Gerhard Rammes, Marc Aurel Busche, Thomas Koeglsperger and Stefan F Lichtenthaler.. Under revision

Author´contributions

MP prepared the samples for mass spectrometry analysis, performed all the experiments in HEK293T cells, in neurons and in mouse brain *ex-vivo*, contributed in designing the study and writing the manuscript

JH performed the electrophysiology experiments

JN contributed to cell culture experiments

MDS performed the Lectin Chip analysis

PHK, SAM performed the mass spectrometry analysis

PG contributed to the electrophysiology experiments

BB, MLT performed the RUSH experiment

ALHE performed the global glycome analysis via mass spectrometry

CM provided reagents, read and corrected the manuscript

JVB, JMG, MW, GR, MAB, TK supervised the analysis and participated in the drafting of the manuscript.

SFL designed the study and wrote the manuscript.

All authors read and approved the final manuscript.

“O frati", dissi "che per cento milia
perigli siete giunti a l'occidente,
a questa tanto picciola vigilia

d'i nostri sensi ch'è del rimanente,
non vogliate negar l'esperienza,
di retro al sol, del mondo sanza
gente.

Considerate la vostra semenza:
fatti non foste a viver come bruti,
ma per seguir virtute e
canoscenza"

And then I said: “O brothers, ye who now
have through a hundred thousand perils reached
the West, to this so short a waking-time

still left your senses, will not to refuse
experience of that world behind the sun
which knows not man!

Bethink you of the seed! Whence ye have sprung; for ye
were not created to lead the life of stupid animals,
but manliness and knowledge to pursue.”

La Divina Commedia, Dante Alighieri, Inferno Canto XXVI